OFFICIAL JOURNAL OF THE SCIENTIFIC SOCIETY OF ANATOMISTS, HISTOLOGISTS, EMBRYOLOGISTS AND TOPOGRAPHIC ANATOMISTS OF UKRAINE

DOI: 10.31393
ISSN 1818-1295
eISSN 2616-6194

ВІСНИК МОРФОЛОГІЇ
REPORTS OF MORPHOLOGY

Vol. 24, №3, 2018

Scientific peer-reviewed journal in the fields of normal and pathological anatomy, histology, cytology and embryology, topographical anatomy and operative surgery, biomedical anthropology, ecology, molecular biology, biology of development

Published since 1993
Periodicity: 4 times a year

Vinnytsya • 2018

ВІСНИК МОРФОЛОГІЇ - REPORTS OF MORPHOLOGY

Founded by the "Scientific Society of Anatomists, Histologists, Embryologists, and Topographic Anatomists of Ukraine" and National Pyrogov Memorial Medical University, Vinnytsya in 1993

Certificate of state registration КВ №9310 from 02.11.2004

Professional scientific publication of Ukraine in the field of medical sciences (approved by the order of the Ministry of Education and Science of Ukraine No. 528 dated 12.05.2015, annex 10); professional scientific publication of Ukraine in the field of biological sciences by specialty groups 14.01.00-14.03.00 (approved by the order of the Ministry of Education and Science of Ukraine No. 747 dated 13.07.2015, annex 17)

Approved by the Academic Council of National Pyrogov Memorial Medical University, Vinnytsya, protocol №2 from 27.09.2018

Indexation: CrossRef, elibrary.ru, Google Schoolar Metrics, National Library of Ukraine Vernadsky

Address editors and publisher:
Pyrogov Str. 56,
Vinnytsya, Ukraine - 21018
Tel.: +38 (0432) 553959
E-mail: nila@vnmu.edu.ua

Computer page-proofs - Klopotovska L.O.
Translator - Gunas V.I.
Technical support - Levenchuk S.S., Lunik A.Yu.
Scientific editing - editorship

The site of the magazine - https://morphology-journal.com

CONTENT

DOI: 10.31393/morphology-journal-2018-24(3)-01 Reports of Morphology, Vol. 24, №3, Pages 5-10

ISSN 1818-1295 eISSN 2616-6194

REPORTS OF MORPHOLOGY

Official Journal of the Scientific Society of Anatomists, Histologists, Embryologists and Topographic Anatomists of Ukraine

journal homepage: https://morphology-journal.com

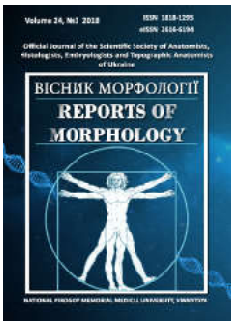

Modeling of sonographic parameters of the kidneys in practically healthy women of the middle intermediate somatotype depending on the constitutional parameters of the body

Cherkasov V.G.[1], Ustymenko O.S.[1], Shayuk A.V.[2], Prokopenko S.V.[3], Gunas I.V.[3]

[1]Bogomolets National Medical University, Kyiv, Ukraine;
[2]Zhytomyr Ivan Franko State University, Zhytomyr, Ukraine;
[3]National Pirogov Memorial Medical University, Vinnytsya, Ukraine

ARTICLE INFO

Received: 11 July, 2018
Accepted: 31 July, 2018

UDC: 616-073.4-8:616.61:616-055.1:616-055.2

CORRESPONDING AUTHOR

e-mail: iryna.tymoshenko@i.ua
Cherkasov V. G.

The scientific literature presents quite a large number of works, in which the priority role of mathematical modeling in providing high-quality medical care, health and active longevity of a person is determined. The purpose of the work is to construct and analyze the regression models of individual sonographic sizes of kidneys in practically healthy women of the middle intermediate somatotype, depending on the features of the anthropometric and somatotypological indicators. Within the framework of the agreement on scientific cooperation from the database of National Pirogov Memorial Medical University, Vinnytsya primary sonographic parameters (length, width, anterior-posterior dimension, area of longitudinal and cross-section of the kidneys and their sinuses, as well as volume of the right and left kidneys) and anthropometric indices (obtained by the method of V.V. Bunak in the modification of P.P. Shaparenko) of 17 practically healthy women of the first mature age of the middle intermediate somatotype, who in the third generation live in the Podillya region of Ukraine. The construction of regression models of individual sonographic sizes of the kidneys, depending on the features of anthropo-somatotypological parameters of the body of women of the middle intermediate somatotype, was carried out in the licensed package "Statistica 6.1". In women of the middle intermediate somatotype all 16 possible reliable regression models of sonographic parameters of the kidneys were constructed depending on the anthropo-somatotypological parameters with the determination coefficient R^2 from 0.891 to 0.978. The analysis of reliable regression models (with a coefficient of determination greater than 0.6), the sonographic parameters of the kidneys in practically healthy women of the middle intermediate somatotype revealed that most often models of both kidneys, as well as separately of the right and left kidneys, include the circumferential dimensions of the body (respectively, 35.9 - 33.3 - 38.5% of the total number of indicators included in the models). In addition, models of both kidneys most often include cephalometric indices (12.6%), thickness of skin-fat folds and body diameters (by 11.7%); models of the right kidney - body diameters (15.7%), cephalometric indices and width of distal epiphyses of long tubular bones of extremities (by 11.8%); models of the right kidney - the thickness of skin and fat folds (17.3%) and cephalometric indices (13.5%). Attention is drawn to the lack of entry into models of sonographic sizes of kidneys total body sizes.

Keywords: *regression analysis, sonographic parameters of the kidneys, indicators of body structure and body sizes, practically healthy women, middle intermediate somatotype.*

Introduction

Huge factual material collected during the century of observation by practicing doctors and enriched with modern hardware researches of the kidneys, requires careful attention of specialists in the field of mathematical forecasting [11, 13, 19]. A fairly large number of works in which the fundamental scientific component comes to the fore, defining in the future the priority role of mathematical modeling in providing high-quality health care, health and

active longevity of man [20, 29].

For today, sufficiently effective approaches have been developed to quantitatively model the various properties of the kidneys [21, 29]. Let's consider only one very important aspect of scientific research concerning the problem of predicting the size of the kidneys, since their increase or decrease serves as an important indicator of renal and extra-renal disorders [2, 14, 22]. Moreover, mathematical prediction of their size may be one of the most affordable tools for testing effectiveness and the possibility of implementing such new ideas as the use of miniature endoscopic camera designed for diagnostic studies and minimally invasive surgical interventions unattainable for traditional technologies [5]. Such studies are carried out on the basis of regression equations with the reproduction of real parameters of the kidneys, which are matched with experimental and sectional data [6].

The basis for mathematical modeling is proved association of parameters of kidneys with features of a structure of a human body [7, 10-12]. The results of a number of scientific studies indicate the possibility of situations where a significant reduction or increase in one or several parameters of physical development correlates with the corresponding dimensional variations of the organ [8, 9, 18, 21, 23].

Thus, mathematical modeling, in direct conjunction with the revolution in the field of instrumental and diagnostic equipment, can provide penetration to fundamentally new levels of understanding of medical and biological processes [17, 20, 21, 24].

The *purpose* of the work is to construct and analyze the regression models of individual sonographic sizes of kidneys in practically healthy women of the middle intermediate somatotype, depending on the features of the anthropometric and somatotypological indicators.

Materials and methods

Within the framework of the agreement on scientific cooperation between the Department of Human Anatomy of the Bogomolets National Medical University, Kyiv and the research center of the National Pirogov Memorial Medical University, Vinnytsya from the database of the latter taken the primary sonographic parameters and anthropometric indices of practically healthy men and women of the first mature age, who in the third generation live in the Podillia region of Ukraine.

With the help of the ultrasound diagnostic system "CAPASEE" SSA-220A (Toshiba, Japan), a convective sensor with a working frequency of 3.75 MHz and a diagnostic ultrasound system Voluson 730 Pro (Austria), a convective sensor of 4-10 MHz, a sonographic study of kidneys was performed [16], which included determination of length, width, anterior-posterior size, longitudinal and cross-sectional area of the kidneys and their sinuses. According to the generally accepted formula: V = 0.524 x L x W x AP, where, V is the volume of the kidney, L is the length of the kidney, W is the width of the kidney, S - the anterior-posterior size of the kidney, the volume of the right and left kidneys is counted.

Anthropometric survey was conducted by V. V. Bunak method in the modification of P.P. Shaparenko [25]; estimation of the somatotype - according to the mathematical scheme J. Carter and B. Heath [3]; indicators of the body composition (fat, bone and muscle) according to the formulas of J. Matiegka [15], as well as the muscular component of the body mass according to the formulas of the American Institute of Nutrition [26].

The construction of regression models of individual sonographic sizes of the kidneys, depending on the features of anthropo-somatotypological parameters of the body of women of the middle intermediate somatotype, was carried out in the licensed package "Statistica 6.1". In the direct stepwise regression analysis, we determined the following conditions: the final version of the model should have a determination coefficient (R^2) of at least 0.60, the F-criterion value of not less than 3.0, and the number of free members included in the model must be minimal.

Results

In practically healthy women of the middle intermediate somatotype (n=17), the following reliable models of sonographic parameters of the kidneys were constructed depending on the features of the anthropometric and somatotypological parameters:

RE_R_DL (*length of the right kidney in the longitudinal section, mm*) = 70.73 + 1.423 x ACR + 3.573 x OBPL1 - 1.377 x ATP - 1.467 x $OBPR_1$ - 7.351 x EPPR + 3.694 x EPG + 1.539 x $OBPR_2$ (R^2=0.976; $F_{(7.9)}$=51.33; p<0.001; St. Error of estimate=1.322),

where (here and thereafter), R^2 - determination factor; $F_{(!.!!)}$ = !!.!! - critical (!.!!) and received (!!.!!) values of Fisher's criterion; St. Error of estimate - standard error of standardized regression coefficient; ACR - shoulder width (cm); OBPL1 - shoulder girth in a tense state (cm); ATP is the height of the finger point (cm); $OBPR_1$ - the forearm circumference in the upper third (cm); EPPR - the width of the distal epiphysis of the forearm (cm); EPG - width of the distal epiphysis of the shin (cm); $OBPR_2$ - the forearm's girth in the lower third (cm).

RE_L_DL (*the length of the left kidney in the longitudinal section, mm*) = 117.5 + 1.484 x ACR + 20.70 x EPPL - 10.66 x $OBPR_2$ - 10.23 x LX - 3.364 x GGR + 0.974 x CRIS (R^2=0.953; $F_{(6.10)}$=33.51; p<0.001; St. Error of estimate = 2.640),

where (here and thereafter), EPPL - the width of the distal epiphysis of the shoulder (cm); LX - ectomorphic component of somatotype for Heath-Carter (score); GGR - thickness of skin and fat folds on the chest (mm); CRIS - interspinous pelvis size (cm).

RE_R_PO (*width of the right kidney in the longitudinal section, mm*) = 111.4 - 4.885 x $OBPR_2$ + 0.843 x OBT - 0.821 x ATP + 3.707 x EPPL - 0.619 x SAG_DUG + 0.226 x GB (R^2=0.961; $F_{(6.10)}$=40.82; p<0.001; St. Error of estimate=0.978),

where (here and in the future), OBT - waist circumference (cm); SAG_DUG - sagittal arch of the head (cm);

RE_L_PO (*width of the left kidney in the longitudinal section, mm*) = 163.8 - 6.903 x $OBPR_2$ + 3.116 x GPR - 2.387 x GGR - 4.649 x LX + 1.685 x OBK - 0.995 x $OBPL_2$ (R^2=0.891; $F_{(6.10)}$=13.60; p<0.001; St. Error of estimate=2.205),

where (here and thereafter), GPR - thickness of skin and fat folds on the forearm (mm); OBK - hands brush circumference (cm); $OBPL_2$ - shoulder girth in a calm condition (cm);

RE_R_TO (*anterior-posterior size of the right kidney on a cross-section, mm*) = 61.13 + 2.221 x ATL - 3.017 x OBG_2 - 2.673 x B_SH_GL - 6.882 x LX - 2.126 x SGK - 0.478 x GB - 0.644 x OBB (R^2=0.969; $F_{(7.9)}$=40.47; p<0.001; St. Error of estimate=1.255),

where (here and in the future), ATL - height of the pubic point (cm); OBG_2 - girth of the shin in the lower third (cm); B_SH_GL - maximum head width (cm); SGK - anterior-posterior size of the chest (cm); GB - thickness of skin-fat fold on the side (mm); OBB - hip circumference (cm);

RE_L_TO (*anterior-posterior size of the left kidney on the cross-section, mm*) = 60.79 - 3.693 x $OBPR_2$ + 0.954 x ATL - 0.496 x GB + 0.442 x GPR - 0.881 x OBG_1 + 0.458 x GL - 0.544 x B_DL_GL (R^2=0.957; $F_{(7.9)}$=28.49; p<0.001; St. Error of estimate=1.008),

where (here and thereafter), OBG_1 - girth of the shin in the upper third (cm); GL - thickness of skin and fat folds under the shoulder blade (mm); B_DL_GL - the largest length of the head (cm);

RE_R1SRE (*area of the longitudinal section of the right kidney, cm²*) = -115.9 + 4.521 x $OBPL_2$ - 1.195 x ATP - 1.646 x MM + 3.460 x OB_GL - 6.465 x EPPL - 0.695 x B_DL_GL + 2.284 x EPG (R^2=0.972; $F_{(7.9)}$=45.31; p<0.001; St. Error of estimate=0.861),

where (here and thereafter), MM - muscle component of the body mass, by Matiegka (kg); OB_GL - head girth (cm);

RE_R2SRE (*square cross-section of the right kidney, cm²*) = 7.650 - 0.734 x ACR + 0.599 x PSG - 4.236 x $OBPR_2$ + 0.403 x OBT + 1.727 x OBK + 0.335 x ATV (R^2=0.926; $F_{(6.10)}$=20.82; p<0.001; St. Error of estimate=1.273),

where (here and thereafter), PSG - transverse middle-thoracic size (cm); ATV - height of the trochanteric point (cm);

RE_L1SRE (*area of the longitudinal section of the left kidney, cm²*) = 135.1 + 2.595 x GPPL - 6.421 x LX - 6.239 x $OBPR_2$ - 3.284 x GGR + 3.672 x OM - 1.315 x ACR + 0.820 x OBB (R^2=0.942; $F_{(7.9)}$=20.85; p<0.001; St. Error of estimate=1.867),

where (here and thereafter), GPPL - the thickness of the skin-fat fold on the front surface of the shoulder (mm); OM - bone component of body weight by Matiegka (kg);

RE_L2SRE (*square cross-section of the left kidney, cm²*) = -18.93 + 0.358 x ATL - 2.898 x $OBPR_2$ + 1.332 x OBK - 0.281 x $OBGK_2$ + 0.930 x SH_LICA + 0.667 x OB_GL (R^2=0.938; $F_{(6.10)}$=25.11; p<0.001; St. Error of estimate=0.727),

where (here and in the future), $OBGK_2$ - the girth of the chest on the exhalation (cm); SH_LICA - face width (cm);

RE_R1SSI (*area of the longitudinal section of the sinus of the right kidney, cm²*) = 11.95 - 3.243 x $OBPR_2$ + 5.816 x EPPL + 0.307 x OBT - 0.352 x OBG_1 + 0.334 x ACR - 1.101 x FX (R^2=0.895; $F_{(6.10)}$=14.14; p<0.001; St. Error of estimate=0.919),

where (here and in the future), FX is the endomorphic component of the somatotype by Heath-Carter (score);

RE_R2SSI (*square cross section of the sinus of the right kidney, cm²*) = 987.6 - 55.04 x CRIS + 76.44 x PSG - 33.31 x PNG + 28.05 x OBK - 28.21 x SGK - 72.22 x LX (R^2=0.918; $F_{(6.10)}$=18.74; p<0.001; St. Error of estimate=48.31),

where (here and thereafter), PNG - transverse lower-thoracic size (cm);

RE_L1SSI (*area of longitudinal section of the sinus of the left kidney, cm²*) = 0.366 + 4.079 x OM + 0.667 x B_SH_GL - 1.248 x $OBPR_2$ - 2.225 x SH_LICA + 0.221 x GG + 1.537 x SH_N_CH (R^2=0.961; $F_{(6.10)}$=40.53; p<0.001; St. Error of estimate=0.684),

where (here and thereafter), GG - thickness of skin and fat folds on the abdomen (mm); SH_N_CH - width of the lower jaw (cm);

RE_L2SSI (*square cross-section of the sinus of the left kidney, cm²*) = -4003 + 69.22 x ATPL - 99.40 x $OBPR_2$ + 18.02 x OBS + 201.6 x EPPL - 45.20 x $OBPL_1$ - 34.52 x ATL - 17.54 x OBB (R^2=0.978; $F_{(7.9)}$=56.39; p<0.001; St. Error of estimate=18.46),

where (here and in the future), ATPL - height of the shoulder point (cm); OBS - foot girth (cm);

RE_R_VRE (*volume of the right kidney, cm³*) = -304.3 - 16.98 x $OBPR_2$ + 9.919 x GPPL + 14.78 x OB_GL - 27.17 x OM - 6.252 x N_SH_GL + 1.191 x $OBGK_1$ (R^2=0.966; $F_{(6.10)}$=47.55; p<0.001; St. Error of estimate=5.548),

where (here and in the future), N_SH_GL - the smallest width of the head (cm); $OBGK_1$ - girth of the chest on the inspiration (cm);

RE_L_VRE (*volume of the left kidney, cm³*) = -53.17 - 32.56 x $OBPR_2$ + 4.207 x OBBB + 3.148 x ATV + 5.879 x OBS - 7.411 x SH_LICA + 7.072 x SGK - 4.605 x OBSH (R^2=0.934; $F_{(7.9)}$=18.19; p<0.001; St. Error of estimate=8.429).

where, OBBB - hips girth (cm); OBSH - neck circumference (cm).

Discussion

The problems associated with an adequate description of the dimensional characteristics of the kidneys in individuals with different somatotypes are still open for research. Let's start from the fact that the values of the model parameters should be determined as basal, that is, they correspond to the normal state of a healthy organism. The "weak place" of these models may also be that the calculation of the sizes in most works is based on the introduction of a small number of constitutional parameters (height, weight and surface area of the body) into a model based on averaged anthropometric measurements without taking into account the ethnic and age factors [1, 5, 21, 23].

In practically healthy women of the middle intermediate somatotype all 16 possible reliable regression models of sonographic parameters of the right and left kidneys, based on the anthropometric and somatotypological parameters with determination coefficient R^2 from 0.891 to 0.978 (for right kidney R^2 from 0.895 to 0.976, for left kidney R^2 from 0.891 to 0.978) were constructed.

The constructed regression models of sonographic parameters of both kidneys in practically healthy women of the middle intermediate somatotype most often include the circumferential dimensions of the body (35.9% of the total number of indicators included in the models), cephalometric indices (12.6%), thickness of skin and fat folds and body diameters (by 11.7%). Among the individual anthropometric and somatotypological indicators, models most often include the forearm circumcision in the lower third (up to 13 models), the width of the distal epiphysis, the shoulder width and the ectomorphic component of the somatotype (up to 5 models), the height of the pubic point and the hands brush circumference (up to 4 models).

The regression models of sonographic parameters of the right kidney in women of the middle intermediate somatotype most often include the circumferential dimensions of the body (33.3% of the total number of indices included in the right kidney models), body diameters (15.7%), and cephalometric indices and width of distal epiphyses of long tubular limb bones (by 11.8%). Among the individual anthropo-somatotypological parameters of the body models of the right kidney most often include the forearm girth in the lower third (up to 5 models), the height of the finger point, the width of the distal epiphysis of the shoulder, the waist circumference and the shoulder width (up to 3 models).

The regression models of the sonographic parameters of the left kidney in women of the middle intermediate somatotype most often include the circumferential dimensions of the body (38.5% of the total number of indicators included in the models of the left kidney), the thickness of skin and fat folds (17.3%) and cephalometric indices (13.5%). Among the individual anthropo-somatotypological parameters of the body models of the left kidney most often include the circumference of the forearm in the lower third (up to 8 models), the width of the face, the height of the pubic point, the thickness of the skin-fat fold on the chest and the magnitude of the ectomorphic component of the somatotype, according to Heath-Carter (up to 3 models).

Attention is drawn to the lack of entry into models of sonographic sizes of the kidneys in women of the middle intermediate somatotype of total body sizes.

In previous studies [4, 27, 28] we determined that from 16 possible sonographic parameters of the kidneys, based on the anthropometric and somatotypological indices in practically healthy women of the mesomorphic somatotype, 7 reliable models with a determination coefficient from 0.607 to 0.641 were constructed; in women of ectomorphic somatotype - all 16 models with a determination coefficient from 0.607 to 0.973; in women endo-mesomorphic somatotype - 14 models with a determination coefficient from 0.672 to 0.912. The most frequently constructed models included: women with mesomorphic somatotype - circumferential body dimensions (29.8%) and cephalometric indexes (19.1%); in women with ectomorphic somatotype body diameters (24.2%), body girth sizes (20.9%), cephalometric indices (19.8%) and thickness of skin and fat folds (14.3%); in women of the endo-mesomorphic somatotype, the cephalometric indexes (to the right kidney 24.2%, to the left kidney 15.6%), body diameters (to the right kidney 24.2%, to the left kidney 17.8%) and the circumferential body size (to the right kidney 24.2%, to left kidney 22.2%), and also only to the left kidney thickness of skin and fat folds (17.8%).

The construction of the regression equations of the kidneys sizes according to the constitutional parameters of a healthy organism becomes rapid and is considered to be an exceptional tool for the study of biomedical problems.

Conclusions

1. In practically healthy women of the middle intermediate somatotype of 16 possible sonographic parameters of the

right and left kidneys, depending on the anthropometric and somatotypological parameters, all 16 valid models with a determination coefficient from 0.895 to 0.976 and from 0.891 to 0.978, respectively, were constructed.

2. Constructed models in women of the middle intermediate somatotype most often include: for the right kidney - the circumferential body dimensions (33.3%), body diameters (15.7%), cephalometric indices and width of distal epiphyses of long tubular bones of the extremities (by 11.8%); for the left kidney - the circumferential dimensions of the body (38.5%), the thickness of skin and fat folds (17.3%) and cephalometric indices (13.5%).

References

[1] Arooj, A., Lam, J., Wui, Y. J., & Supriyanto, E. (2011). Comparison of Renal Size among Different Ethnicities. *International Journal of Biology and Biomedical Engineering,* 5(4), 221-229.

[2] Bakker, H., Kooijman, M. N., van der Heijden, A. J., Hofman, A., Franco, O. H., Taal, H. R., & Jaddoe, V. W. (2014). Kidney size and function in a multi-ethnic population-based cohort of school-age children. *Pediatr. Nephrol.,* 29(9), 1589-1598. doi: 10.1007/s00467-014-2793-8

[3] Carter, J. L., & Heath, B. H. (1990). *Somatotyping - development and applications.* Cambridge University Press.

[4] Cherkasov, V. G., & Ustymenko, O. S. (2017). Modeling using regression analysis of sonographic parameters of kidneys depending on the features of the size of practical healthy women with mesomorphic somatotype. *World of Medicine and Biology,* 3(61), 73-76. doi: 10.26724/2079-8334-2017-3-61-73-76

[5] Correas, J.-M., Anglicheau, D., Joly, D., Gennisson, J.-L., Tanter, M., & Helenon, O. (2016). Ultrasound-based imaging methods of the kidney-recent developments. *Official J. of Int. Society of Nephrology,* 90(6), 1199-1210. doi: 10.1016/j.kint.2016.06.042

[6] Draper, N., & Smith, G. (2016). *Applied Regression Analysis.* M.: Williams.

[7] El-Reshaid, W., & Abdul-Fattah, H. (2014). Sonographic assessment of renal size in healthy adults. *Med. Princ. Pract.*, 23(5), 432-436. doi: 10.1159/000364876

[8] Gunas I. V., Kovalenko, D. A., Fomina, L. V., Belik, N. V., & Fedonyuk, L. Ya. (2010). Modeling, using regression analysis, sonographic parameters of the kidneys, depending on the anthropometric and somatotypological parameters of men and women of the first mature age. *Reports of Morphology,* 16(4), 915-920.

[9] Harmse, W. S. (2011). Normal variance in renal size in relation to body habitus. *South African Journal of Radiology,* 15(4), 123-126. https//doi.org/10.4102/sajr.v15i4.355

[10] Hyun, Y. Y., Lee, K. B., Rhee, E. J., Park, C. Y., Chang, Y., & Ryu, S. (2016). Chronic kidney disease and high eGFR according to body composition phenotype in adults with normal BMI. *Nutr. Metab. Cardiovasc.,* 26(12), 1088-1095. doi: 10.1016/j.numecd.2016.09.003

[11] Jaroszynski, A., Dereziński, T., Jaroszyńska, A., Zapolski, T., Wasikowska, B., Wysokiński, A., … Horoch, A. (2016). Association of anthropometric measures of obesity and chronic kidney disease in elderly women. A*nn. Agric. Environ. Med.*, 23(4), 636-640. doi: 10.5604/12321966.1226859

[12] Jovanović, D., Gasic, B., Pavlovic, S., & Naumovic, R. (2013). Correlation of kidney size with kidney function and anthropometric parameters in healthy subjects and patients with chronic kidney diseases. *Ren. Fail.*, 35(6), 896-900. doi: 10.3109/0886022X.2013.794683

[13] Kolchanova, N. A., Goncharova, S. S., Lihovshaya, V. A., & Ivanisenko, V. A. (2008). *System Computer Biology.* Novosibirsk: Publishing SO RAS.

[14] Maaji, S. M., Daniel, O., & Adamu, B. (2015). Sonographic measurement of renal dimensions of adults in North western Nigeria: a preliminary report. *Sub-Saharan African journal of medicine,* 2(3), 123-127. doi: 10.4103/2384-5147.164420

[15] Matiegka, J. (1921). The testing of physical effeciecy. *Amer. J. Phys. Antropol.*, 2(3), 25-38. https://doi.org/10.1002/ajpa.1330040302

[16] Mitkov, V. V. (2006). A *practical guide to ultrasound diagnostics. General ultrasound diagnosis.* M.: Vidar.

[17] Niyyar, V. D., & O'Neill W. C. (2018). Point-of-care ultrasound in the practice of nephrology. *Kidney Int.*, 93(5), 1052-1059. doi: 10.1016/j.kint.2017.11.032

[18] Okur, A., Serin, H. I., Zengin, K., Erkoc, M. F., Tanik, S., Yildirim, U., … Akyol, L. (2014). Relationship between kidney volume and body indexes in the Turkish population determined using ultrasonography. *Int. Braz. J. Urol.*, 40(6), 816-822. doi: 10.1590/S1677-5538.IBJU.2014.06.13

[19] Oparin, O. A., Lavrova, N. V., Blahoveshchenska, A. V., & Korenovskuy, I. P. (2010). *Clinical and ultrasound parallel diagnostics of diseases of internal organs. Tutorial. Recommended by the Ministry of Education and Science of Ukraine.* Kharkiv: Fact.

[20] Petrov, V. I., & Nedogoda, S. V. (2009). *Evidence-based medicine: study guide.* M.: "GOETAR-MED".

[21] Quaia, E., Nocentini, A., & Torelli, L. (2009). Assessment of a new mathematical model for the computation of numerical parameters related to renal cortical blood flow and fractional blood volume by contrast-enhanced ultrasound. *Ultrasound Med. Biol.,* 35(4), 616-627. doi: 10.1016/j.ultrasmedbio.2008.10.003

[22] Raza, M., Hameed, A., & Khan, M. I. (2011). Ultrasonographic assessment of renal size and its correlation with body mass index in adults without known renal disease. *J. Ayub. Med. Coll. Abbottabad.*, 23(3), 64-68.

[23] Saeed, Z., Mirza, W, Sayani, R., Sheikh, A., Yazdani, I., & Hussain, S. A. (2012). Sonographic Measurement of Renal Dimensions in Adults and its Correlates. *International Journal of Collaborative Research on Internal Medicine & Public Health,* 4(9), 1626-1641.

[24] Salsberg, E., Quigley, L., Masselink, L., Wu, X., & Collins, A. (2015). The US Nephrology Workforce 2015: Developments and Trends. Washington, American Society of Nephrology.

[25] Shaparenko, P. P. (2000). *Anthropometry.* Vinnytsya: [w. p.].

[26] Shephard, R. J. (1991). *Body composition in biological anthropology*. Cambridge.

[27] Ustymenko, O. S. (2018). Regression models of sonographic parameters of the kidneys in practically healthy women of the ectomorphic somatotype depending on the peculiarities of body size. *Biomedical and Biosocial Anthropology,* 31, 53-58. doi: 10.31393/bba31-2018-07

[28] Ustymenko, O. S. (2018). Sonographic model parameters of kidney in men and women endo-mesomorphic somatotype depending on the anthropometric indices characteristics. *Biomedical and Biosocial Anthropology,* 30, 43-49. doi: 10.31393/bba30-2018-06

[29] Voropaeva, O. F., & Shokin, Yu. I. (2012). Numerical simulation in medicine: Some problem statements and calculation results. Computational Technologies, 17(4), 29-55.

МОДЕЛЮВАННЯ СОНОГРАФІЧНИХ ПАРАМЕТРІВ НИРОК У ПРАКТИЧНО ЗДОРОВИХ ЖІНОК СЕРЕДНЬОГО ПРОМІЖНОГО СОМАТОТИПУ В ЗАЛЕЖНОСТІ ВІД КОНСТИТУЦІОНАЛЬНИХ ПАРАМЕТРІВ ТІЛА

Черкасов В. Г., Устименко О. С., Шаюк А. В., Прокопенко С. В., Гунас І. В.

В науковій літературі представлено досить велике число робіт, в яких визначається пріоритетна роль математичного моделювання в забезпеченні високоефективного медичного обслуговування, здоров'я та активного довголіття людини. Мета роботи - у практично здорових жінок середнього проміжного соматотипу побудувати та провести аналіз регресійних моделей індивідуальних сонографічних розмірів нирок в залежності від особливостей антропометричних і соматотипологічних показників. У рамках договору про наукове співробітництво із бази даних Вінницького національного медичного університету ім. М.І. Пирогова взяті первинні сонографічні параметри (довжина, ширина, передньо-задній розмір, площа поздовжнього та поперечного перерізу нирок та їх синусів, а також об'єм правої і лівої нирок) і антропометричні показники (отримані за методикою В.В. Бунака у модифікації П.П. Шапаренка) 17 практично здорових жінок першого зрілого віку середнього проміжного соматотипу, які у третьому поколінні проживають на території Подільського регіону України. Побудова регресійних моделей індивідуальних сонографічних розмірів нирок в залежності від особливостей антропо-соматотипологічних параметрів тіла жінок середнього проміжного соматотипу проведена в ліцензійному пакеті "Statistica 6.1". У жінок середнього проміжного соматотипу побудовані усі 16 можливих достовірних регресійних моделей сонографічних параметрів нирок в залежності від антропо-соматотипологічних показників із коефіцієнтом детермінації R^2 від 0,891 до 0,978. При аналізі достовірних регресійних моделей (з коефіцієнтом детермінації більшим 0,6) сонографічних параметрів нирок у практично здорових жінок середнього проміжного соматотипу встановлено, що найчастіше до моделей обох нирок, а також окремо правої і лівої нирок, входять обхватні розміри тіла (відповідно 35,9 - 33,3 - 38,5% від загальної кількості показників, що входять до моделей). Крім того, до моделей обох нирок найчастіше входять кефалометричні показники (12,6%), товщина шкірно-жирових складок і діаметри тіла (по 11,7%); до моделей правої нирки - діаметри тіла (15,7%) та кефалометричні показники й ширина дистальних епіфізів довгих трубчастих кісток кінцівок (по 11,8%); до моделей правої нирки - товщина шкірно-жирових складок (17,3%) та кефалометричні показники (13,5%). Привертає увагу відсутність входження до моделей сонографічних розмірів нирок тотальних розмірів тіла.

Ключові слова: *регресійний аналіз, сонографічні параметри нирок, показники будови та розмірів тіла, практично здорові жінки, середній проміжний соматотип.*

МОДЕЛИРОВАНИЕ СОНОГРАФИЧЕСКИХ ПАРАМЕТРОВ ПОЧЕК У ПРАКТИЧЕСКИ ЗДОРОВЫХ ЖЕНЩИН СРЕДНЕГО ПРОМЕЖУТОЧНОГО СОМАТОТИПА В ЗАВИСИМОСТИ ОТ КОНСТИТУЦИОНАЛЬНЫХ ПАРАМЕТРОВ ТЕЛА

Черкасов В. Г., Устименко Е. С., Шаюк А. В., Прокопенко С. В., Гунас И. В.

В научной литературе представлено достаточно большое число работ, в которых определяется приоритетная роль математического моделирования в обеспечении высокоэффективного медицинского обслуживания, здоровья и активного долголетия человека. Цель работы - у практически здоровых женщин среднего промежуточного соматотипа построить и провести анализ регрессионных моделей индивидуальных сонографических размеров почек в зависимости от особенностей антропометрических и соматотипологических показателей. В рамках договора о научном сотрудничестве из базы данных Винницкого национального медицинского университета им. Н.И. Пирогова взяты первичные сонографические параметры (длина, ширина, передне-задний размер, площадь продольного и поперечного сечения почек и их синусов, а также объем правой и левой почек) и антропометрические показатели (получены по методике В.В. Бунака в модификации П.Ф. Шапаренко) 17 практически здоровых женщин первого зрелого возраста среднего промежуточного соматотипа, которые в третьем поколении проживают на территории Подольского региона Украины. Построение регрессионных моделей индивидуальных сонографических размеров почек в зависимости от особенностей антропо-соматотипологических параметров тела женщин среднего промежуточного соматотипа проведено в лицензионном пакете "Statistica 6.1". У женщин среднего промежуточного соматотипа построены все 16 возможных достоверных регрессионных моделей сонографических параметров почек в зависимости от антропо-соматотипологических показателей с коэффициентом детерминации R^2 от 0,891 до 0,978. При анализе достоверных регрессионных моделей (с коэффициентом детерминации большим 0,6) сонографических параметров почек у практически здоровых женщин среднего промежуточного соматотипа установлено, что чаще всего к моделям обеих почек, а также отдельно правой и левой почек, входят обхватные размеры тела (соответственно 35,9 - 33,3 - 38,5% от общего количества показателей, входящих в модели). Кроме того, в модели обеих почек чаще всего входят кефалометрические показатели (12,6%), толщина кожно-жировых складок и диаметры тела (по 11,7%); в модели правой почки - диаметры тела (15,7%), кефалометрические показатели и ширина дистальных эпифизов длинных трубчатых костей конечностей (по 11,8%); в модели правой почки - толщина кожно-жировых складок (17,3%) и кефалометрические показатели (13,5%). Привлекает внимание отсутствие вхождения в модели сонографических размеров почек тотальных размеров тела.

Ключевые слова: *регрессионный анализ, сонографические параметры почек, показатели строения и размеров тела, практически здоровые женщины, средний промежуточный соматотип.*

DOI: 10.31393/morphology-journal-2018-24(3)-02 Reports of Morphology, Vol. 24, №3, Pages 11-18

ISSN 1818-1295 eISSN 2616-6194

REPORTS OF MORPHOLOGY

Official Journal of the Scientific Society of Anatomists, Histologists, Embryologists and Topographic Anatomists of Ukraine

journal homepage: https://morphology-journal.com

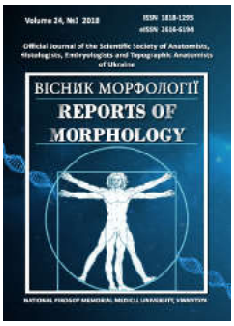

The role of the CagA gene in the occurrence of the inflammatory response of the gastric mucosa in patients with chronic Helicobacter pylori-associated gastritis

Vernigorodskiy S.V., Sukhan D.S.
National Pirogov Memorial Medical University, Vinnytsya, Ukraine

ARTICLE INFO
Received: 03 July, 2018
Accepted: 06 August, 2018

UDC: 616.33-002.2:579.835:575.113

CORRESPONDING AUTHOR
e-mail: vernset@ukr.net
Vernygorodskyi S.V.

Currently, Helicobacter pylori infection (H. pylori) is recognized as one of the most important risk factors for gastrocarcinogenesis. It is known that this infection does not directly cause neoplastic changes in the gastric mucosa, and this is due to a number of consecutive events due to the long persistence of the pathogen in the human body. The initial stage of this cascade, of course, is the inflammatory response, due to the body's ability to adapt to extraneous infection, which is the inevitable result of the interaction of H. pylori with cells of the gastric epithelium. This direct damaging effect is enhanced by the production of vacuolating cytotoxin and the release of products of the cytotoxin-associated CagA gene, which, at a pathomorphological level, is manifested by inflammatory infiltration of the gastric mucosa (GM) to some extent. On the relationship between the degree of contamination and the activity of the inflammation of the GM in people infected with the CagA strain, today there are different, often conflicting opinions, which is why in this work we set the goal of establishing the relationship between the nature of the inflammatory response and the presence of the CagA gene in H. pylori- infected patients. The purpose of the study is to determinate the relationship between the nature of the inflammatory response and the genetic features of the H. pylori strain (CagA genotype).We examined 365 patients, among whom 40 people were included in the control group (18 women and 22 men, whose average age was 45,33±15,46 and 42,82±12,31, respectively) without any gastroenterological pathology in the anamnesis , patients with chronic non-atrophic gastritis (188 people) and chronic atrophic gastritis (137 people). A close relationship was established between the presence of the CagA gene, activity and the degree of contamination for chronic non-atrophic gastritis (CNG): for a low degree of contamination, Fisher's exact test was = 0.002, $p<0.05$, for a moderate degree - 0.012, $p<0.05$, for a high degree - 0,012, $p<0.05$. Accordingly, in chronic atrophic gastritis (CAG): for a low degree of contamination Fisher's exact test = 0.011, $p<0.05$, for a moderate degree - 0.003, $p<0.05$, for a high degree - 0.001, $p<0.05$. There is also a close relationship between the degree of contamination and the activity of chronic gastritis (CG): in patients with a high degree of contamination, CG activity was determined, as a rule, for stage 2-3. In our study, the inflammatory response depended on the presence or absence of the H. pylori strain in the patient, which contains the CagA genotype, which, in our opinion, plays a key role in triggering a cascade of inflammatory changes in the GM and progression of chronic gastritis.

Keywords: *Helicobacter pylori, CagA, chronic gastritis, morphological changes.*

Introduction

The correlation of chronic inflammation with gastric cancer was established in 1863 by the famous German pathologist R. Virchow [27]. The discovery of Helicobacter pylori has revolutionized previous perceptions of the nature of gastroduodenal pathology and noted this unique infectious agent as a specific cause of CG, peptic ulcers and stomach cancer. The International Kyoto Consensus first proposed an etiological classification of gastritis and recommended that H. pylori-induced CG should be considered as an infectious disease requiring treatment

not so much to alleviate symptoms as to prevent complications such as peptic ulcer and gastric cancer [7, 32, 36]. The property of H. pylori to induce the development of inflammatory, dysplastic, metastatic and neoplastic changes depends on factors related to the microorganism itself, the organism of the host and the environment. The main pathogenicity genes include: CagA (cytotoxin-associated gene A); VacA (vacuolating cytotoxin); IceA (induced by contact with epithelium); BabA (blood group antigen-binding adhesin). H. pylori genes in the so-called "pathogenicity island" cag (cagA pathogenicity island, cag PAI) due to the activation of NF-kB (nucleic factor kappa-B) are involved in the development of an inflammatory response by initiating a cascade of signal transduction, leading to interleukin IL-8 production. As a result, proinflammatory cytokines and cellular (Th-1-mediated) immune response lead to further progression of inflammatory response [4, 17, 18, 28, 22].

The high frequency of peptic ulcer disease and the onset of MALT-lymph in Europe is due to the presence of CagA. CagA strains of H. pylori are also associated with pronounced epithelial cell proliferation and GM metaplasia [6]. In western countries, there have also been reports that individuals infected with CagA-positive strains are more likely to develop stomach ulcer and cancers than those infected with H. pylori CagA-negative strains. However, there was no such dependence on the inhabitants of East Asia [40]. Most authors argue that there is a close correlation [9, 10, 11, 14, 24, 26], others believe that CagA-positive / negative strains of H.pylori are not related to the development of severe gastroduodenal pathology and do not find any significant differences in the activity of inflammation and colonization in different types of H. pylori infection [4, 13, 19].

That is why the *purpose* of our study was to establish the relationship between the nature of the inflammatory response and the genetic features of the H. pylori strain (presence of CagA genotype).

Materials and methods

The study group consisted of 325 people with CG diagnosis: 111 women (mean age 49.85±13.41) and 214 men (mean age 48.81±13.61). The control group included 40 persons (18 female and 22 male, mean age 45.33±15.46 and 42.82±12.31, respectively) without gastrointestinal pathology in history (Table 1). Among patients with CG, the following groups were isolated: chronic non-atrophic gastritis (188 persons) and chronic atrophic gastritis (137 people). In the survey, the ethical principles of the Helsinki Declaration of the World Medical Association (World Medical Association Declaration Helsinki, 1964) were followed. All patients were informed and signed informed consent, confirming their voluntary participation in the study.

In the course of fibroesophagogastroduodenoscopy, multiple biopsies were performed - 2 biopsies from the body and antrum of the stomach and 1 from the angle of the stomach. Pathologist examination of biopsies for the diagnosis was performed in accordance with the requirements of the morphological section of the modified Sydney-Houston system [5, 23]. Determination of the persistence of H. pylori in GM was performed using urease test [20], cytologically by Pappenheimer [21] and histologically - colored by Giemsa and toluidine blue by B. Slater [31]. The genotyping of helicobacter infection was performed using a polymerase chain reaction. For further comparative analysis with the results of genotyping H. pylori we used own data obtained from the inspection of 40 practically healthy persons, among which 17 were infected with H. pylori. To determine the degree of dysplasia, the criteria proposed by WHO experts [3], and developed on the basis of the Vienna classification of neoplasia of the gastrointestinal epithelium [30] were used. In the presence of H. pylori infection, all cases of observations were divided into two groups: H. pylori-positive and H. pylori-negative.

Table 1. Distribution of patients according to nosology depending on age.

Age (years) / Nosology	up to 25 (m/f)	26-44 (m/f)	45-59 (m/f)	60 and >(m/f)
Normal GM	4 (2/2)	19 (11/8)	11 (7/4)	6 (2/4)
CNG without dysplasia	10 (7/3)	27 (18/9)	14 (9/5)	5 (3/2)
CNG with dysplasia: Mild Severe	4 (3/1) 3 (2/1) 1 (1/0)	42 (29/13) 29 (20/9) 13 (9/4)	56 (36/20) 33 (21/12) 23 (15/8)	30 (20/10) 17 (11/6) 13 (9/4)
CAG without dysplasia	-	8(5/3)	10(6/4)	22 (14/8)
CAG with dysplasia: Mild Severe	2 (1/1) 2 (1/1) -	19 (14/5) 15 (12/3) 4 (2/2)	43 (28/15) 31 (19/12) 12 (9/3)	33 (21/12) 19 (13/6) 14 (8/6)
Total	**20 (13/7)**	**115 (77/38)**	**134 (86/48)**	**96 (60/36)**

Statistical processing was performed using Microsoft Office Excel 2007 and "Statistica 5.0". Calculated the average arithmetic value M, its error m. The reliability of the difference between the average values was estimated by the Students criterion, the difference was considered to be valid at $p<0.05$. In order to check the statistical hypotheses of absolute and relative frequencies in independent samples, the chi square (χ^2) criterion was used, with the frequency of the investigated event less than 5 observations for the analysis of frequency differences in the two independent groups used Fisher's exact criterion, the confidence intervals given in the work, were constructed for confidence probability p=95%. In all statistical analysis procedures, the achieved level of significance (p) was calculated, with the critical level of significance taken equal to 0.05.

Results

In the control group, both in H. pylori-negative patients (-) and in H. pylori-positive (+), GM maintained its histoarchitectonics, regardless of the presence of CagA +.

The cytological smear is usually clean. In the two H. pylori (+) individuals, focal degenerative changes in the pyloric glands were established. At the same time, according to anamnesis, they also had signs of dyspepsia. In histological analysis, GM in practically healthy individuals consisted of a subepithelial layer which width was determined by the depth of the pits and glands, the ratio of which was approximately 1:3. Gastric pits were located close to each other. Surface epithelium cells, as a rule, had a highly prism form and a clear polar differentiation.

At morphological analysis of GM of patients with CNG CagA negative (CagA-) helicobacter infection without dysplasia it was established that in the group of inactive CNG surface and pit epithelium cells, exocrinocytes of fundal and pyloric glands in histological sections and smears-imprints retained their structure, were located predominantly in layers and groups, looked monomorphic, the nuclei were pushed to the periphery of cells, round-oval, their contour was equal. Chromatin homogeneous coarse-grained, intensely colored. The cytoplasm is weakly basophilic. Exocrinocytes of the glandular epithelium of the antral department of GM were located in groups and palisade-like structures, had larger sizes in comparison with superficial ones. The nuclei in them were located eccentrically, more oval, some of them containing single small correct form of the nucleolus.

In 15 (55.56%) patients with acute H. pylori (CagA-) CNG without dysplasia and 8 with mild dysplasia (29.63%) epithelial cells had a similar look, but dystrophic changes were accompanied by the appearance of dysregeneration in the form of hyperchromatosis, a violation of the location of nuclei and a nuclear-cytoplasmic ratio, as well as a basophilia of the cytoplasm of individual epithelial cells, more often present a few neutrophils and lymphocytes that were mainly infiltrated in GM lamina propria with its slight perivascular edema (Fig. 1), indicating weak activity and corresponded to the first stage according to L.Y. Aruina et al. (1998) [1].

The division of gastritis in the stage of activity was determined by the degree of neutrophilic infiltration of GM lamina propria. At the first stage of activity there was a slight leukocyte infiltration of GM lamina propria, while in the second occurred infiltration of the surface and pit epithelium with enhanced leukodiapedesis and the inflow of inflammatory cells to the lumen of the stomach. In the third stage, along with the pronounced infiltration of GM lamina propria and the epithelial layer, there were so-called "intra-pit abscesses", similar to "crypt-abscesses" in inflammatory diseases of the colon [1, 2, 16]. Their formation was through massive leukodiapedesis through the thickness of the epithelium to the lumen of the pits, and also accompanied by a powerful destruction of the epithelial layer.

At moderate and high levels of contamination, which corresponded to the 2nd and 3rd stages of CNG activity, both in CagA- and CagA+ H. pylori-infected patients, the above features increased significantly. At the same time,

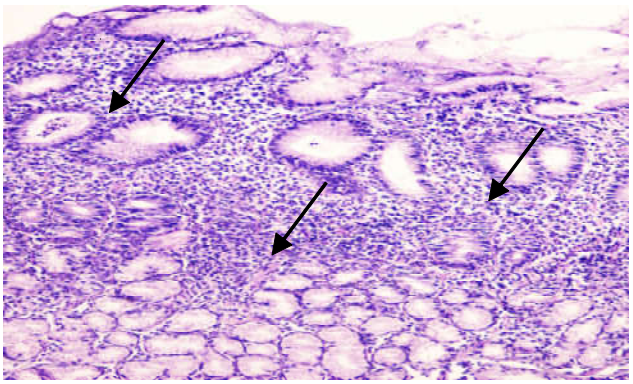

Fig. 1. Lymphoplasmacytic infiltration of the mucous membrane lamina propria with admixture of segmental neutrophils and dystrophic changes of surface and pit epithelium. Chronic non-atrophic active (stage 1) gastritis without dysplasia. CagA-. The arrows show the areas of lymphoplasmacytic infiltration of the mucous membrane lamina propria. Hematoxylin-eosin. x100.

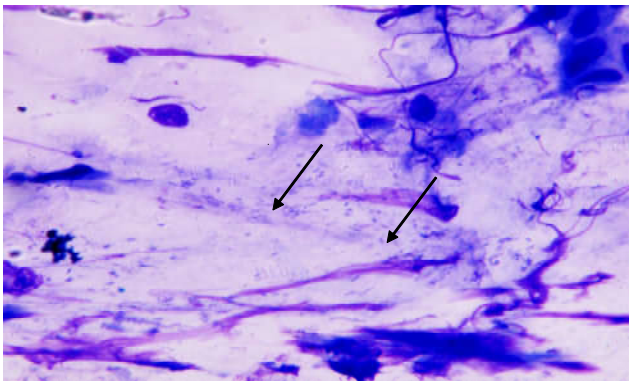

Fig. 2. Moderate degree of contamination of GM, more than 20 H. pylori bacteria in the field of vision (x1000) in a patient with CNG (CagA+). The arrows show the areas of the H. pylori conglomeration. Bacterioscopy by Pappenheimer. x1000.

among and intraepithelial localization of microorganisms in comparison with the low degree of contamination and the first stage of activity prevailed in the cytoplasm of the superficial and pit epithelium with a high degree of contamination and 3 stages of activity in 76% of H. pylori CagA+ patients.

At the same time, in patients with CNG with CagA-negative (CagA-) among and intraepithelial localization of microorganisms was observed in 10% of patients with high degree of contamination and 3 stages of activity compared with low and 1 stage. However, in patients with CAG CagA+, among and intraepithelial localization of microorganisms was observed only in 35% of cases with a high degree of contamination and 3 stages of activity, and CagA- in 5%. With a low degree of contamination and 1 stage of activity in both groups of CG H. pylori was determined predominantly in the adjacent to the surface epithelium mucus.

For CNG (CagA+) with moderate and high contamination in smears-imprints, an increase in the number of layer and groups of epithelial cells, as well as in the glandular structures, was likely to be attributed to the weakening of

intercellular connections (associated with both the activity of inflammation - leukopedesis and with the persistence of helicobacter infection) and easier getting into the imprint (Fig. 2).

Part of the epithelial structures was characterized by signs of dystrophy, manifested by the flattening of cellular forms, vacuolation of the cytoplasm, weakening of the contours of the membranes, loosening of the chromatin structure. The cells of the glandular epithelium were also represented in a greater number, among them observed moderate polymorphism. Along with the epithelial cells producing mucus, the presence of groups and glandular structures of proliferating cells with basophilic cytoplasm and absence of signs of secretion in the part of cells, a small increase in the nuclear-cytoplasmic ratio, starting with the generative zone of the gland, was confirmed. Such a picture created the impression of some polymorphism of epithelial cells. The intensity of mononuclear infiltration (degree of inflammation) in patients with CNG and CAG showed mild, moderate and severe degree of inflammation. At a significant degree of inflammation, along with the increase in the density of infiltration, formed clusters, which pushed the glands with the spread of it deep into the mucous membrane, up to the basal part. The accumulation of lymphocytes in mucous membrane lamina propria was diverse in terms of volume, cell density, structure and depth of occurrence. At a minimal and moderate extent, the formation of small groups of lymphocytes in the basal parts of the mucous membrane was observed. An increase in the volume of mononuclear inflammatory infiltrates in mucous membrane lamina propria occurred due to the formation of follicles. They were observed as bundles of oval or round shape, which consisted of tightly adjacent small lymphocytes. In a number of follicles there were light centers - reproduction, indicating a sufficient immune response of the body. The level of colonization of the mucosal by CagA (+) strains of H. pylori directly correlated with activity and degree of inflammation, both patients with CNG and CAG.

Dysplastic changes in the gastric epithelium in patients with CNG were detected in 43 H. pylori-, among which light dysplasia was observed in 28 (65.12%), and severe in 15 (34.88%). While GM dysplasia was registered at 89 H. pylori + patients with CNG, among which in CagA- 12 patients with dysplasia - 8 cases were with mild dysplasia (66.67%), while the severity was twice as low - 4 (33.33%). In the morphological analysis of dysplastic changes in GM of patients with CNG CagA+ H. pylori strains, it was found that among 77 patients with dysplasia, it was mild in 46 (59.74%) and severe in 31 (40.26%) (Table 2).

The activity of CAG, as well as CNG, irrespective of the presence of dysplasia, correlated positively with the bacterial colonization of GM: cases with severe (+++) infection respectively was mainly second or third stage of CAG activity (Table 3).

CAG with the first stage of activity in cytological preparations and on histological sections, painted with toluidine blue, heliobacteria were well visualized in the form of curved sticks. At a weak degree colonization - single (up to 20 in the field of view with an increase of 1000 times) bacterial bodies were found in the pit mucus, more often outside the epithelium in some fields of view.

For moderate colonization of GM by heliobacteria, the location of microbes, in the mucus, and in the lumen of the pits near the epithelium, was typically, where we observed from 20 to 50 bacteria in the field of view, which coincides with the data of Aruin, 1998 [1]. In cases of severe contamination along with epithelial cells and glandular structures, more than 50 microbial bodies were found as in the pits in the form of bacterial accumulation in many fields of vision and in adjacent to the surface epithelium of the mucus, gastric pits, and sometimes in the lumen of the glands.

Histological analysis of GM of patients with CAG for 2 stages of activity was characterized by diffuse leukocyte infiltration both in the surface and in the pit epithelium, and segmental leukocytes sometimes destroy the neck of the glands (Fig. 3). In the 3 stages of CAG activity, neutrophils were detected in both the surface and pit epithelium and in

Table 2. Characteristics of the examined patients depending on the presence of the gene CagA H. pylori.

Nosology	*CagA (-)N, m/f*	*CagA (+)N, m/f*
Normal GM	12 (6/6)	5 (3/2)
CNG without dysplasia	15 (8/7)	11 (7/4)*
CNG with dysplasia Mild Severe	12 8 (5/3) 4 (2/2)	77 * 46 (30/16)* 31 (21/10)*
CAG without dysplasia	12 (7/5)	9 (6/3)
CAG with dysplasia Mild Severe	16 12 (8/4) 4 (2/2)	48* 31 (22/9)* 17 (11/6)*
Total:	**67 (38/29)**	**150 (100/50)**

Notes: * p < 0,05- in comparison with the norm.

Table 3. Characteristics of the examined patients depending on the stage of contamination, the stage of activity and the presence of CagA.

Nosology	*CagA(-)*			*CagA(+)*		
	+	++	+++	+	++	+++
CNG inactive	11	5	4	7	5	0
CNG active	**3**	**2**	**2**	**20**	**23**	**33**
1 stage	2	1	1	9	6	3
2 stage	1	1	1	8	10	13
3 stage	0	0	0	3	7	17
CAG inactive	7	6	5	3	0	1
CAG active	**3**	**3**	**4**	**15**	**10**	**28**
1 stage	1	2	1	8	2	3
2 stage	2	1	3	6	7	8
3 stage	0	0	0	1	1	17
Total	**24**	**16**	**15**	**45**	**38**	**62**

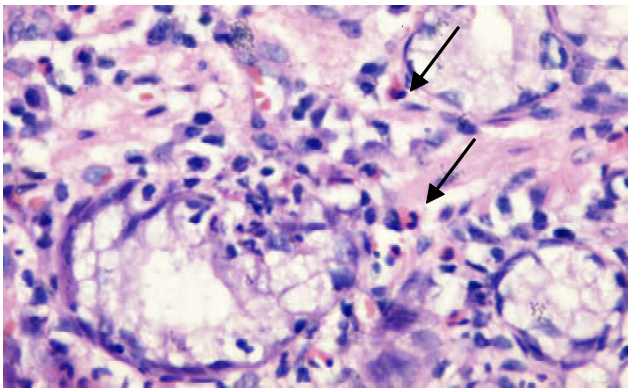

Fig. 3. Chronic atrophic active (stage 2) gastritis CagA+. Leukocyte infiltration of the mucous membrane lamina propria of the antral part of the stomach. The arrows show segmented neutrophils in mucous membrane lamina propria. Hematoxylin-eosin. x1000.

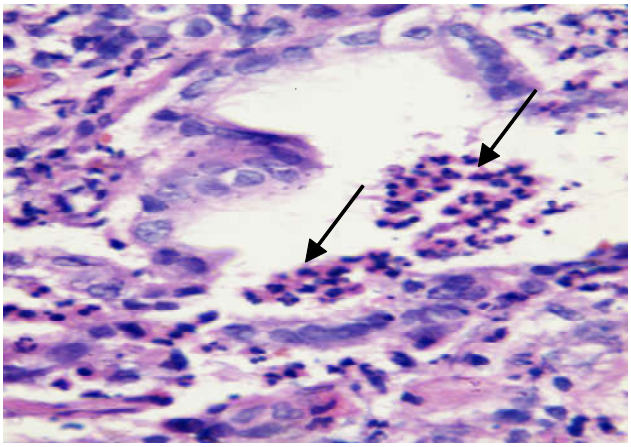

Fig. 4. Chronic atrophic active (stage 3) gastritis. CagA+. Leukodiapedesis with the formation of "intra-pit abscess". The arrows show the accumulation of segmental leukocytes inside the stomach pits. Hematoxylin-eosin. x1000.

the lumen of the glands with the formation of intrapit and glandular abscesses (Fig. 4).

In some sites, micro-erosions were observed as a small surface defect of the epithelial layer. Also, areas of epithelium of regenerative type with basophilic nuclei with high activity of inflammation were observed. Most often erosions were combined with the 2nd and 3rd stage of inflammation activity, as well as with the strong H. pylori contamination.

The parameters for CAG patients were follow: 31 (64%) of 48 patients had mild dysplasia and 17 (36%) with severe (see Table 2). At a severe degree of dysplasia, the severity of cellular atypia increased in patients both with CAG and CNG.

In the comparative pathomorphological analysis of GM in H. pylori+ and H. pylori-patients with CAG with dysplastic changes, it should be noted that 1 stage of atrophy was positively correlated with the degree of infectivity ($\chi^2 = 0.046$, $p < 0.05$), while for 2, 3, 4 stages of atrophy ($\chi^2 = 0,2773$, $p > 0,05$; $\chi^2 = 0,382$, $p > 0,05$; $\chi^2 = 0,555$; $p > 0,05$ respectively), such dependence has not been established. In our opinion, this is due to the key role of helicobacter infection, which triggers a cascade of pathological changes in GM. With further progression of atrophic changes in the gastric epithelium, GM loses the ability to synthesize mucin, which leads to the reduction of adhesive properties and the inability of H. pylori to bind to glycoproteins of gastric mucus.

Thus, conducted studies indicate that the presence of CagA positive genotype of helicobacter infection in patients with CG complicates the prognosis of the underlying disease, causing a cascade of pathological changes in GM.

Histologic and molecular genetic comparisons conducted in the studied groups of patients showed that the lowest degree of chronic gastritis activity was observed in GM of body and anthrax in uninfected patients and infected with H. pylori CagA (-) strains, and the minimum bacterial insemination rates - in the body of the stomach in patients infected with the strains of CagA (-) H. pylori.

Study of the activity of inflammation (neutrophil infiltration) of GM in chronic gastritis confirmed the association with helicobacter infection (see Table 3). The statistical analysis revealed a high reliability between inflammation activity and the presence of helicobacter infection (CagA+), and with CNG: for a low degree of contamination, the exact Fisher criterion = 0.002, $p < 0.05$, for moderate degree - 0.012, $p < 0.05$, for high degree - 0.012, $p < 0.05$. Accordingly, for CAG: for a low degree of contamination, the exact Fisher criterion = 0,011, $p < 0,05$, for a moderate degree - 0,003, $p < 0,05$, for a high degree - 0,001, $p < 0,05$. The highest values of gastric activity rates were noted for the antrum department in patients with CNG infected with CagA (+) H. pylori strains and in patients with the third stage of CAG activity infected with H. pylori (+) strains. The highest degree of bacterial insemination was recorded by us in the antral department of the stomach in patients with CNG of the third stage of activity infected with the strains of CagA (+) H. pylori.

Discussion

The main role in the mechanism of neutrophilic chemotaxis plays an epithelium, in which the expression of cytokines, leukotriene B4 and complement activation products occurs with adhesion [15, 28, 42]. The protein that activates neutrophils stimulates the adhesion of leukocytes to endothelial cells, which in turn changes microcirculation, leads to degranulation of tissue basophil granulocytes (mast cells), leukocytes and platelet aggregation and transudation. The leading role in chemotaxis belongs to interleukin-8, the main source of which is the gastric epithelium. Adhesion causes in epitheliocytes reorganization of actin cytoskeleton and increases the expression of the gene encoding interleukin-8, and then triggers the inflammatory cascade with the secretion of various cytokines [33, 39, 41]. In addition to direct bacterial stimulation of the epithelial production of interleukin-8, its expression is enhanced by the factor of tumor necrosis and interleukin-1, which are produced by macrophages and leukocytes, which migrate to the sites of colonization [25, 29]. A vicious circle with a long active process is created. The data we receive are in agreement with the data of N. Tegtmeyer et al. [34], which also revealed the

association of CagA + strains infection of the H. pylori with CG activity, due to the ability to directly stimulate the secretion of the epithelium of interleukin-8, with almost exclusively strains of type 1 (CagA +, VacA +) [34] and do not coincide with the data given by Y. Yamaoka in 1999 [40], which did not establish a significant difference in the relationship between the activity of inflammation with the colonization in different types of H. pylori infection.

It should be noted that most studies have shown that with the presence of H. pylori in the cytotoxin-associated gene, the relative risk of these diseases increases by 2-3 times, and some authors point to an increased risk of developing gastric cancer in CagA + H. pylori infection in 28.4 times [35, 37, 38]. The cellular composition of inflammatory infiltrates of GM is undergoing significant changes in the H. pylori infection, which are more non-specific, and in terms of prediction regarding the risk of pre-cancerous development, should be interpreted in conjunction with other factors and indicators involved in the pathogenesis of dysplastic changes in SOS. In our study, the degree of colonization, as a rule, corresponded to the stage of activity, as in cases of CNG, and in patients with CAG, which coincides with the data [8, 12].

By initiating damage, H. pylori causes chronic inflammation in GM. This inflammation is mediated by multitude pro- and anti-inflammatory cytokines. Genetic polymorphism directly influences changes in the intensity of the cytokine response, which causes definitive clinical effects in humans [35]. Clinical and morphological manifestations of helicobacter infection depend on genetic factors of pathogenicity of the microorganism and genetic predisposition of the infected organism.

The data obtained by us is sufficiently promising for further research of the relationship between helicobacter infection in the epithelium of GM and precancerous changes in the stomach with the features of the clinical course of the disease and the composition of cellular infiltration. Although the role of another H. pylori infectious agent in the gastric cancer etiology has been substantiated, however, not all pathogenetic links in the participation of H. pylori in gastro-carcinogenesis have been fully elucidated. Perhaps they are also due to the effect on the composition of inflammatory cellular infiltration of GM and the production of some cytokines by H. pylori-induced epithelial cells, macrophages and other cells.

Further study of genetic factors of virulence with the use of polymerase chain reaction is promising, since it will allow not only the prediction of the course of chronic gastritis, depending on the strain detected, but also to optimize and develop new differentiated approaches to eradication therapy.

Conclusions

The degree of activity of both chronic non-atrophic and atrophic gastritis depended on the presence of CagA. At the same time, the closest correlation is recorded between the degree of infectivity and the stage of activity. Thus, in chronic non-atrophic gastritis: for a low degree of contamination, the exact Fisher criterion was 0.002, with $p<0.05$, for a moderate degree - 0.012 ($p<0.05$), and for high -0.012 ($p<0.05$). Accordingly, for chronic atrophic gastritis: for a low degree of contamination, Fisher's exact criterion was 0.011, at $p<0.05$, for a moderate degree - 0.003 ($p<0.05$), for a high degree -0.001 ($p<0.05$).

References

[1] Aruin, L. I., Kapuller, L. L., & Isakov, V. A. (1998). *Morphological diagnosis of diseases of the stomach and intestines*. M.: "Triad-X".

[2] Aruin, L. I., Kononov, A. V., & Mozgovoy, S. I. (2009). International classification of chronic gastritis: what should be accepted and what is in doubt. *Archive of pathology,* 4, 11-18.

[3] Bosman, F. T., Carneiro, F., Hruban, R. H., & Theise, N. D. (2010). *World Health Organization Classification of Tumours. Pathology and Genetics of Tumours of the Digestive System*. IARC Press. Lyon, 417.

[4] Chukov, S. Z., & Pasechnikov, V. D. (2001). Do H. pylori virulence factors determine the nature of the gastroduodenal pathology? *Russian Journal of Gastroenterology, Hepatology, Coloproctology*, 11(2), 75-81.

[5] Dixon, M. F., Michael, D., & Path, F. R. (1996). Classification and Grading of Gastritis: The Updated Sydney System. *The American Journal of Surgical Pathology*, 20(10), 1161-1181.

[6] Evstigneev, I. V. (2011). Infection caused by Helicobacter pylori: state of the problem and prospects. *Klinichna Imunologiya.* Allergology Infectology, 6-7, 14-19.

[7] Gaddy, J. A., Radin, J. N., Loh, J. T., Zhang, F., Washington, M. K., Peek, R. M., & Cover, T. L. (2013). High Dietary Salt Intake Exacerbates Helicobacter pylori-Induced Gastric Carcinogenesis. *Infection and Immunity*, 81(6), 2258-2267. doi:10.1128/iai.01271-12.

[8] Ghasemi Basir, H. R., Ghobakhlou, M., Akbari, P., Dehghan, A., & Seif Rabiei, M. A. (2017). Correlation between the Intensity of Helicobacter pylori Colonization and Severity of Gastritis. *Gastroenterology Research and Practice*, 1-5. doi:10.1155/2017/8320496.

[9] Hatakeyama, M. (2014). Helicobacter pylori CagA and Gastric Cancer: A Paradigm for Hit-and-Run Carcinogenesis. *Cell Host & Microbe,* 15(3), 306-316. doi:10.1016/j.chom.2014.02.008.

[10] Isaeva, G. S., &Valiyeva, R. I. (2018). Biological properties and virulence of Helicobacter pylori. KMAH, 1 (20), 14-23.

[11] Iunusova, A. I., Litvinova, I. S., Karpeno, P. A., & Tohidpour, A. (2017). The Cytotoxin-Associated Gene A (CagA) of Helicobacter pylori: the Paradigm of an Oncogenic Virulence Factor. *Journal of Siberian Federal University. Biology,* 1-12. doi:10.17516/1997-1389-0015.

[12] Ivanova, N. L., Sokolova, I. L., Sadovnikova, V. V., & Smirnova, E. M. (2003). The activity of the inflammatory process in the gastric mucosa, depending on the degree of contamination of helicobacter pylori in children. *Medikum,* 3-4, 24-31.

[13] Jenks, P. J., Megraud, F., & Labigne, A. (1998). Clinical outcome after infection with Helicobacter pylori does not appear to be reliably predicted by the presence of any of the genes of the cag pathogenicity island. *Gut,* 43, 752-758.

[14] Kamogawa-Schifter, Y., Yamaoka, Y., Uchida, T., Beer, A., Tribl, B., Schöniger-Hekele, M., & Dolak, W. (2018). Prevalence

of Helicobacter pylori and its CagA subtypes in gastric cancer and duodenal ulcer at an Austrian tertiary referral center over 25 years. *PLOS ONE*, 13(5), e0197695. doi:10.1371/journal.pone.0197695

[15] Kido, M., Tanaka, J., Aoki, N., Iwamoto, S., Nishiura, H., Chiba, T., & Watanabe, N. (2009). Helicobacter pylori Promotes the Production of Thymic Stromal Lymphopoietin by Gastric Epithelial Cells and Induces Dendritic Cell-Mediated Inflammatory Th2 Responses. *Infection and Immunity,* 78(1), 108-114. doi:10.1128/iai.00762-09

[16] Kononov, A. V. (2006). Inflammation as the basis of Helicobacter pylori - associated diseases. *Archive of pathology,* 5, 3-10.

[17] Kononov, A. V. (2009). Genetic regulation and phenotype of inflammation in Helicobacter pylori infection. *Archive of pathology,* 5, 57-63.

[18] Lee, J. Y., Kim, N., Choi, Y. J., Nam, R. H., Choi, Y. J., Kwon, Y. H., & Lee, D. H. (2014). Histologic Findings and Inflammatory Reactions After Long-term Colonization of Helicobacter felis in C57BL/6 Mice. *Journal of Cancer Prevention,* 19(3), 224-230. doi:10.15430/jcp.2014.19.3.224

[19] Maeda, S., Yoshida, H., Ikenoue, T., Ogura, K., Kanai, F., Kato, N. ... Omata, M. (1999). Structure of the cag pathogenicity island in Japanese Helicobacter pylori isolates. *Gut,* 44, 336-341.

[20] Medvetsky, Ye. B., & Vilcanyuk, I. O. (2001). Method of staining Helicobacter pylori in cytological preparations. *Reports of morphology,* 7(1), 154-155.

[21] Morozov, I. A. (2000). Cytological diagnosis of Helicobacter pylori infection in the stomach. *Russian Journal of Gastroenterology, Hepatology, Coloproctology,* 2, 7-10.

[22] Mozgovoy, S. I., Novikov, D. G., & Kononov, A. V. (2010). Assessment of the integral indicator of mucosal atrophy in chronic gastritis in the prognosis of gastric cancer. *Omsk Scientific Herald,* 1, 81-83.

[23] Mozgovoy, S. I., Shimanskaya, A. G., & Osintseva, I. L. (2010). Russian revision of the international classification of chronic gastritis: evaluation of a new diagnostic approach using Capa-statistics methods. *Omsk Scientific Herald*, 1, 84-88.

[24] Nizhevich, A. A., Kuchina, E. S., & Akhmadeeva, E. N. (2012). The value of anti-CagA serological immune response in children with gastric ulcer and duodenal ulcer associated with helicobacter pylori. *Basic research,* 4(1), 212-215; URL: http://www.fundamental-research.ru/ru/article/view?id=29746.

[25] Nomura, S., Yamaguchi, H., Ogawa, M., Wang, T. C., Lee, J. R., & Goldenring, J. R. (2005). Alterations in gastric mucosal lineages induced by acute oxyntic atrophy in wild-type and gastrin-deficient mice. *American Journal of Physiology-Gastrointestinal and Liver Physiology*, 288(2), G362-G375. doi:10.1152/ajpgi.00160.2004.

[26] Park, J., Forman, D., Waskito, L., Yamaoka, Y., & Crabtree, J. (2018). Epidemiology of Helicobacter pylori and CagA-Positive Infections and Global Variations in Gastric Cancer. *Toxins*,10(4), 163. doi:10.3390/toxins10040163.

[27] Perwez Hussain, S., & Harris, C. C. (2007). Inflammation and cancer: An ancient link with novel potentials. *International Journal of Cancer*, 121(11), 2373-2380. doi:10.1002/ijc.23173

[28] Polyzos, S. A. (2017). Helicobacter pylori infection and esophageal adenocarcinoma: a review and a personal view. *Annals of Gastroenterology.* doi:10.20524/aog.2017.0213

[29] Potrokhova, E. A., Pomorgailo, E. G., & Kononov, A. V. (2012). Variants of the course of H. pylori-associated gastritis in adolescents after eradication of the pathogen. *Russian Bulletin of Perinatology and Pediatrics*, 2, 46-51.

[30] Schlemper, R., Riddell, R., & Kato, Y. (2000). Vienna classification of gastrointestinal epithelial neoplasia. *Gut*,47(2), 251-255.

[31] Slater, B. (1990). Superiorstain for Helicobacter pylori usingtoluidine. *Journal of Clinical Pathology*, 43(11), 961.

[32] Sugano, K., Tack, J., Kuipers, E. J., Graham, D. Y., El-Omar, E. M., Miura, S., & Malfertheiner, P. (2015). Kyoto global consensus report on Helicobacter pylorigastritis. *Gut,* 64(9), 1353-1367. doi:10.1136/gutjnl-2015-309252

[33] Suzuki, N., Murata-Kamiya, N., Yanagiya, K., Suda, W., Hattori, M., Kanda, H., & Hatakeyama, M. (2015). Mutual reinforcement of inflammation and carcinogenesis by the Helicobacter pylori CagA oncoprotein. *Scientific Reports,* 5(1). doi:10.1038/srep10024.

[34] Tegtmeyer, N., Wessler, S., & Backert, S. (2011). Role of the cag-pathogenicity island encoded type IV secretion system in Helicobacter pylori pathogenesis. *FEBS Journal*, 278(8), 1190-1202. doi:10.1111/j.1742-4658.2011.08035.x

[35] Tkach, S. M. (2009). H. pylori infection as a major cause of gastric carcinogenesis. *Health of Ukraine*, 1, 32-33.

[36] Tkach, S. M. (2016). Modern approaches to the classification, diagnosis and management of patients with chronic gastritis in the light of the international Kyoto consensus. *Gastroenterologiya*, 1, 110-116.

[37] Tsukamoto, T., Nakagawa, M., Kiriyama, Y., Toyoda, T., & Cao, X. (2017). Prevention of Gastric Cancer: Eradication of Helicobacter Pylori and Beyond. *International Journal of Molecular Sciences,* 18(8), 1699. doi:10.3390/ijms18081699

[38] Vieth, M., Dirshmid, K., Oehler, U., Helpap, B., von Luckner, A. G., & Stolte, M. (2001). Acute measles gastric infection. *The American Journal of Surgical Pathology,* 25(2), 259-62.

[39] Walduck, A., Schmitt, A., Lucas, B., Aebischer, T., & Meyer, T. F. (2004). Transcription profiling analysis of the mechanisms of vaccine-induced protection against H. pylori. *The FASEB Journal,* 18(15), 1955-1957. doi:10.1096/fj.04-2321fje.

[40] Yamaoka, Y., Kodama, T., Gutierrez, O., Kim, J. G., Kashima, K., & Graham, D. Y.(1999).Relationship between Helicobacter pylori iceA, cagA and vacA status and clinical outcome: studies in four different countries. *Journal of Clinical Microbiology,* 37(7), 2274-2279.

[41] Zhang, X.-Y., Zhang, P.-Y., & Aboul-Soud, M. A. M. (2016). From inflammation to gastric cancer: Role of Helicobacter pylori. *Oncology Letters,* 13(2), 543-548. doi:10.3892/ol.2016.5506.

[42] Zhang, Y., Pan, K., Zhang, L., Ma, J., Zhou, T., & Li, J. (2015). Helicobacter pylori, cyclooxygenase-2 and evolution of gastric lesions: results from an intervention trial in China. *Carcinogenesis*, bgv147. doi:10.1093/carcin/bgv147.

РОЛЬ CagA ГЕНА У ВИНИКНЕННІ ЗАПАЛЬНОЇ ВІДПОВІДІ СЛИЗОВОЇ ОБОЛОНКИ ШЛУНКУ У ХВОРИХ НА ХРОНІЧНИЙ HELICOBACTER PYLORI-АСОЦІЙОВАНИЙ ГАСТРИТ

Вернигородський С.В., Сухань Д.С.

В теперішній час інфекція Helicobacter pylori (H. pylori) визнана одним із найважливіших факторів ризику гастроканцерогенезу. Відомо, що дана інфекція не викликає безпосередньо неопластичні зміни в слизовій оболонці шлунку, а відбувається це внаслідок ряду послідовних подій за рахунок тривалої персистенції збудника в організмі людини. Початковим етапом даного каскаду, безумовно, є запальна відповідь, яка обумовлена здатністю організму адаптуватися до сторонньої інфекції та є неминучим результатом взаємодії H. pylori з клітинами шлункового епітелію. Цей пошкоджуючий прямий ефект посилюється

продукцією вакуолізуючого цитотоксину й вивільненням продуктів цитотоксин-асоційованого гена CagA, що на патоморфологічному рівні проявляється запальною інфільтрацією слизової оболонки шлунку (СОШ) того чи іншого ступеня. Щодо зв'язку між ступенем обсіменіння (контамінації) та активності запалення СОШ у людей, інфікованих штамом CagA, на сьогодні існують різні, часто суперечливі думки, ось чому в даній роботі ми поставили за мету встановлення взаємозв'язку між характером запальної відповіді та наявності гену CagA у H. pylori-інфікованих хворих. Мета дослідження - встановлення взаємозв'язку між характером запальної відповіді та генетичнихми особливостями штаму H. pylori (наявності генотипу CagA). Нами було обстежено 365 пацієнтів, серед яких до контрольної групи увійшли 40 осіб (18 жіночої та 22 чоловічої статі, середній вік яких становив 45,33±15,46 та 42,82±12,31 років, відповідно) без наявності будь-якої гастроентерологічної патології в анамнезі, хворих на хронічний неатрофічний гастрит (188 осіб) та хронічний атрофічний гастрит (137 осіб). Встановлений, тісний зв'язок між наявністю гену CagA, активністю та ступенем контамінації для хронічного неатрофічного гастриту: для низького ступеня контамінації точний критерій Фішера становив =0,002, p<0,05, для помірного ступеня - 0,012, p<0,05, для високого ступеня - 0,012, p<0,05. Відповідно, при хронічному атрофічному гастриті: для низького ступеня контамінації точний критерій Фішера =0,011, p<0,05, для помірного ступеня - 0,003, p<0,05, для високого ступеня - 0,001, p<0,05. Зареєстрований також тісний зв'язок між ступенем контамінації та активністю хронічного гастриту (ХГ): у хворих з високим ступенем контамінації виявляли, як правило, 2-3 стадію активності ХГ. У нашому дослідженні запальна відповідь залежала від наявності, або відсутності у пацієнта штаму H. pylori, що містив генотип CagA, котрий, на нашу думку, займає ключову роль у запуску каскада запальних змін СОШ та прогресуванні хронічного гастриту.
Ключові слова: *Helicobacter pylori, CagA, хронічний гастрит, морфологічні зміни.*

РОЛЬ CagA ГЕНА В ВОЗНИКНОВЕНИИ ВОСПАЛИТЕЛЬНОГО ОТВЕТА СЛИЗИСТОЙ ОБОЛОЧКИ ЖЕЛУДКА У БОЛЬНЫХ ХРОНИЧЕСКИМ HELICOBACTER PYLORI-АССОЦИИРОВАННЫМ ГАСТРИТОМ

Вернигородский С.В., Сухань Д.С.

В настоящее время инфекция Helicobacter pylori (H. pylori) признана одним из важнейших факторов риска гастроканцерогенеза. Известно, что данная инфекция не вызывает непосредственно неопластические изменения в слизистой оболочке желудка, а происходит это вследствие ряда последовательных событий за счет длительной персистенции возбудителя в организме человека. Начальным этапом данного каскада, безусловно, является воспалительный ответ, который обусловлен способностью организма адаптироваться к посторонней инфекции и является неизбежным результатом взаимодействия H. pylori с клетками желудочного эпителия. Этот повреждающий прямой эффект усиливается продукцией вакуолизирующего цитотоксина и высвобождением продуктов цитотоксин-ассоциированного гена CagA, что на патоморфологическом уровне проявляется воспалительной инфильтрацией слизистой оболочки желудка (СОЖ) той или иной степени. По связи между степенью обсеменения (контаминации) и активности воспаления СОЖ у людей, инфицированных штаммом CagA, на сегодняшний день существуют различные, часто противоречивые мнения, вот почему в данной работе мы поставили цель установления взаимосвязи между характером воспалительного ответа и наличием гена CagA у H. Pylori-инфицированных больных. Цель исследования - установление взаимосвязи между характером воспалительного ответа и генетическими особенностяими штамма H. pylori (наличия генотипа CagA). Нами было обследовано 365 пациентов, среди которых в контрольную группу вошли 40 человек (18 женского и 22 мужского пола, средний возраст которых составлял 45,33±15,46 и 42,82±12,31 лет соответственно) без наличия какой-либо гастроэнтерологической патологии в анамнезе, больных хроническим неатрофическим гастритом (188 человек) и хроническим атрофическим гастритом (137 человек). Установлена тесная связь между наличием гена CagA, активностью и степенью контаминации для хронического неатрофического гастрита: для низкой степени контаминации точный критерий Фишера составлял 0,002, p<0,05, для умеренной степени - 0,012, p<0,05, для высокой степени - 0,012, p<0,05. Соответственно, при хроническом атрофическом гастрите: для низкой степени обсеменения точный критерий Фишера был равен 0,011, p<0,05, для умеренной степени - 0,003, p<0,05, для высокой степени - 0,001, p<0,05. Зарегистрирована также тесная связь между степенью контаминации и активностью хронического гастрита (ХГ): так у больных с высокой степенью контаминации определяли, как правило, 2-3 стадию активности ХГ. В нашем исследовании воспалительный ответ зависел от наличия или отсутствия у пациента штамма H. pylori, содержащий генотип CagA, который, по нашему мнению, занимает ключевую роль в запуске каскада воспалительных изменений СОЖ и прогрессировании хронического гастрита.
Ключевые слова: *Helicobacter pylori, CagA, хронический гастрит, морфологические изменения.*

DOI: 10.31393/morphology-journal-2018-24(3)-03 Reports of Morphology, Vol. 24, №3, Pages 19-25

ISSN 1818-1295 eISSN 2616-6194

REPORTS OF MORPHOLOGY

Official Journal of the Scientific Society of Anatomists, Histologists, Embryologists and Topographic Anatomists of Ukraine

journal homepage: https://morphology-journal.com

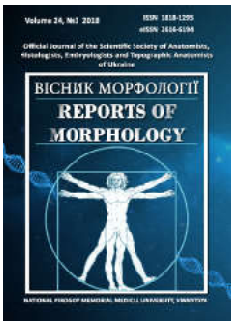

Determination of individual teleroentgenographic characteristics of the lower medial incisors position in Ukrainian young men and young women with orthognathic bite

Dmitriev M.O.[1], Gunas I.V.[1], Dzevulska I.V.[2], Glushak A.A.[1]

[1]National Pirogov Memorial Medical University, Vinnytsya, Ukraine
[2]Bogomolets National Medical University, Kyiv, Ukraine

ARTICLE INFO
Received: 09 July, 2018
Accepted: 15 August, 2018

UDC: 616.716.8-071-084:613.956:
617.52: 616.34.25-007.481-7

CORRESPONDING AUTHOR
e-mail: dmitriyevnik@gmail.com
Dmitriev M.O.

Ethnic, sexual and age features of the incisors positions point to the need for the development of techniques that allow to determine their individual characteristics, since commonly accepted standards recommended for optimal positioning of incisors can only be used as indicative. The purpose of the study - by studying teleroentgenographic indices and conducting direct stepwise regression analysis in young men and young women of Ukraine with orthognathic bite, to develop and analyze the mathematical models of individual characteristics of the position of the lower medial incisors. With the Veraviewepocs 3D device, Morita (Japan) in 38 young men (17 to 21 years of age) and 55 young women (aged from 16 to 20 years) with occlusion close to orthognathic bite and balanced faces received side teleroentgenograms. Cephalometric analysis was performed using OnyxCeph³™ software. Cephalometric points and measurements were performed according to the recommendations of A.M. Schwarz, J. McNamara, W.B. Downs, R.A. Holdway, P.F. Schmuth, C.C. Steiner and C.H. Tweed. According to the above methods, in the licensed package "Statistica 6.0" using direct straight line regression analysis, the teleroentgenographic characteristics of the position of the lower medial incisors (distance 1I_NB, distance 1I_APog, angle 1I_DOP, IMPA angle, Mand1_NB angle, FMIA angle and Mand1_MeIm angle) were performed. In young men with orthognathic bite of 7 possible models of teleroentgenographic characteristics of the lower medial incisors, 5 were constructed with determination coefficient R^2 from 0.694 to 0.849, and in young women, all 7 possible models with determination coefficient R^2 from 0.595 to 0.794. In young men most often the regression equations included - the angle ANB and facial vertical index GL_SN_S (by 11.5%); lower face height ANS_ME, face angle NBA_PTGN and distance S_E (by 7.7%). In young women most often the regression equations included - the angle of N_POG (16.7%); Wits indicator (13.9%); inclination angle I (8.3%); H-angle, maxillo-mandibular angle MM and angle of facial axis NBA_PTGN (by 5.6%). Thus, in the work with the help of the method of stepwise regression with inclusion, among Ukrainians of juvenileage, on the basis of features teleroentgenographic indicators, the analysis of reliable models of individual teleroentgenographic characteristics of the position of the lower medial incisors was developed and carried out.

Keywords: *lower medial incisors position, teleroentgenographic, regression analysis, orthognathic bite, young men, young women.*

Introduction

Determination of the position of the lower incisors in the sagittal plane is one of the key positions in the diagnosis, planning and control of treatment of dental ankles [9, 25]. First of all, because together with the upper incisors, in addition to the function of biting, they also play an aesthetic function. Their position provides the formation of a soft profile of the lower third of the face. The position of the incisors in the sagittal plane (inclination), the position of the lips and the chin morphology play a key role in the evaluation and perception of the results of orthodontic treatment from the position of aesthetics, both doctors and patients themselves [16].

To objectivize the determination of the position of the lower incisors, the researchers studied the location of the central axes and the position of the cutting edge and the vestibular (lip) surface to different cephalometric planes [8, 24, 26-28, 30]. But the use of unified standards is criticized by many researchers, proving the variability of these indicators. So E. Hernandez-Sayago et al. [14] determined the presence of a statistically significant difference in the inclination of the lower incisors in relation to the length of the anterior base of the skull, the angle of McHorris, the closure and mandibular planes, and offer a differentiated approach that determines the inclination of incisors, depending on the nature of the bite and the face type.

R. MoraHurtado, M.E. VeraSerna and E. Uribe-Querol [25] point to the importance of choosing an orthodontic device that affects the position of the lower incisors, depending on the type of patient's face. Namely, their study in individuals with normognatic type of closure of molars (class 1 by Engle) revealed statistically significant differences in the characteristics of the lower incisors between the mesocephalic and brachiocephalic types and the increase in the inclusions of the latter in dolichocephalic compared with brachycephalic.

A number of studies have found that the position of the lower incisors is not only closely related to the morphology of the chin symphysis and the direction of face growth [23], but also with the features of the closing plane itself [20], as well as the position of the lower incisors affects the nature of the closure and the nature of the movement of the dentition relative to each other [10]. Moreover, M.M. Alabdullah et al. [1] found a direct linear relationship between the force of chewing muscles and the angular characteristics of the incisors.

In addition to its aesthetic and functional significance, the literature constantly poses questions about the influence of the position of the lower incisors on the state of periodontal tissues, that is, the structures that hold and allow the tooth function to function properly. It is the emergence of a gum recession and is the most undesirable and potentially dangerous complication in the orthodontic displacement of incisors, which is indicated by the study of D. Ciavarella et al. [2], D.T. Garlock et al. [11], M. Tepedino et al. [29].

The *purpose* of the study - by studying tele-roentgenographic indices and conducting direct stepwise regression analysis in young men and women of Ukraine with orthognathic bite, to develop and analyze the mathematical models of individual characteristics of the position of the lower medial incisors.

Materials and methods

With the Veraviewepocs 3D device, Morita (Japan) in 38 young men (17 to 21 years of age) and 55 young women (aged from 16 to 20 years) with occlusion close to orthognathic bite and balanced faces received side teleroentgenograms. Cephalometric analysis was performed using OnyxCeph³™ software. Cephalometric points and measurements were performed according to the recommendations of A.M. Schwarz [27], J. McNamara [24], W.B. Downs [8], R.A. Holdway [15], P.F. Schmuth [26], C.C. Steiner [28] and C.H. Tweed [30]. The analysis of teleroentgenograms and the results of their researches for Ukrainian young men and young women is described in detail and set out in a number of articles [4-7, 12, 13].

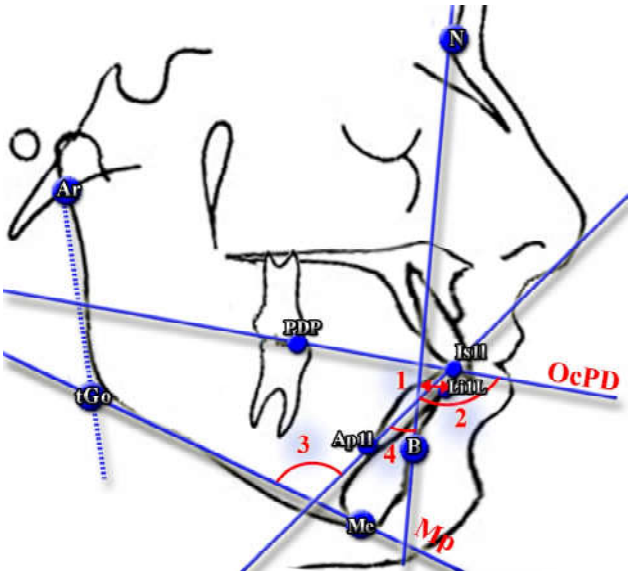

Fig. 1. Teleroentgenographic characteristics position of the lower medial incisors. **1 - NB_1l** (distance 1l_NB), distance from the point Li1L to the line N-B (*determines the anterior-posterior location of the crown part of the lower medial incisor to the line N-B*); **2 - DOP_1l** (angle 1l_DOP), formed by the Ap1L-Is1L (*center axis of the lower medial incisor*) and ADP-PDP lines (*occlusion plane by Downs, OcPD*), measure of deviation from a straight angle with a positive value in the clockwise direction, with a negative against the course of the latter; **3 - IMPA** (IMPA angle, Incisor Mandibular Plane Angle) - is formed by lines Ap1L-Is1L (*center axis of the lower medial incisor*) and tGo-Me (*mandibular plane Mp*) (*characterizes the inclination of the lower medial incisor to the mandibular plane*). By Downs method, this indicator for convenience and more clinical practicality is used at a reduced size of 90° and can take both negative and positive values, and is called *MEGO_1L*; in *Schwarz* method this figure is called *MAND1_ML* (angle Mand1_ML); **4 - MAND1_NB** (angle Mand1_NB), formed by lines Ap1L-Is1L (*tilt central axis of the lower medial incisor*) and N-B.

We, in accordance with the above-mentioned methods, simulated the teleroentgenographic characteristics of the position of the lower medial incisors (Fig. 1, 2).

The statistical processing of the obtained results was carried out in the license package "Statistica 6.0" using a direct stepwise regression analysis.

Results

As a result of modeling teleroentgenographic characteristics of the position of the lower *medial* incisors in young men and women with orthognathic bite, depending on the metric parameters of the skull, we have constructed linear equations for the following indices.

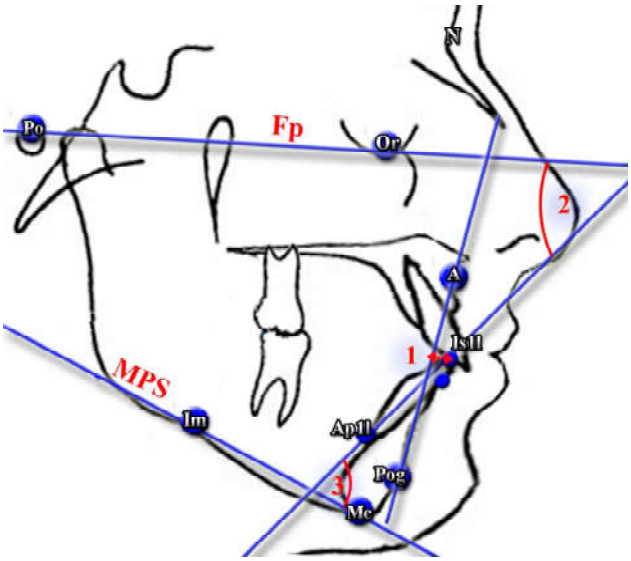

Fig. 2. Teleroentgenographic characteristics position of the lower medial incisors. **1 - APOG_1L** (distance 1I_APog) - the distance from the point Is1L to the line A-Pog (if the distance is medial, that is, the cutting edge of the incisor is in the front with respect to the line position, then the indicator takes a positive value, and if the distance is distal, that is the cutting edge of the incisor is in the posterior with respect to the line position, then the indicator takes a negative value); **2 - FMIA** (angle FMIA, *Frankfort Mandibular Incisor Angle*), formed by the lines Is1L-Ap1L (*center axis of the lower medial incisor*) and Po-Or (*Frankfurter plane, Fp*) (*angle of inclination of the lower median incisor to the Frankfurter plane, Fp*); **3 - MAND1_ME** (angle Mand1_MeIm) - is formed by lines Ap1L-Is1L (*inclination of the central axis of the lower medial incisor*) and Im-Me (mandibular plane by *Schwarz, MPS*).

For young men:

FMIA = 153.1 - 1.931 x ANB + 0.714 x PN_POG - 0.829 x NBA_PTGN - 0.362 x S_E (R^2=0.804; $F_{(4.31)}$=31.87; p<0.001; Error of estimate=3.263);

IMPA = 108.2 - 0.518 x ARGOME + 0.828 x WITS + 0.893 x S_E + 0.316 x F + 0.564 x N_POG_ + 0.213 x AFH_PFH - 0.181 x GL_SN_S (R^2=0.848; $F_{(7.28)}$=22.31; p<0.001; Error of estimate=3.462);

MAND1_ME = 175.2 + 0.989 x B - 1.271 x MM - 0.546 x MAND + 0.243 x GL_SN_S + 0.424 x ANS_ME (R^2=0.849; $F_{(5.30)}$=33.67; p<0.001; Error of estimate=3.351);

MAND1_NB = 30.38 + 1.872 x ANB - 0.221 x GL_SN_S + 0.463 x COND_A - 0.424 x ANS_ME (R^2=0.694; $F_{(4.31)}$=17.58; p<0.001; Error of estimate=3.295);

NB_1L = 10.56 + 0.792 x ANB - 0.049 x N_SP_SP - 0.350 x MAX + 0.136 x NBA_PTGN + 0.122 x N_SE - 0.082 x H (R^2=0.729; $F_{(6.30)}$=13.44; p<0.001; Error of estimate=0.798).

For young women:

APOG_1L = -21.09 + 0.349 x N_POG_ + 0.279 x AFH - 0.144 x GL_SNPOG - 0.242 x S_L + 0.342 x NBA_PTGN - 0.122 x NSBA (R^2=0.614; $F_{(6.47)}$=12.48; p<0.001; Error of estimate=1.222);

DOP_1L = 95.29 + 1.822 x WITS + 0.838 x N_POG_ + 0.716 x MAX_MAND - 0.964 x SND - 0.396 x POR_GNS (R^2=0.641; $F_{(6.47)}$=14.00; p<0.001; Error of estimate=4.011);

FMIA = 98.34 - 0.351 x MM - 0.279 x N_POG_ + 0.775 x PN_POG - 0.986 x WITS - 0.815 x PN_A (R^2=0.794; $F_{(5.45)}$=34.62; p<0.001; Error of estimate=3.652);

IMPA = -48.78 + 1.484 x WITS + 0.599 x NAPOG + 1.390 x I - 0.565 x P_OR_N + 1.010 x H - 0.727 x ML_NL (R^2=0.771; $F_{(6.44)}$=24.76; p<0.001; Error of estimate=3.658);

MAND1_ME = 144.2 - 1.677 x WITS + 0.456 x FMA - 0.395 x MM - 0.500 x N_POG_ - 0.326 x I (R^2=0.742; $F_{(5.45)}$=25.90; p<0.001; Error of estimate=3.679);

MAND1_NB = -76.80 + 0.597 x NAPOG + 1.085 x WITS + 0.669 x I + 0.504 x H + 0.362 x N_POG_ - 0.333 x S_E (R^2=0.736; $F_{(6.44)}$=20.50; p<0.001; Error of estimate=3.608);

NB_1L = -7.468 + 0.183 x N_POG_ + 0.157 x ANS_ME + 0.163 x A_N_PO (R^2=0.595; $F_{(3.50)}$=24.47; p<0.001; Error of estimate=1.097).

In these models:

R^2 - coefficient of determination;

$F_{(!,!!)}$=!!,!! - critical $_{(!,!!)}$ and got (!!,!!) value of Fisher's criterion;

St. Error of estimate - standard error of the standardized regression coefficient;

A_N_Po (distance A_N_Pog) - distance from the point A to the line N-Pog (the face plane, characterizes the degree of convexity of the face);

AFH (distance AFH or front height of the face) - distance from the point Me to the line ANS-PNS;

AFH_PFH (ratio AFH_PFH) - distance ratio from the point Me to the line ANS-PNS and from the point Ar to the point tGo (the ratio between the front (AFH) and rear (PFH) face height);

ANB (angle ANB) - is formed by lines A-N and N-B (indicates an angular interstitial relation in the anterior-posterior direction; angle ANB is considered positive if point A is in front of NB; if the lines NA and NB overlap, then the ANB angle is 0°; if point A is behind the NB line, then the angle is considered negative);

ANS_ME (lower face height) - distance from the point ANS to the point Me;

ARGOME (angle Ar-Go-Me, or the angle of the mandible) - is formed by lines Ar-tGo and tGo-Me;

B (basal angle) - formed by lines ANS-PNS (palatine plane SpP) and Im-Me (mandibular plane MPS by Schwarz) (indicates the angle between the upper and lower jaws);

COND_A (effective length of the upper jaw) - distance from the point Cond to the point A;

F (face angle or angle F) - formed by lines Se-N and N-A (determines the location of the anterior contour of the upper jaw in the jet plane to the base of the skull);

FMA (POr_MeGo) (angle FMA, Frankfort Mandibular Angle) - formed by lines tGo-Me (mandibular plane Mp) and Po-Or (Frankfurt plane Fp);

GL_SN_S (index Gl'_Sn_Sn_Gn' or facial vertical index) - distance ratio of Gl'-Sn and Sn-Gn' (defines vertical relationships in the face profile);

GL_SNPOG (angle Gl'SnPog' or indicator of convexity

of the soft tissue profile) - formed by lines Gl'-Sn and Sn-Pog';

H (H-angle) - formed by lines Po-Or (Frankfurt plane Fp) and Pn (nasal perpendicular, perpendicular to the line from the point N' to the line Se-N), defines the angle of the inclination of the Frankfurt plane to the base of the skull;

I (angle I, inclination angle) - angle formed by line ANS-PNS and Pn (nasal perpendicular, perpendicular to the line from the point N' to the line Se-N), angle of inclination of the upper jaw (spinal plane) to the nasal perpendicular;

MAND (length of the lower jaw) - distance from the constructive point tGoS to the constructive point apMandS;

MAX (length of the upper jaw) - distance from the constructive point apMax to the point PNS;

MAX_MAND (maxillo-mandibular difference) - difference between distances Cond-A and Cond-Gn;

ML_NL (SpP_GoMe, base angle) - formed by lines ANS-PNS and tGo-Me (the angle between the palatal SpP and the mandibular MP planes);

MM (maxillo-mandibular angle) - is formed by lines A-B and ANS-PNS (defines the angle below which the upper jaw is located in relation to the lower jaw in the jet plane);

N_POG_ (angle N'Hold_Pog'_Hline) - angle between lines Ls-Pog' (H line, Holdway line) and N'Hold-Pog';

N_SE (distance Se_N or the length of the front of the skull base by Steiner) - distance from the point Se to the point N;

N_SP_SP (coefficient N_Sp'_Sp'_Me) - distance ratio N-Sp' and Sp'-Me (the ratio of the upper and lower height of the face);

NAPOG (angle of the skeletal face obliquity, or angle NaPog) - formed by lines N-A and A-Pog;

NBA_PTGN (angle NBa-PtGn or the angle of the front axle) - formed by lines N-Ba and Pt-Gn (determines the direction of development of the mandible);

NSBA (angle NSBA) - formed by lines S-N (the front part of the skull base) and S-Ba;

P_OR_N (soft tissue angle, or angle P_Or_N'Hold_Pog') - formed by lines Po-Or and N'Hold-Pog';

PN_A (distance PN_A) - distance from the point A to the point PNm (perpendicular line from the point N to the line Po-Or). If the point A is distal from the nasal perpendicular, then the indicator takes a negative value, and if the medial than a positive value;

PN_POG (distance PN_Pog) - distance from the point Pog to the nose perpendicular PN (perpendicular line from the point N to the line Po-Or);

POR_GNS (У-axis or angle POr_GnS) - angle formed by lines Po-Or and S-Gn (angle of inclination У-axis relative to the Frankfurt horizontal);

S_E (distance S_E or the length of the back of the skull base by Steiner) - distance from the point S to a constructive point E, which is located at an intersection of the perpendicular carried out from the point ppCond to the line S-N;

S_L (distance S_L or the front length of the skull base by Steiner) - from the point S to a constructive point L, which is formed at the intersection of the perpendicular carried out from the point Pog to the line Se-N;

SND (angle SND) - formed by lines S-N and N-D (indicates the anterior-posterior location of the symphysis (D - the center of the symphysis ossification) of the lower jaw to the base of the skull);

WITS (indicator Wits) - distance between constructive points AOclP and BOclP - projections of the corresponding points A and B on the line apOcP-ppOcP (OcPSt, closing plane by Steiner), indicates a linear interjaw ratio in the anterior-posterior direction (if the projection of point A lies ahead of the projection of point B then the indicator takes a positive value; if the projection of point A lies behind the projection of point B then the indicator takes a negative value).

Discussion

One of the important indicators of the quality of orthodontic treatment is the stability of the results. Unfortunately, to date, the search for its solution is still ongoing, as relapses of tooth-jaw disease in one degree or another occur according to M.M. Khalil', E.V. Filimonova and M.V. Vologina data in 20% of cases [17]. Investigation of A. Koniarova et al. [18] indicate that the number of stable cases is only 16% higher than the number of relapses with which the statistically proven connections of some indices of the incisors positions.

Ethnic [19, 22], sexual and age [21] features of the incisors positions point to the need for the development of techniques that allow to determine their individual characteristics, since commonly accepted standards recommended for optimal positioning of incisors can only be used as indicative [3].

With the help of the step regression method, for Ukrainian young men and women with orthognathic bite, taking into account peculiarities of teleroentgenographic indices, developed reliable models (with a determination coefficient greater than 0.50) of individual teleroentgenographic characteristics of the position of the lower medial incisors. It was found that in young men from 7 possible models, 5 were constructed with determination coefficient R^2 from 0.694 to 0.849, and in young women - all 7 possible models with determination coefficient R^2 from 0.595 to 0.794.

In the analysis of constructed models with a determination coefficient of greater than 0.50, it was found that in young men with orthognathic bite most often the regression equations included - an angle **ANB**, parameters of which indicate the angular interjaw ratio in the anterior-posterior direction and the vertical facial index **GL_SN_S**, whose parameters are determined by vertical correlations in the face profile (by 11.5%); lower face height **ANS_ME**, face angle **NBA_PTGN**, whose parameters determine the direction of development of the mandible and the distance **S_E**, or the length of the back part of the skull base by Steiner (by 7.7%). In young women with orthognathic bite most often the models included - the

angle **N_POG** (16.7%); the **Wits** indicator, whose parameters are determined by the linear interjaw ratio in the anterior-posterior direction (13.9%); inclination angle **I**, whose parameters determine the angle of inclination of the upper jaw to the nasal perpendicular (8.3%); the **H**-angle, whose parameters determine the angle of the Frankfurt plane to the base of skull, the maxillo-mandibular angle **MM**, whose parameters determine the angle at which the upper jaw is located in relation to the lower jaw in the sagittal plane, as well as the angle of the face axis **NBA_PTGN**, whose parameters determine the direction development of the mandible (by 5.6%).

The models developed by us allow to develop a computer program that can automatically calculate the individual teleroentgenographic characteristics of the position of the lower medial incisors, which, in turn, will help orthodontists achieve the maximum physiological and aesthetic results.

Conclusions

In young men with orthognathic bite of 7 possible models, 5 were constructed with a determination coefficient from 0.694 to 0.849, and in young women - all 7 models with a determination coefficient from 0.595 to 0.794. In young men, the most commonly included models were the angle ANB, the vertical vertical index **GL_SN_S** (by 11.5%); lower face height **ANS_ME**, face angle **NBA_PTGN** and distance **S_E** (by 7.7%); in young women - the angle **N_POG** (16.7%); **Wits** indicator (13.9%); inclination angle I (8.3%); **H**-angle, maxillo-mandibular angle **MM** and angle of facial axis **NBA_PTGN** (by 5.6%).

References

[1] Alabdullah, M. M., Saltaji, H., Abou-Hamed, H., & Youssef, M. (2014). The relationship between molar bite force and incisor inclination: a prospective cross-sectional study. *Int. Orthod.,* 12(4), 494-504. doi: 10.1016/j.ortho.2014.10.001

[2] Ciavarella, D., Tepedino, M., Gallo, C., Montaruli, G., Zhurakivska, K., Coppola, L., … Lo Russo, L. (2017). Postorthodontic position of lower incisors and gingival recession: A retrospective study. *J. Clin. Exp. Dent.,* 12(9), 1425-1430. doi: http://dx.doi.org/10.4317/jced.54261

[3] Dallel, I., Khemiri, M., Fathallah, S., Ben Rejeb, S., Tobji, S., & Ben Amor, A. (2015). Incisor repositioning: a new approach in orthodontics. *Orthod. Fr.,* 86(4), 327-338. doi: 10.1051/orthodfr/2015031

[4] Dmitriev, M. O. (2016). Definition of normative cephalometric parameters by Steiner method for Ukrainian young men and women. *World of Medicine and Biology,* 3(57), 28-32.

[5] Dmitriev, M. O. (2017). Identification of normative cephalometric parameters based on G. Schmuth method for young male and female Ukrainians. *Reports of Morphology,* 23(2), 288-292.

[6] Dmitriev, M. O. (2018). Determination of standard cephalometric parameters using the Downs method for Ukrainian adolescents. *Reports of Morphology,* 24(2), 22-26. doi: 10.31393/morphology-journal-2018-24(2)-03

[7] Dmitriev, M. O., Chugu, T. V., Gerasymchuk, V. V., & Cherkasova, O. V. (2017). Determination of craniometric and gnatometric indicators by A. M. Schvartz metod for Ukrainian boys and girls. *Biomedical and Biosocial Anthropology,* 29, 53-58.

[8] Downs, W. B. (1956). Analysis of the dentofacial profile. *Angle Orthodontist*, 26, 191-212.

[9] Duncan, L. O., Piedade, L., Lekic, M., Cunha, R. S., & Wiltshire, W. A. (2016). Changes in mandibular incisor position and arch form resulting from Invisalign correction of the crowded dentition treated nonextraction. *The Angle Orthodontist,* 86(4), 577-583. doi: https://doi.org/10.2319/042415-280.1

[10] Feng, F., Liu, Y., Chi, J., Wang, Y., Xing, B., Wang, Y., & Liu, W. (2018). Effects of anterior tooth crown inclination on occlusal relationship-A study in three-dimensional reconstruction. *Arch. Oral. Biol.,* 94, 48-53. doi: 10.1016/j.archoralbio.2018.06.015

[11] Garlock, D. T., Buschang, P. H., Araujo, E. A., Behrents, R. G., & Kim, K. B. (2016). Evaluation of marginal alveolar bone in the anterior mandible with pretreatment and posttreatment computed tomography in nonextraction patients. American *Journal of Orthodontics and Dentofacial Orthopedics,* 149(2), 192-201. doi: 10.1016/j.ajodo.2015.07.034

[12] Gunas, I. V., Dmitriev, M. O., Tikholaz, V. O., Shinkaruk-Dykovytska, M. M., Pastukhova, V. A., Melnik, M. P., & Rudiy, Yu. I. (2018). Determination of normal cephalometric parameters by J. McNamara method for Ukrainian boys and girls. *World of Medicine and Biology,* 1(63), 19-22. doi: 10.26724/2079-8334-2018-1-63-19-22

[13] Gunas, I. V., Dmitriev, M. O., Prokopenko, S. V., Shinkaruk-Dykovytska, M. M., & Yeroshenko, G. A. (2017). Determination regulatory cephalometric options by the method of Tweed International Foundation for Ukrainian boys and girls. *World of Medicine and Biology,* 4(62), 27-31. doi: 10.26724/2079-8334-2017-4-62-27-31

[14] Hernandez-Sayago, E., Espinar-Escalona, E., Barrera-Mora, J. M., Ruiz-Navarro, M. B., Llamas-Carreras, J. M., & Solano-Reina, E. (2013). Lower incisor position in different malocclusions and facial patterns. *Med. Oral. Patol. Oral. Cir. Bucal.,* 1, 18(2), 343-350. PMID: 23229262

[15] Holdaway, R. A. (1984). A soft-tissue cephalometric analysis and its use in orthodontic treatment planning. Part II. *Am. J. Orthod.,* 85, 279-293. doi: https://doi.org/10.1016/0002-9416(84)90185-4

[16] Huang, Y. P., & Li, W. R. (2015). Correlation between objective and subjective evaluation of profile in bimaxillary protrusion patients after orthodontic treatment. *Angle Orthod.,* 85(4), 690-6988. doi: 10.2319/070714-476.1

[17] Khalil', M. M., Filimonova, E. V., Vologina, M. V. (2008). The results of the study of the effectiveness of orthodontic treatment in the retention period. Abstracts are presented in the collection of scientific works of Volgograd State Medical University "Actual issues of experimental, clinical and preventive dentists". Collection of scientific papers of Volgograd State Medical University, 65(1), 346.

[18] Koniarova, A., Sedlata Juraskova, E., Spidlen, M., & Statelova, D. (2017). The influence of orthodontic non-extraction treatment on the change in the inclination and position of incisors in the Europoid race. Bratisl. Lek. Listy, 118(11), 662-668. doi: 10.4149/BLL_2017_126

[19] Kumari, L., & Das, A. (2017). Determination of Tweed's cephalometric norms in Bengali population. Eur. J. Dent., 11(3), 305-310. doi: 10.4103/ejd.ejd_274_16

[20] Kumari, N., Fida, M., & Shaikh, A. (2016). Exploration of variations in positions of upper and Lower incisors, overjet, overbite, and irregularity Index in orthodontic patients with dissimilar depths of Curve of spee. J. Ayub. Med. Coll.

Abbottabad, 28(4), 766-772.
[21] Linjawi, A I. (2016). Age- and gender-related incisor changes in different vertical craniofacial relationships. J. Orthod. Sci., 5(4), 132-137. doi: 10.4103/2278-0203.192116
[22] Lombardo, L., Perri, A., Arreghini, A., Latini, M., & Siciliani, G. (2015). Three-dimensional assessment of teeth first-, second- and third-order position in Caucasian and African subjects with ideal occlusion. Prog. Orthod., 16, 11. doi: 10.1186/s40510-015-0086-9
[23] Manea, I., Abascal-Pineda, I., Solano-Mendoza, B., Solano-Reina, A., & Solano-Reina, J. E. (2017). Facial growth pattern: Association between lower incisor position and symphyseal morphology. *Journal of the World Federation of Orthodontists,* 6(4), 147-151. doi: https://doi.org/10.1016/j.ejwf.2017.09.001
[24] McNamara, J. A. Jr. (1984). A method of cephalometric evaluation. *Am. J. Orthod.*, 86(6), 449-469. PMID: 6594933
[25] MoraHurtado, R., VeraSerna, M. E., & Uribe-Querol, E. (2016). Lower incisor inclination in relation to facial biotype in skeletal Class I patients. Inclinacion del incisivo inferior respecto al biotipo facial en pacientes clase I esqueletal. *Revista Mexicana de Ortodoncia,* 4(3), 157-162. doi: https://doi.org/10.1016/j.rmo.2016.10.031
[26] Schmuth, G. P. F. (1971). Methodische Schwierigkeiten bei der Anwendung der Röntgenkephalometrie in der Kieferorthopadie. *Fortschritte der Kieferorthopadie*, 32(2), 317-325.
[27] Schwarz, A. M. (1960). *Röntgenostatics; practical evaluation of the tele-X-ray-photo.* Publisher: Brooklyn, N.Y.: Leo L. Bruder.
[28] Steiner, C. C. (1959). Cephalometrics in clinical practice. Angle Orthod., 29, 8-29.
[29] Tepedino, M., Franchi, L., Fabbro, O., & Chimenti, C. (2018). Post-orthodontic lower incisor inclination and gingival recession-a systematic review. *Prog. Orthod.*, 19(1), 17. doi: 10.1186/s40510-018-0212-6
[30] Tweed, C. H. (1954). The Frankfort-Mandibular Incisor Angle (FMIA) in Orthodontic Diagnosis, Treatment Planning and Prognosis. *Angle Orthod.,* 3, 121-169.

ВИЗНАЧЕННЯ ІНДИВІДУАЛЬНИХ ТЕЛЕРЕНТГЕНОГРАФІЧНИХ ХАРАКТЕРИСТИК ПОЛОЖЕННЯ НИЖНІХ ПРИСЕРЕДНІХ РІЗЦІВ У УКРАЇНСЬКИХ ЮНАКІВ І ДІВЧАТ ІЗ ОРТОГНАТИЧНИМ ПРИКУСОМ

Дмітрієв М.О., Гунас І.В., Дзевульська І.В., Глушак А.А.

Етнічні, статеві та вікові особливості положення різців вказують на необхідність розробки методик, що дозволяють визначити їх індивідуальні характеристики, оскільки загально прийняті стандарти, рекомендовані для оптимального позиціонування різців, можуть бути використані лише як орієнтовні. Мета дослідження - шляхом вивчення телерентгенографічних показників і проведення прямого покрокового регресійного аналізу в юнаків і дівчат України з ортогнатичним прикусом розробити та провести аналіз математичних моделей індивідуальних характеристик положення нижніх присередніх різців. За допомогою пристрою Veraviewepocs 3D, Morita (Японія) у 38 юнаків (віком від 17 до 21 року) та 55 дівчат (віком від 16 до 20 років) з оклюзією, наближеною до ортогнатичного прикусу та збалансованими обличчями, були отримані бокові телерентгенограми. Цефалометричний аналіз проводили за допомогою програмного забезпечення OnyxCeph³™. Цефалометричні точки та виміри проводили згідно рекомендацій A.M. Schwarz, J. McNamara, W.B. Downs, R.A. Holdway, P.F. Schmuth, C.C. Steiner та C.H. Tweed. Згідно вищенаведених методик, в ліцензійному пакеті "Statistica 6,0" з використанням прямого покрокового регресійного аналізу проведено моделювання телерентгенографічних характеристик положення нижніх присередніх різців (відстань 1I_NB, відстань 1I_APog, кут 1I_DOP, кут IMPA, кут Mand1_NB, кут FMIA та кут Mand1_MeIm). В юнаків із ортогнатичним прикусом із 7 можливих моделей телерентгенографічних характеристик положення нижніх присередніх різців побудовано 5 з коефіцієнтом детермінації R^2 від 0,694 до 0,849, а у дівчат - усі 7 можливих моделей з коефіцієнтом детермінації R^2 від 0,595 до 0,794. В юнаків найбільш часто до регресійних рівнянь входили - кут ANB та лицевий вертикальний індекс GL_SN_S (по 11,5%); нижня висота обличчя ANS_ME, кут лицевої вісі NBA_PTGN та відстань S_E (по 7,7%). У дівчат найбільш часто до моделей входили - кут N_POG (16,7%); показник Wits (13,9%); інклінаційний кут I (8,3%); H-кут, верхньощелепно-нижньощелепний кут MM та кут лицевої вісі NBA_PTGN (по 5,6%). Таким чином, за допомогою методу покрокової регресії з включенням, в українців юнацького віку на основі особливостей телерентгенографічних показників розроблені та проведений аналіз достовірних моделей індивідуальних телерентгенографічних характеристик положення нижніх присередніх різців.

Ключові слова: *положення нижніх присередніх різців, телерентгенографія, регресійний аналіз, ортогнатичний прикус, юнаки, дівчата.*

ОПРЕДЕЛЕНИЕ ИНДИВИДУАЛЬНЫХ ТЕЛЕРЕНТГЕНОГРАФИЧЕСКИХ ХАРАКТЕРИСТИК ПОЛОЖЕНИЯ НИЖНИХ ЦЕНТРАЛЬНЫХ РЕЗЦОВ У УКРАИНСКИХ ЮНОШЕЙ И ДЕВУШЕК С ОРТОГНАТИЧЕСКИМ ПРИКУСОМ

Дмитриев Н.А., Гунас И.В., Дзевульская И.В., Глушак А.А.

Этнические, половые и возрастные особенности положения резцов указывают на необходимость разработки методик, позволяющих определить их индивидуальные характеристики, поскольку общепринятые стандарты, рекомендованные для оптимального позиционирования резцов, могут быть использованы только как ориентировочные. Цель исследования - путем изучения телерентгенографических показателей и проведения прямого пошагового регрессионного анализа у юношей и девушек Украины с ортогнатическим прикусом разработать и провести анализ математических моделей индивидуальных характеристик положения нижних центральных резцов. С помощью устройства Veraviewepocs 3D, Морита (Япония) у 38 юношей (в возрасте от 17 до 21 года) и 55 девушек (в возрасте от 16 до 20 лет) с окклюзией, приближенной к ортогнатическому прикусу и сбалансированными лицами, были получены боковые телерентгенограммы. Цефалометрический анализ проводили с помощью программного обеспечения OnyxCeph³™. Цефалометрические точки и измерения проводили согласно рекомендациям A.M. Schwarz, J. McNamara, W.B. Downs, R.A. Holdway, P.F. Schmuth, C.C. Steiner и C.H. Tweed. Согласно вышеприведенных методик, в лицензионном пакете "Statistica 6.0" с использованием прямого пошагового регрессионного анализа проведено моделирование телерентгенографических характеристик положения нижних центральных резцов (расстояние 1I_NB, расстояние 1I_APog, угол 1I_DOP, угол IMPA, угол Mand1_NB, угол FMIA и угол Mand1_MeIm). У юношей с ортогнатическим прикусом из 7 возможных моделей телерентгенографических характеристик

положения нижних центральных резцов построено 5 с коэффициентом детерминации R^2 от 0,694 до 0,849, а у девушек - все 7 возможных моделей с коэффициентом детерминации R^2 от 0,595 до 0,794. У юношей наиболее часто в регрессионные уравнения входили - угол ANB и лицевой вертикальный индекс GL_SN_S (по 11,5%); нижняя высота лица ANS_ME, угол лицевой оси NBA_PTGN и расстояние S_E (по 7,7%). У девушек наиболее часто в модели входили - угол N_POG (16,7%); показатель Wits (13,9%); инклинационный угол I (8,3%); H-угол, верхнечелюстной-нижнечелюстной угол MM и угол лицевой оси NBA_PTGN (по 5,6%). Таким образом, с помощью метода пошаговой регрессии с включением, у украинцев юношеского возраста на основе особенностей телерентгенографических показателей разработаны и проведен анализ достоверных моделей индивидуальных телерентгенографических характеристик положения нижних центральных резцов.

Ключевые слова: *положение нижних центральных резцов, телерентгенография, регрессионный анализ, ортогнатический прикус, юноши, девушки.*

DOI: 10.31393/morphology-journal-2018-24(3)-04 Reports of Morphology, Vol. 24, №3, Pages 26-31

ISSN 1818-1295 eISSN 2616-6194

REPORTS OF MORPHOLOGY

Official Journal of the Scientific Society of Anatomists, Histologists, Embryologists and Topographic Anatomists of Ukraine

journal homepage: https://morphology-journal.com

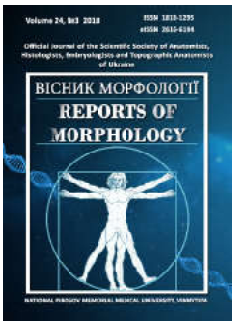

Features of structural-morphological changes in cases of experimental intestinal antibiotic-induced dysbiosis

Bobyr V.V.[1], Poniatovskyi V.A.[1], Chobotar A.P.[1], Stechenko L.O.[1], Kryvosheyeva O.I.[1], Nazarchuk O.A.[2], Kovalenko O.O.[1]

[1]Bogomolets National Medical University Ministry of Health of Ukraine, Kyiv, Ukraine;
[2]National Pirogov Memorial Medical University, Vinnytsya, Ukraine

ARTICLE INFO
Received: 25 July, 2018
Accepted: 20 August, 2018

UDC: 616.34: 615.211.099

CORRESPONDING AUTHOR
e-mail: vitalibobyr@ukr.net
Bobyr V.V.

Nowadays, scientists often define dysbiosis as a condition of a microbial ecological system, in which there is a simultaneous abnormality of the functions and interaction mechanisms of its key components: macroorganism and indigenous microbiota associated with the mucous membranes of cavities and skin. At the same time, obviously, the basis of all these processes is changes of structural intestinal components that are caused by qualitative and quantitative changes in the normal microflora. Purpose: to study the ultrastructural organization of the mucous membrane of the small intestine of mice after the formation of dysbiosis of the intestine. Outbred white mice in the number of 40 units (20 - experimental and 20 control) was served as an experimental model. Antibacterial drugs (ampicillin, metronidazole and gentamicin) are used to form dysbiosis. The conducted experiments are allowed to establish that the using of antibacterial drugs in the above-mentioned doses contributes to shortening the length of the microvillus and their reduction (disappearance) in some places, destruction with subsequent disintegration. According to the results of electronograms analysis, the assumption was made about stimulating the secretory function of the small intestine enterocytes by powerful doses of antibacterial drugs. In addition, it was found that the formation of dysbiotic disorders is accompanied by a defect of the connection between epithelial cells due to the expansion of the intercellular space and the disappearance of the dense plate. Research results also indicate that antibiotics that were used in the experiment can cause development of apoptosis. In addition, it has been shown that, on the background of the dysbiotic disorders formation, the activation of immune processes is taking place, as evidenced by the appearance of a significant number of Paneth cells, plasma cells with enlarged tubules, apparently due to their filling with immunoglobulins, as well as the growth of numbers of luminalis eosinophils and basophils. The ability of antibiotics to form dysbiotic states with pronounced cytodestructive disorders in the epithelium of the small intestine with the development of apoptosis was substantiated; the argument about the immune stimulating effect of antibiotic induced dysbiosis is argued.

Keywords: *antibiotics, dysbiosis, intestine, microbiota, electron microscopy.*

Introduction

According to the latest data human intestine contains about 100 trillion bacteria, 70-80% of which today cannot be cultivated yet [2, 8, 13]. Nowadays, scientists often consider the intestinal microbiota as a kind of extracorporeal organ, which provides vital aspects of human vital activity [2, 6, 22, 23]. Every man is considered to have several hundred of bacterial species. Among them there are predominantly Gram-positive *Firmicutes* (first of all *Clostridium, Enterococcus, Lactobacillus*) and Gram-negative ones *Bacteroides*. In general, the human microbe is characterized by pronounced multifunctional activity that provides the vital functions of the macroorganism. But, at the same time, according to scientists view the normal microflora differs and expressed susceptibility, and even, may be a kind of indicator of adverse effects on the body [25]. The composition of a normal microflora can be influenced by a number of factors such as inflammatory bowel disease, psycho-emotional overload, unfavorable ecological picture, etc. [14,

24]. However, the effect of chemotherapeutic drugs, especially with the oral mechanism of administration is thought among the prior ones. Earlier, a violation of the quantitative and qualitative composition of the normal intestinal microflora was called dysbiosis. Although, the term "dysbiosis", was proposed was proposed by A. Nissle in 1916, and was associated with fungal and fermentative intestinal dyspepsia, had been caused by a decrease in the concentration of the *Escherichia coli* in the intestine. For sure, this term does not correspond to modern postulates about the nature of violations in human microbiocenosis, because it is limited to the statement of changes exclusively to the bacterial component of the intestinal consortium [21].

Because of this, the term "dysbiosis" is more often used today. This one more in detail characterizes the microbial ecology and, in particular, indicates that in the case of dysbiosis disturbances, the ratio between different representatives of microbial world (bacteria, fungi, viruses, protozoa) changed, the latter is accompanied changes in their biological properties and mechanisms of interaction with macroorganism [15, 17].

Nowadays, scientists most often identify dysbiosis as a condition of a microbial ecological system, in which there is a simultaneous violation of the functions and mechanisms of interaction of its key components: macroorganism and indigenous microbiota associated with the mucous membranes of the cavities and skin [4, 11, 17].

At the same time, obviously, changes in the structural components of the intestine, which are caused by qualitative and quantitative changes of normobiota are the basis of all these processes. It is important that the intestinal microflora of a person does not differ much from the intestinal microflora of other mammals, which facilitates the methodology of its study. [11, 12].

The *aim* - to study the ultrastructural organization of the mucous membrane of the small intestine of mice after the formation of dysbiosis of the intestine.

Materials and methods

As experimental model there were used 40 laboratory white mice (20 - experimental and 20 - control ones). These animals were kept in accordance with "Standard rules on the ordering, equipping and maintenance of experimental biological clinics (vivarium)". All animal experiments complied with the ARRIVE guidelines and were carried out in accordance with the general ethical principles of experiments on animals, adopted by the First National Congress of Ukraine on Bioethics (Kyiv, 2001), Law of Ukraine No. 3447-IV of February 21, 2006 "On the Protection of Animals from Cruel Treatment" and associated guidelines, EU Directive 2010/63/EU for animal experiments, certified by the Ethics Commission of Bogomolets National Medical University (protocol No. 65 of October 3, 2012) [1].

For the formation of dysbiotic states there were used antibacterial drugs, daily doses of which were for ampicillin and metronidazole 10 mg, for gentamicin 2.9 mg [3]. Animals were injected intragastrically using a tuberculin syringe with a needle with thickening at the end. Simultaneously with the drinking water, the specified antibiotics were added (1 g of ampicillin, 1 g of metronidazole and 290 mg of gentamicin per 1000 ml of water). The selection of feces and the administration of antibiotic solutions to animals were repeated for 5 days, with a daily determination of the total number of fecal microflora and its individual representatives (*Escherichia, Bifidobacteria, Lactobacilli*).

The animals were killed on the six day of the experiment for the purpose of pathology section examination. For the electron microscopic examination small pieces of small intestine of 1 mm3 in size were prepared. The specimens of intestine were prior fixed with a buffer solution of glutaraldehyde fixation for 1 hour, and then, after washing with a buffer, they were finished with 1% osmium tetroxide solution for 1 hour.

After dehydration in ethanol of increasing concentration and acetone, the material was poured into a mixture of epoxy resins (epon and araldite) and polymerized at +60°C for 36 hours. Cutting-up the samples were obtained using glass knives on ultra-microcrystal "LKB III, Sweden" and investigated in electron microscopes Jeol JEM 100 CX II (Japan) and PEM-125 (Ukraine). Before microscopy, the sections were contrasted with uranyl acetate and lead citrate according to the standard procedure [9, 20].

Results

The method used to simulate dysbiosis allowed us to obtain qualitative and quantitative disturbances in the composition of normal intestinal microflora of animals, which were confirmed bacteriologically. In a result of our experiments there was found that after the use of antibacterial drugs at the above doses, a visual shortening of the length of the microvilli was observed, and in places reduction (disappearance) or degradation with subsequent disintegration (Fig. 1, 2) compared with the control (Fig. 3). In this case, the total desquamation of microvilli was also often noted; in such cells, the brush border was absent, the plasma membrane

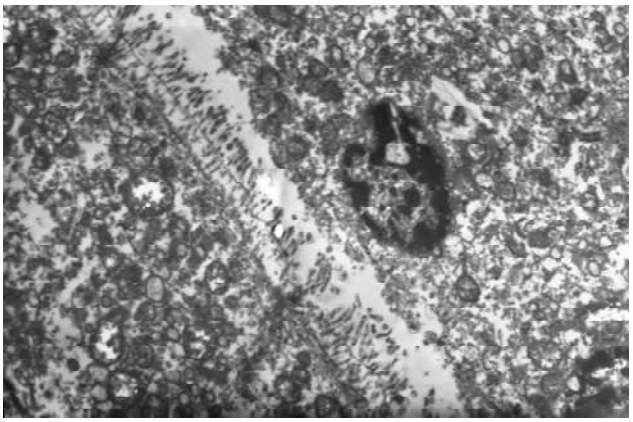

Fig. 1. Electronic microphotography. Local reduction of the brush border of enterocytes of the small intestine of the mouse with antibiotic induced dysbiosis. x4200.

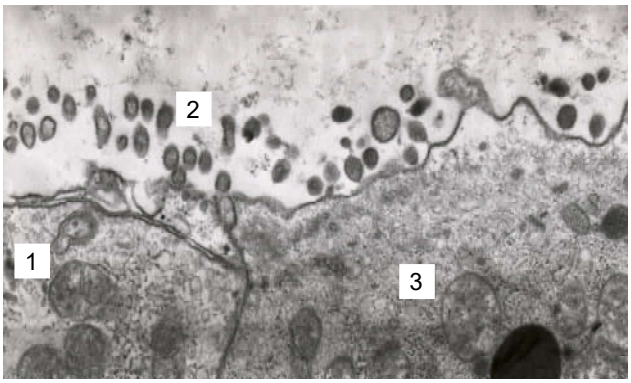

Fig. 2. Electronic microphotography. Desquamated microvilli. x4200. 1 - autophagosome; 2 - microvilli; 3 - mitochondria.

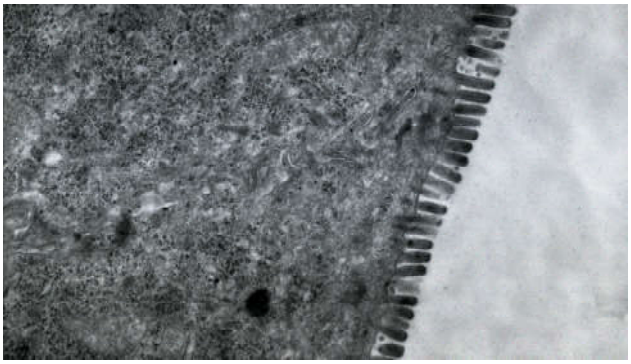

Fig. 3. Electronic microphotography. Brush border of enterocytes of the small intestine of the mouse. Control. x4200.

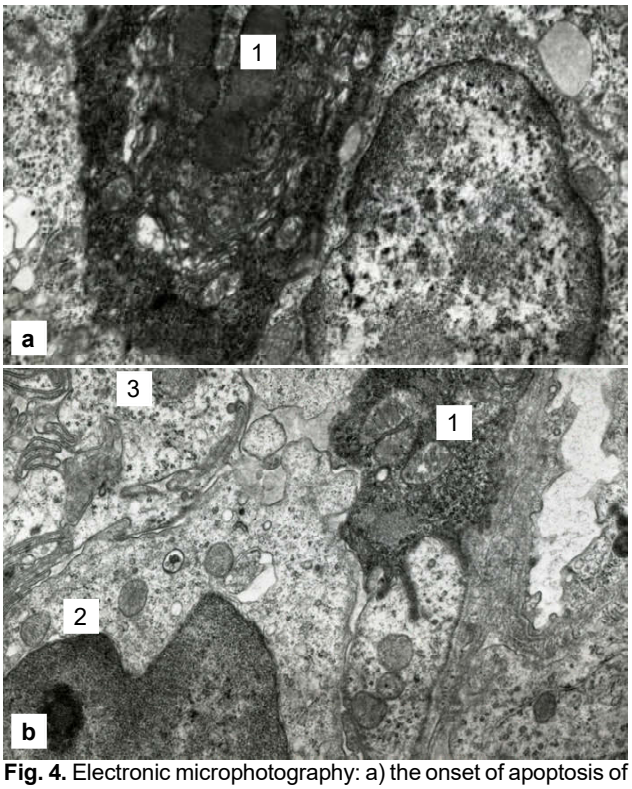

Fig. 4. Electronic microphotography: a) the onset of apoptosis of enterocytes of the small intestine (1); b) prolonged apoptosis of enterocytes of the small intestine. The death of enterocytes (1); lymphocytes between enterocytes (2); enterocytes (3). x4200.

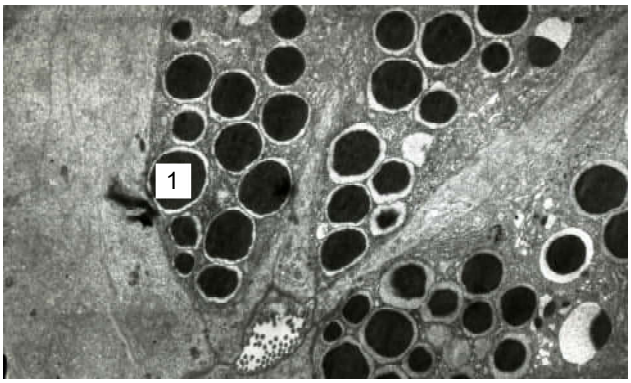

Fig. 5. Electronic microphotography. The accumulation of Paneth cells after the formation of dysbiosis. Paneth cell granules (1). x4200.

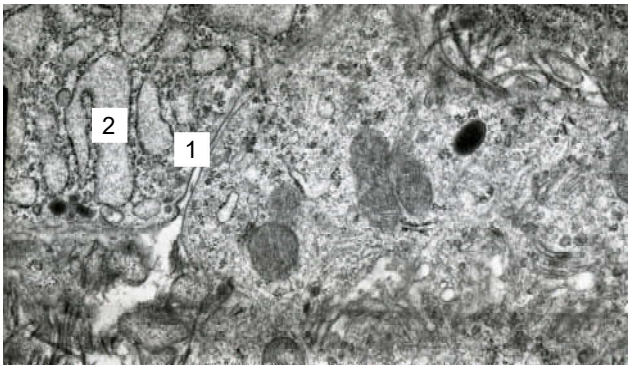

Fig. 6. Electronic microphotography. Lamina propria of mucous membrane. Plasmocytes (1). Expanded tubules of plasmocytes (2). x4200.

was smoothed, and in the enterocytes the edema of the mitochondria and the formation of autophagosoms were noted.

The clarification of the matrix of the cytoplasm, which indicated an insignificant edema was determined. At the same time, the locking lamina of the contacts was considerably thinned - as a result of which the expansion of contacts between the cells was observed.

We have found that the formation of dysbiotic disorders is accompanied by a violation of the relationship between epithelial cells due to the expansion of the intercellular space. The results of the studies also indicate the ability of the antibiotics, have been used in the experiment, to induce apoptosis: the cells were displaced to the basement membrane, they were densified, especially in the cytoplasm, there were no nuclei already visualized in electronogram, all organelles and predecessors of apoptosis were condensed and displaced to the basement membrane with subsequent exclusion from a number of epithelial cells (Figures 4a-b). The conducted experiments also allowed to establish, that activation of immune processes took place against the background of the formation of dysbiotic disorders, as evidenced by the appearance of a significant number of Paneth cells (Fig. 5). A significant response from the immune system was also proved by the presence of a significant number of plasma cells. In some electronic micro-photographs, the expansion of the tubule cells of the plasma

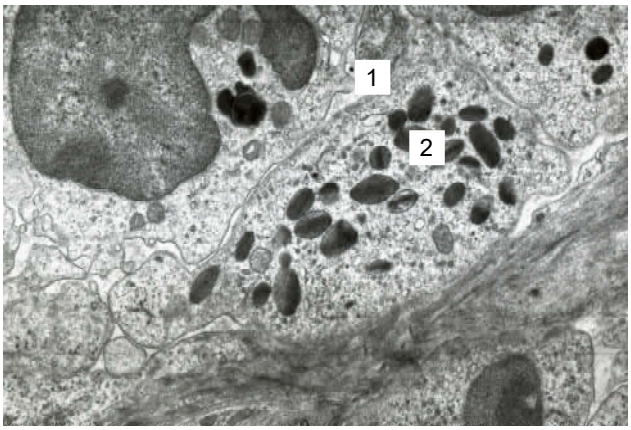

Fig. 7. Electronic microphotography. Eosinophil in the lumen of the capillary (1) with characteristic longitudinal beads with core (2). x4200.

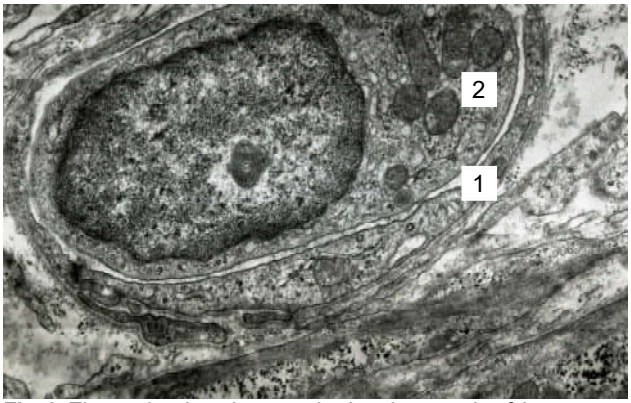

Fig. 8. Electronic microphotography. Lamina propria of the mucous membrane of the small intestine. Enlightenment of the capillary (1), which contains B-lymphocyte (2). x4200.

cells was clearly traceable, apparently due to their filling with immunoglobulins (Fig. 6). In addition, the analysis of electronic microphotographs showed that in the case of antibiotic induced dysbiosis, the number of educational eosinophils and basophils increased (Fig. 7).

These cells were like indicators of allergic reactions because of their direct involvement in the protective allergic and anaphylactic reactions of the body. An increase in the number of B-lymphocytes between enterocytes and in the lumen of capillaries was evidenced by the formation of the immune response (Fig. 8).

Discussion

Normal microflora of the human body is represented by an extraordinary qualitative and quantitative diversity of microorganisms. The microbiota of the intestine, as one of the most numerous biotops in the body, is the consortium of microorganisms, been very sensitive to many factors [2, 7, 10, 23]. There is an assumption that dysbiosis, or a violation of the quantitative and qualitative composition of the normal intestinal microflora, leads to violations of the microbial ecological system, functions, mechanisms of interaction of the macroorganism and indigenous microbiota, and changes in the structural components of the intestine. The scientific interest is the in-depth study of the ultrastructural organization of the mucous membrane of the small intestine under conditions of dysbiotic changes [4, 16].

According to the data of bacteriological analysis there was proved, that modeling of dysbiosis allowed to obtain qualitative and quantitative violations of the composition of normal intestinal microflora of experimental animals. Obviously, the oral administration of antibacterial drugs can contribute to the development of functional disorders in the intestine, which are already manifested at the ultrastructure level. According to the researchers' reports the effect of dysbiotic disturbances on the suction and secretory activity of the small intestine with destructive changes in columnar enterocytes with a rim was known [18]. The cytoplasmic matrix, which was registered in the study, showed a slight edema. At the same time, there was observed the considerably thinned locking lamina gut, that resulted in the expansion of the contacts between the enterocytes.

According to a various studies, the ability of some drugs, including acetaminophen, has been shown to cause dysbiotic disturbances in animals. Electronic microscopy picture characterises these violations as one accompanied by structural changes in stem cells, namely, hypertrophy of mitochondria, which manifests itself as a clarification of the matrix and reduction of crypt [5]. In the formation of antibiotic induced dysbiosis in mice such changes were not registered. The formation of dysbiotic disorders was established to be accompanied by a violation of the relationship between epithelial cells due to the expansion of the intercellular space. In our study, the emergence of a significant number of Paneth cells in the background of the formation of dysbiotic violations was found to indicate the activation of immune processes. Recent studies have proved the important role of these cells in the regulation of intestinal homeostasis, and identified Paneth cells as an important component of the protective mechanisms of congenital immunity [5, 6].

The prospect of further research is the in-depth study of mechanisms stimulating the influence of antibiotic-induced dysbiosis on local immune reactivity.

Conclusions

1. The ability of antibacterial drugs to form dysbiotic states in animals accompanied by marked cytodestructive disorders in the small intestine epithelium, namely, the shortening and desquamation of microvilli, edema of mitochondria, cytoplasmic matrix enlightenment, the violation of the relationship between epithelial cells and the development of apoptosis, have been substantiated experimentally.

2. An argumentative assumption has been made about the stimulating effect of antibiotic induced dysbiosis on the activation of immune defense reactions. This has been confirmed by the growth in the number of Paneth cells, plasma cells filled with immunoglobulins, educational eosinophils and basophils, as well as an increase in the number of B-lymphocytes that are recorded between enterocytes and the lumen of the capillaries.

References

[1] *About protecting animals from abuse.* (2006). The Law of Ukraine science 21.02.2006, № 3447-IV.

[2] Bilen, M., Dufour, J. C., Lagier, J. C., Cadoret, F., Daoud, Z., Dubourg, G., & Raoult, D. (2018). The contribution of culturomics to the repertoire of isolated human bacterial and archaeal species. *Microbiome,* 6(1), 94. doi: 10.1186/s40168-018-0485-5

[3] Bobyr, V. V., Ponyatovsky, V. A., Djugikowa, E. M., & Shyrobokov V. P., (2015). Modeling of dysbiotic disorders with laboratory animals. *Biomedical and Biosocial Anthropology,* 24, 230-233.

[4] Bron, P., Van Baarlen, P., & Kleerebezem M. (2011). Emerging molecular in-sights into the interaction between probiotics and the host intestinal mucosa. *Nat. Rev. Microbiol*., 10, 66-78.

[5] Bykov, V. L., (2014). Paneth cells: history of discovery, structural and functional characteristics and the role in the maintenance of homeostasis in the small intestine. *Morphology: Archives of anatomy, histology, and embryology,* 145(1), 67-80.

[6] Chang, P. V., Hao, L., Offermanns, S., & Medzhitov, R. (2014). The microbial metabolite butyrate regulates intestinal macrophage function via histone deacetylase inhibition. *Proceedings of the National Academy of Sciences of the United States of America,* 111(6), 2247-2252. doi: 10.1073/pnas.1322269111

[7] Dethlefsen, L., & Relman, D. A. (2011). Incomplete recovery and individualized responses of the human distal gut microbiota to repeated antibiotic perturbation. *Proc. Natl. Acad. Sci. USA,* 108(1), 4554-4561. doi: 10.1073/pnas.1000087107

[8] Duvallet, C., Gibbons, S. M., Gurry, T., Irizarry, R. A., & Alm, E. J. (2017). Meta-analysis of gut microbiome studies identifies disease-specific and shared responses. *Nat. Commun.,* 8, 1-46. doi: 10.1038/s41467-017-01973-8

[9] Dykstra, M. J., & Reuss, L. E. (2003). *Biological electron microscopy: theory, techniques, and troubleshooting.* Springer Science & Business Media.

[10] Falcony, G., Joossens, M., Vieira-Silva, S., Wang, J., Darzi, Y., Faust, K., … Raes, J. (2016). Population-level analysis of gut microbiome variation. *Science*, 352(6285), 560-564. doi: 10.1126/science.aad3503

[11] Johnson, C. D., & Kudsk, K. A. (1999). Nutritional and intestinal mucosal immunity. *Clin. Nutr.*, 18(6), 337-344. doi: https://doi.org/10.1016/S0261-5614(99)80012-0

[12] Kravchuk, R. I., Sheybak, V. M., Zhmakin, A. I., Goretsky, M. V., & Egorov, A. S. (2007). Characteristics of ultrastructural changes in the mucous membrane of the jejunum after acetaminophen-induced rats dysbacteriosis. J*ournal of Grodno State Medical University*, 1, 106-109.

[13] Lagier, J. C., Edouard, S., Pagnier, I., Mediannikov, O., Drancourt, M., & Raoult, D. (2015). Current and past strategies for bacterial culture in clinical microbiology. *Clinical microbiology reviews,* 28(1), 208-236. doi: 10.1128/CMR.00110-14

[14] Lin, L., & Zhang, J. (2017). Role of intestinal microbiota and metabolites on gut homeostasis and human diseases. *BMC immunology,* 18(1), 2. doi: 10.1186/s12865-016-0187-3.

[15] Lloyd-Price, J., Abu-Ali, G., & Huttenhower, C. (2016). The healthy human microbiome. *Genome Med.,* 8(1), 51. doi: 10.1186/s13073-016-0307-y

[16] Mokili, J. L., Rohwer, F., & Dutilh, B. E. (2012). Metagenomics and future perspectives in virus discovery. *Current Opinion in Virology*, 2(1), 63-77. doi: 10.1016/j.coviro.2011.12.004

[17] Moore, H. C., Jacoby, P., Taylor, A., Harnett, G., Bowman, J., Riley, T. V., … Lehmann, D. (2010). The interaction between respiratory viruses and pathogenic bacteria in the upper respiratory tract of asymptomatic Aboriginal and non-Aboriginal children. *Pediatr. Infect. Dis. J.*, 29(6), 540-545. doi: 10.1097/INF.0b013e3181d067cb

[18] Ovcharova, A. N. (2012). *The morphological characteristics of the small and large intestine in experimental primary dysbiosis and its correction by probiotics.* (Abstract dis. Cand. Biol. Sciences). Scientific research Institute of Human Morphology, Moscow, RAMS.

[19] Qin, J., Li, R., Raes, J., Arumugam, M., Burgdorf, K. S., Manichanh, C. … Wang, J. (2010). A human gut microbial gene catalogue established by metagenomic sequencing. *Nature,* 464, 59-65. doi: 10.1038/nature08821

[20] Sarkisova, D. S., & Perova, Yu. L. (Edit.) (1996). *Microscopic technique. Guide for doctors and laboratory technicians.* Moscow: Medicine.

[21] Shirobokov, V. P., Yankovsky, D. S., & Dyment, G. S. (2014). *Microbes in biogeochemical processes, the evolution of the biosphere and the existence of mankind*. K.: Veres.

[22] The Human Microbiome Project Consortium (2012). A framework for human microbiome research. *Nature,* 486(7402), 215-221. doi: 10.1038/nature11209

[23] Thursby, E., & Juge, N. (2017). Introduction to the human gut microbiota. *The Biochemical journal,* 474(11), 1823-1836. doi: 10.1042/BCJ20160510

[24] Williams, M. D., Ha, C. Y., & Ciorba, M. A. (2010). Probiotics as therapy in gastroenterology: A study of physician opinions and recommendations. *J. Clin. Gastroenterol*, 44(9), 631-636. doi: 10.1097/MCG.0b013e3181d47f5b

[25] Yankovsky, D. S., Shirobokov, V. P., Volosovets, A. P., & Moiseenko, R. A., Dyment, G. S. (2013). Human microbiome and modern methods of its improvement. *Journal of the National Academy of Medical Sciences of Ukraine*, 19(4), 411-420.

ОСОБЛИВОСТІ СТРУКТУРНО-МОРФОЛОГІЧНИХ ЗМІН ПРИ ЕКСПЕРИМЕНТАЛЬНОМУ АНТИБІОТИКОІНДУКОВАНОМУ ДИСБІОЗІ КИШКІВНИКА

Бобир В.В., Понятовський В.А., Чоботар А.П., Стеченко Л.О., Кривошеєва О.І., Назарчук О.А., Коваленко О.О.

Сьогодні вчені найчастіше визначають дисбіози як такий стан мікробної екологічної системи, при якому спостерігається одночасне порушення функцій та механізмів взаємодії її ключових компонентів: макроорганізму та індигенної мікробіоти, асоційованої зі слизовими оболонками порожнин та шкірних покривів. Разом із тим, очевидно, в основі всіх цих процесів лежать зміни структурних компонентів кишківника, які викликані якісними та кількісними змінами нормофлори. Мета роботи - вивчити ультраструктурну організацію слизової оболонки тонкої кишки мишей після формування дисбіотичних станів кишківника. Експериментальною моделлю слугували безпородні білі миші у кількості 40 одиниць (20 дослідних та 20 контрольних). Для формування дисбіотичних станів використано антибактеріальні препарати (ампіцилін, метронідазол та гентаміцин). Проведені експерименти дозволили встановити, що використання антибактеріальних препаратів у вищезазначених дозах сприяє вкороченню довжини мікроворсинок та місцями їх редукції (зникнення), деструкції із подальшим розпадом. За результатами аналізу електронограм зроблено припущення про стимуляцію секреторної функції ентероцитів

тонкої кишки потужними дозами антибактеріальних препаратів. Встановлено, що формування дисбіотичних порушень супроводжується порушенням зв'язку між епітеліальними клітинами за рахунок розширення міжклітинного простору і зникненням щільної пластинки. Результати досліджень також свідчать про здатність використаних в експерименті антибіотиків викликати розвиток апоптозу. Показано, що на фоні формування дисбіотичних порушень відбувається активізація імунних процесів, про що свідчить поява значної кількості клітин Панета, плазматичних клітин з розширеними канальцями, очевидно, за рахунок їх наповнення імуноглобулінами, а також зростання кількості просвітних еозинофілів і базофілів. Таким чином, обґрунтована здатність антибіотиків формувати дисбіотичні стани з вираженими цитодеструктивними порушеннями в епітелії тонкої кишки з розвитком апоптозу; аргументовано припущення про імуностимулюючий вплив антибіотикоіндукованого дисбіозу.

Ключові слова: *антибіотики, дисбіоз, кишківник, мікробіота, електронно-мікроскопічне дослідження.*

ОСОБЕННОСТИ СТРУКТУРНО-МОРФОЛОГИЧЕСКИХ ИЗМЕНЕНИЙ ПРИ ЭКСПЕРИМЕНТАЛЬНОМ АНТИБИОТИКОИНДУЦИРОВАННОМ ДИСБИОЗЕ КИШЕЧНИКА

Бобирь В.В., Понятовский В.А., Чоботар А.П., Стеченко Л.А., Кривошеева О.И., Назарчук А.А., Коваленко А.О.

Сегодня ученые чаще всего определяют дисбиозы как такое состояние микробной экологической системы, при котором наблюдается одновременное нарушение функций и механизмов взаимодействия ее ключевых компонентов: макроорганизма и индигенной микробиоты, ассоциированной со слизистыми оболочками полостей и кожных покровов. Вместе с тем, очевидно, в основе всех этих процессов лежат изменения структурных компонентов кишечника, вызванные качественными и количественными изменениями нормофлоры. Цель работы - изучить ультраструктурную организацию слизистой оболочки тонкой кишки мышей после формирования дисбиотических состояний кишечника. Экспериментальной моделью служили беспородные белые мыши в количестве 40 единиц (20 исследовательских и 20 контрольных). Для формирования дисбиотических состояний использованы антибактериальные препараты (ампициллин, метронидазол и гентамицин). Проведенные эксперименты позволили установить, что использование антибактериальных препаратов в вышеуказанных дозах способствует укорочению длины микроворсинок и местами их редукции (исчезновению), деструкции с последующим распадом. По результатам анализа электроннных микрофотографий сделано предположение о стимуляции секреторной функции энтероцитов тонкого кишечника мощными дозами антибактериальных препаратов. Кроме того, установлено, что формирование дисбиотических нарушений сопровождается нарушением связи между эпителиальными клетками за счет расширения межклеточного пространства и исчезновением плотной пластинки. Результаты исследований также свидетельствуют о способности использованных в эксперименте антибиотиков вызвать развитие апоптоза. Показано, что на фоне формирования дисбиотических нарушений происходит активация иммунных процессов, о чем свидетельствует появление значительного количества клеток Панета, плазматических клеток с расширенными канальцами, очевидно, за счет их наполнения иммуноглобулинами, а также увеличение количества просветительных эозинофилов и базофилов. Таким образом, обоснована способность антибиотиков формировать дисбиотические состояния с выраженными цитодеструктивными нарушениями в эпителии тонкого кишечника с развитием апоптоза; аргументировано предположение об иммуностимулирующем влиянии антибиотик-индуцированного дисбиоза.

Ключевые слова: *антибиотики, дисбиоз, кишечник, микробиота, электронно-микроскопическое исследование.*

DOI: 10.31393/morphology-journal-2018-24(3)-05 Reports of Morphology, Vol. 24, №3, Pages 32-36

ISSN 1818-1295 eISSN 2616-6194

REPORTS OF MORPHOLOGY

Official Journal of the Scientific Society of Anatomists, Histologists, Embryologists and Topographic Anatomists of Ukraine

journal homepage: https://morphology-journal.com

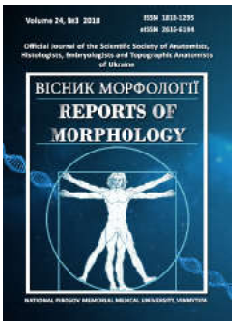

Features of total body sizes and anthropometric torso sizes in female volleyball players of mesomorphic somatotype

Sarafinyuk L.A.[1], Fomina L.V.[1], Khavtur V.O.[2], Fedoniuk L.Ia.[2], Khapitska O.P.[1], Stefanenko I.S.[1]

[1]National Pirogov Memorial Medical University, Vinnytsya, Ukraine;
[2]SHEI "I.Ya. Horbachevsky Ternopil State Medical University of the Ministry of Health of Ukraine", Ternopil, Ukraine

ARTICLE INFO
Received: 17 July, 2018
Accepted: 10 August, 2018

UDC: 572.5:796.325-05:611.018.2

CORRESPONDING AUTHOR
e-mail: Isarafinyuk@gmail.com
Sarafinyuk L.A.

Determination of constitutional parameters that are inherent in highly skilled athletes of a particular sport can serve as reliable predictive markers during sport selection. But the last time an indisputable fact is the somatotypological conditionality of individual sizes that characterize the external structure of the body, and the visceral structures of the organism. The purpose of the work is to establish differences in the anthropometric dimensions between young women volleyball players of high level of athletic skill and non-sports young women belonging to the mesomorphic somatotype. On the base of the research center of the National Pirogov Memorial Medical University, we conducted an anthropo-somatotypological study of 127 female volleyball players of youth age (from 16 to 20 years) with a high level of athletic skill. Sports experience in all cases was greater than 3 years. From the database of research center of the National Pirogov Memorial Medical University was selected 140 practically healthy young women of the same age who were not engaged in sports. Anthropometric measurements were carried out using the method of V.V. Bunak (1941), somatotypological research - according to the estimated modification of the Heath-Carter method (1990). After the conducted somatotyping, it was found that 29 volleyball players and 33 non-sports young women belonged to the mesomorphic type of constitution. The analysis of the obtained results is carried out in the licensed package of Statistica 5.5 using nonparametric methods of evaluation of indicators. In the volleyball players of the mesomorphic somatotype, compared to young women who are not engaged in sports of the same constitutional type, we have found a significantly larger length of the body, the mass and area of the body surface, the height of the suprasternal, pubic, shoulder anthropometric points, chest cords, transverse mid and lower chest and sagittal middle-thigh diameters, intervertebral distance of the pelvis and its external conjugates. Relatively smaller in female volleyball players of mesomorphic type of physique was the thickness of the skin-fat folds under the shoulder blade. One can conclude that within the same somatotype there are significant changes in the anthropometric parameters, in particular total body and longitudinal, transverse, front and rear body dimensions, which is affected by the body of modern young womenvolleyball players with mesomorphic somatotype, under the influence of intensive loads.

Keywords: *anthropometry, mesomorphic somatotype, female volleyball players, juvenile age.*

Introduction

Sports specialization is based on the adequacy of the biological capabilities of a person to the demands of their professional activities [13, 15, 22]. Reserves of the human body, which determine the possibility of achieving high results in sports, are far from exhausted. The question of the timely detection of children and adolescents susceptibility to certain types of motor activity has become relevant, as a result of their development and the growth of professional skills, they also have a sports individuality [12]. Therefore, rational system of sports selection creates favorable conditions for full disclosure of the potential of a young athlete and their improvement [3]. Early diagnostics of the features of the development of morphological characteristics and motor abilities of children in the process of sports selection is possible with the use of genetic markers [4, 8, 11]. The current practice of selecting young athletes takes into account their morphological and functional parameters [7, 9], which have a high degree of genetic determination. It is proved that

athletes with a certain set of constitutional traits have advantages in a separate sport [1, 2,16-18, 21, 23]. Therefore, the definition of constitutional parameters that are inherent to highly skilled athletes of a particular sport can serve as reliable prognostic markers during sports selection. But it is known that the representatives of the elite of a particular sport have a significant variability in the size of total and partial body sizes. This is especially true for representatives of sports games, whose anthropometric parameters are marked by a large variety.

In previous studies, we revealed the marked differences in many anthropometric body sizes and body mass components in volleyball players, compared to non-athletes [23], a significant difference was found in the parameters of the external structure of the body of volleyball players of different sporting roles [19]. These studies confirm the shape-forming effect of volleyball sports activities on the body of athletes. Reserves of the human body, which determine the possibility of achieving high results in sports, are far from exhausted [14, 20]. Therefore, from our point of view, it was interesting to get an answer to the question of whether the somatometric dimensions vary from the representatives of certain constitutional types under the influence of sports activities.

The *purpose* of the work is to establish differences in the anthropometric dimensions between young women volleyball players of high level of athletic skill and non-sports young women belonging to the mesomorphic somatotype.

Materials and methods

On the base of the research center of the National Pirogov Memorial Medical University, we conducted an anthropo-somatotypological study of 127 young women volleyball players of youth age (from 16 to 20 years) with a high level of athletic skill. Sports experience in all cases was greater than 3 years. From the database of research center of the National Pirogov Memorial Medical University was selected 140 practically healthy young women of the same age who were not engaged in sports. Anthropometric measurements were carried out using the method of V.V. Bunak [5]. All surveyed girls had a somatotypological study on the estimated modification of the Heath-Carter method [6]. After the conducted somatotyping, it was found that 29 young women volleyball players and 33 non-sports young women belonged to the mesomorphic type of constitution. A control group was created from persons not engaged in sports and belonging to the mesomorphic somatotype, from the volleyball players with mesomorphic somatotype the main group was created. The analysis of the obtained results is carried out in the licensed package of Statistica 5.5 using nonparametric methods of evaluation of indicators. The reliability of the difference between independent quantitative indicators was determined using the Man-Whitney U-criterion.

Results

We found that volleyball players of the mesomorphic somatotype have significantly higher body mass, body length, and body surface area than young women of the same constitutional type that are not involved in sports (in all cases $p<0.001$) (tabl. 1).

Table 1. Anthropometric total body dimensions in persons with mesomorphic somatotype (M± σ).

Anthropometric dimensions	Control group	Female volleyball players	p
Body weight (kg)	57.96±7.48	65.89±7.36	<0.001
Body length (cm)	160.4±6.6	169.3±5.7	<0.001
Body surface area (m^2)	1.601±0.131	1.757±0.120	<0.001

Table 2. Anthropometric sizes of the body in persons with mesomorphic somatotype (M±σ).

Anthropometric dimensions	Control group	Female volleyball players	p
Height of the suprasternal point (cm)	130.5±6.2	139.5±6.5	<0.001
Height of the pubic point (cm)	81.38±5.36	87.91±4.71	<0.001
Height of the shoulder point (cm)	133.0±6.9	141.7±6.5	<0.001
Waist circumference (cm)	67.83±5.28	70.22±5.01	<0.05
Girth of the chest on the inspiration (cm)	86.47±7.14	95.05±5.99	<0.001
Girth of the chest on the exhalation (cm)	79.41±6.37	85.95±6.34	<0.001
Girth of the chest at rest (cm)	82.07±6.60	89.95±6.29	<0.001
Transverse mid-chest (cm)	25.54±2.96	26.61±1.55	<0.001
Transverse lower chest (cm)	21.15±3.38	23.68±2.31	<0.001
Sagittal mid-chest (cm)	16.96±1.20	18.17±2.02	<0.05
Shoulder width (cm)	35.87±2.66	36.62±2.16	=0.092
Interspinous distance (cm)	24.84±1.77	25.03±2.06	>0.05
Intercristal distance (cm)	27.58±1.65	28.59±2.64	=0.067
Intertrochanteric distance (cm)	31.55±1.65	32.50±2.02	<0.05
External conjugate (cm)	18.55±1.05	19.60±1.76	<0.05
Thickness of the fold under the shoulder blade (mm)	10.39±3.25	8.838±2.268	<0.05
Thickness of the fold on the abdomen (mm)	10.47±4.08	10.76±3.55	>0.05
Thickness of the fold on the side (mm)	8.619±4.180	10.14±3.47	=0.081

It was found that young women volleyball players have significantly higher hematopoietic, pubic and shoulder points (in all cases $p<0.001$) than their peers of mesomorphic somatotype who are not involved in sports (tabl. 2). In young women volleyball players with a mesomorphic somatotype, the waist circumference ($p<0.05$) and thorax at inhalation, exhalation and rest (in all cases $p<0.001$) are higher than in the control group of young women. Transverse mid-chest and lower chest sizes of the chest in athletes are statistically significantly higher than in non-sportsmen ($p<0.001$). The front and rear middle-thigh diameter also has significantly higher values in comparison with the control ($p<0.05$). At

that time, we found that the acromial diameter of the chest, indicating the width of the shoulders, has a large mean value in the sample of volleyball players, although the difference in the comparison of athletes and young women who are not engaged in sports with a mesomorphic somatotype is unreliable.

Analyzing the anthropometric size of the ace, it was found that the intraosseous distance in the mesomorphic somatotype, engaged in and not engaged in sports, has no significant differences. At that time, the values of the intervertebral distance and external conjugates in volleyball players are significantly higher than in the control group young women ($p<0.05$). A tendency towards higher values ($p=0.067$) of the intervertebral distance in a group of volleyball players with a mesomorphic somatotype was established (tabl. 2).

It was established that volleyball players have a significantly lower thickness of skin and fat folds under the shoulder blade than young women in the control group, which also belong to the mesomorphic type of constitution ($p<0.05$) (tabl. 2). The thickness of the fold on the abdomen has no significant differences between the comparison groups. It should be noted that at volleyball players thickness of skin and fat folds on the side has higher average values than in the control, but we did not find statistically significant differences in the value of this indicator when comparing volleyball players and non-athletes.

Discussion

The high level of modern sports requires specific knowledge in the field of morphological and functional characteristics of the organism. The somatotypological approach was used in the study of the indicators of central [24] and peripheral [10] hemodynamics, and it was proved that representatives of a separate somatotype, engaged in a particular sport of high level of athletic skill, have significant differences in the parameters of the cardiovascular system compared with non-athletes of the same constitutional type.

After comparing external somatometric parameters, despite the fact that young women of adolescence of both studied groups belonged to a mesomorphic constitutional type, we found significant differences. In volleyball players the body is more massive, as evidenced by the significantly higher values of all of their total body size. Length, weight and surface area of the body are signs that must be taken into account when carrying out a prognostic and signing sporting selection in volleyball [19]. In previous studies, without division into somatotypes, it has also been proven that volleyball players have significantly higher total body sizes. It was found that the average body length in the general group of volleyball players was 9,4 cm larger than that of non-sportsmen, body weight - by 8,5 kg, body surface area - by 0,2 m^2 [23]. Approximately, the same tendency for the predominance of individual total body sizes in volleyball players persists in considering this problem from the standpoint of belonging to the mesomorphic somatotype.

We have found that volleyball players of mesomorphic somatotype have longitudinal trunk sizes, which can be judged by the height of anthropometric points, are significantly higher compared to young women of the same constitutional type who were not engaged in sports. And the volleyball players of the general group did not have a significant difference in the height of the pubic, shoulder and trochanteric points when compared with non-sportsmen [19]. We found that volleyball players of mesomorphic somatotype all the enveloping dimensions of the chest are significantly larger ($p<0.001$) than in the control. In volleyball players of the general group, compared with non-athletes, reliable differences were detected only for the girth of the chest on the inspiration ($p<0.05$) [23]. In addition, we found that most of the body diameters in athletes are statistically significantly higher than that of young women who are not engaged in sports. This refers to the transverse mid and lower dimensions of the chest, the anterior-posterior mid-thigh, the intervertebral distance and the anterior-posterior size of the pelvis, as evidenced by the value of the external conjugate. In volleyball players of the general group, the reliable differences ($p<0.05$) were characteristic only for indicators that characterized the transverse dimensions of the chest [23]. Regarding indicators of hypodermic fat delivery, it should be noted that volleyball players of the mesomorphic somatotype compared with the control group, the thickness of the fold under the shoulder blade is significantly lower, the abdomen has no significant differences, and on the side has larger mean values at $p> 0,05$. Volleyball players of the general group had less subcutaneous fat removal on the body than young women who were not engaged in sports, as evidenced by a significantly lower value of all skin and fat folds ($p<0.001$) [25]. Thus, we have found that within the same somatotype there are more significant changes in the anthropometric indices of the body, in particular the body, under the influence of intensive loads, which is undergoing the organism of modern volleyball players of the mesomorphic somatotype.

Using the somatotypological approach in the analysis of external parameters of the body will enable more accurate prediction of changes in the anthropometric parameters of volleyball players under the influence of training and competitive activities.

Conclusions

1. It has been established that volleyball players of mesomorphic somatotype, compared to girls who are not engaged in sports of the same constitutional type, have a significantly higher magnitude of length, mass and surface area of the body.

2. The vast majority of the anthropometric dimensions of the trunk (longitudinal, transverse, anterior and posterior) in young women volleyball players of the mesomorphic body type are significantly greater than that of the control group young women.

References

[1] Adhikari, A., Nahida, P., Islam, R. N., & Kitab, A. (2014). Importance of Anthropometric Characteristics in Athletic Performance from the Perspective of Bangladeshi National Level Athletes' Performance and Body Type. *American Journal of Sports Science and Medicine,* 2(4), 123-127. doi: 10.12691/ajssm-2-4-1D.

[2] Bacciotti, S., Baxter-Jones, A., Gaya, A., & Maia, J. (2018). Body physique and proportionality of Brazilian female artistic gymnasts. *J. Sports Sci.,* 36(7), 749-756. doi: 10.1080/02640414.2017.1340655.

[3] Barth, M., Emrich, E., & Daumann, F. (2018). Approaches and methods used for measuring organizational performance in national sport governing bodies from 1986 to 2014. A systematized review. *Current Issues in Sport Science*, 3, 1-22. doi: 10.15203/CISS_2018.010.

[4] Bouchard, C. (2011). Overcoming barriers to progress in exercise genomics. *Exerc Sport Sci Rev.*, 39, 212-217.

[5] Bunak, V. V. (1941). *Anthropometry: a practicalcourse*. M.: Uchpedgiz.

[6] Carter, J. L., & Heath, B. H. (1990). *Somatotyping - development and applications.* Cambridge: University Press.

[7] Di Rienzo, F., Hoyek, N., Collet, C., & Guillot, A. (2014). Physiological changes in response to apnea impact the timing of motor representations: a preliminary study. *Behavioral and Brain Functions.*, 10(1), 15. doi: 10.1186/1744-9081-10-15.

[8] Guilherme, J. P., Tritto, A., North, K. N., Lancha, J. A. H., & Artioli, G. G. (2014). Genetics and sport performance: current challenges and directions to the future. *Rev Bras Educ Fis Esporte*, 28(1), 177-193.

[9] Guillot, A., Moschberger, K., & Collet, C. (2013). Coupling movement with imagery as a new perspective for motor imagery practice. *Behav Brain Funct.,* 9, 8. doi: 10.1186/1744-9081-9-8.

[10] Khapitska, O. P. (2016). Somatotypological features of parameters of peripheral hemodynamics in athletes. *Reports of VNMU*, 20(2), 375-382.

[11] Lippi, G., Maffulli, N., & Longo, U. G. (2009). Genetics and sports. *British Medical Bulletin,* 93(1), 27-47. doi: 10.1093/bmb/ldp007.

[12] Liu, J., Lewis, G., & Evans, L. (2013). Understanding Aggressive Behavior Across the Life Span. *J. Psychiatr Ment Health Nurs.,* 20(2), 156-168. doi: 10.1111/j.1365-2850.2012.01902.x.

[13] Malina, R. M. (2010). Early Sport Specialization: Roots, Effectiveness, Risks Current. *Sports Medicine Reports*, 9(6), 364-371. doi: 10.1249/JSR.0b013e3181fe3166.

[14] Moroz, V. M., Khapitska, O. P., Kyrychenko, Yu. V., Kulibaba, S. O., & Sarafynyuk, P. V. (2018). Peculiarities of rheovasography parameters of the shin in volleyball players, wrestlers, athletes with mesomorphic somatotype. *World of Medicine and Biology,* 1(63), 52-56.

[15] Myer, G. D., Jayanthi, N., Difiori, J. P., Faigenbaum, A. D., Kiefer, A. W., Logerstedt, D., & Micheli, L. J. (2015). Does Early Sports Specialization Increase Negative Outcomes and Reduce the Opportunity for Success in Young Athletes? *Sports Health,* 7(5), 437-442. doi: 10.1177/1941738115598747.

[16] Pastuszak, A., Bu?ko, K., & Kalka, E. (2016). Somatotype and body composition of volleyball players and untrained female students - reference group for comparison in sport. *Anthropological Review*., 79(4), 461-470.

[17] Pyne, D., Gardner, A., & Sheehan, K. (2006). Positional differences in fitness and anthropometric characteristics in Australian football. *Journal of Science and Medicine in Sport,* 9, 143-150.

[18] Raković, A., Savanović, V., Stanković, D., Pavlović, R., Simeonov, A., & Petković, E. (2015). Analysis of the elite athletes somatotypes. *Acta Kinesiologica,* 1, 47-53.

[19] Sarafinyuk, L. A., & Yakusheva, Y. I. (2015). Differences in longitudinal body sizes in volleyball players of different roles. *Actual questions of medical science and practice,* 82(2), 170-176.

[20] Sarafynyuk L. A., Fomina L. V., Kyrychenko Yu. V., Kaminska N. A., & Kyrychenko V. I. (2016). Determination of parameters of central hemodynamics by anthropometric predictors in girls of mesomorphs with different levels of physical activity. *Bulletin of Biology and Medicine,* 2(129), 301-304.

[21] Stanković, D., Pavlović, R., Petković, E., Raković, A., & Puletić, M. (2018). The somatotypes and body composition of elite track and field athletes and swimmers. *International Journal of Sports Science,* 8(3), 67-77. doi: 10.5923/j.sports.20180803.01.

[22] Wiersma, L. D. (2000). Risks and Benefits of Youth Sport Specialization: Perspectives and Recommendations. *Pediatric exercise science,* 12(1), 13-22. doi: 10.1123/pes.12.1.13.

[23] Yakusheva, Y. I., & Sarafinyuk, L. A. (2014). Features of total and separate partial anthropometric sizes in volleyball players of adolescence. *Reports of Morphology,* 20(2), 473-475.

[24] Yakusheva, Y. I. (2015). Indicators of central hemodynamics in volleyball players with different body types. *Bulletin of Biology and Medicine,* 2(123), 344-347.

[25] Yakusheva, Y. I. (2015). Thickness of skin and fat folds, component composition of body weight and somatotype in volleyball players of different roles. *Reports of Morphology,* 21(1), 209-213.

ОСОБЛИВОСТІ ТОТАЛЬНИХ РОЗМІРІВ ТІЛА Й АНТРОПОМЕТРИЧНИХ РОЗМІРІВ ТУЛУБА У ВОЛЕЙБОЛІСТОК МЕЗОМОРФНОГО СОМАТОТИПУ

Сарафинюк Л.А., Фоміна Л.В., Хавтур В.О., Федонюк Л.Я., Хапіцька О.П., Стефаненко І.С.

Визначення конституціональних параметрів, які притаманні висококваліфікованим спортсменам окремого виду спорту, може виступати надійними прогностичним маркером при проведенні спортивного відбору. Але в останній час незаперечливим фактом є соматотипологічна обумовленість окремих розмірів, які характеризують зовнішню будову тіла, та вісцеральних структур організму. Мета роботи - встановити відмінності антропометричних розмірів між волейболістками високого рівня спортивної майстерності та неспортсменками, які належать до мезоморфного соматотипу. На базі науково-дослідного центру Вінницького національного медичного університету ім. М.І. Пирогова нами було проведене антропо-соматотипологічне дослідження 127 волейболісток високого рівня спортивної майстерності юнацького віку (від 16 до 20 років). Спортивний стаж у всіх випадках був більшим 3 років. Із бази даних науково-дослідного центру Вінницького національного медичного університету ім. М.І. Пирогова було відібрано 140 практично здорових дівчат аналогічного віку, які не займалися спортом. Антропометричне вимірювання проводили за методом В.В. Бунака (1941), соматотипологічне дослідження - за розрахунковою модифікацією метода Heath-Carter (1990). Після проведеного соматотипування встановили,

що 29 волейболісток та 33 дівчини, які не займалися спортом, належали до мезоморфного типу конституції. Аналіз отриманих результатів проведений у ліцензійному пакеті Statistica 5.5 з використанням непараметричних методів оцінки показників. Виявлено у волейболісток мезоморфного соматотипу порівняно з дівчатами, які не займаються спортом того ж конституціонального типу, достовірно більшу величину довжини, маси та площі поверхні тіла, висоти надгрудинної, лобкової, плечової антропометричних точок, обхватів грудної клітки, поперечних середньо- і нижньогрудного, сагітального середньогрудинного діаметрів, міжвертлюгової відстані таза та його зовнішньої кон'югати. Достовірно меншою у волейболісток мезоморфного типу статури була товщина шкірно-жирової складки під лопаткою. Можна зробити висновок, що у межах одного соматотипу відбуваються значні зміни антропометричних показників, зокрема тотальних розмірів тіла та поздовжніх, поперечних, передньо-задніх розмірів тулуба під впливом інтенсивних навантажень, яких зазнає організм сучасних волейболісток мезоморфного соматотипу.

Ключові слова: *антропометрія, мезоморфний соматотип, волейболістки, юнацький вік.*

ОСОБЕННОСТИ ТОТАЛЬНЫХ РАЗМЕРОВ ТЕЛА И АНТРОПОМЕТРИЧЕСКИХ РАЗМЕРОВ ТУЛОВИЩА У ВОЛЕЙБОЛИСТОК МЕЗОМОРФНОГО СОМАТОТИПА

Сарафинюк Л.А., Фомина Л.В., Хавтур В.О., Федонюк Л.Я., Хапицкая О.П., Стефаненко И.С.

Определение конституциональных параметров, присущих высококвалифицированным спортсменам отдельного вида спорта, может выступать надежным прогностическим маркером при проведении спортивного отбора. Но в последнее время неоспоримым фактом является соматотипологическая обусловленность отдельных размеров, характеризующих внешнее строение тела, и висцеральных структур организма. Цель работы - установить различия антропометрических размеров между волейболистками высокого уровня спортивного мастерства и неспортсменками, относящихмися к мезоморфному соматотипу. На базе научно-исследовательского центра Винницкого национального медицинского университета имени Н.И. Пирогова нами было проведено антропо-соматотипологическое исследование 127 волейболисток высокого уровня спортивного мастерства юношеского возраста (от 16 до 20 лет). Спортивный стаж во всех случаях был более 3 лет. Из базы данных научно-исследовательского центра Винницкого национального медицинского университета им. М.И. Пирогова было отобрано 140 практически здоровых девушек аналогичного возраста, которые не занимались спортом. Антропометрическое измерение проводили по методу В.В. Бунака (1941), соматотипологические исследования - по расчетной модификации метода Heath-Carter (1990). После проведенного соматотипирования установили, что 29 волейболисток и 33 девушки, которые не занимались спортом, принадлежали к мезоморфному типу конституции. Анализ полученных результатов проведен в лицензионном пакете Statistica 5.5 с использованием непараметрических методов оценки показателей. Выявлено у волейболисток мезоморфного соматотипа по сравнению с девушками, которые не занимаются спортом того же конституционального типа, достоверно большую величину длины, массы и площади поверхности тела, высоты надгрудинной, лобковой, плечевой антропометрических точек, обхватов грудной клетки, поперечных средне- и нижнегрудного, сагиттального среднегрудинного диаметров, межвертельной дистанции таза и его внешней конъюгаты. Достоверно меньше у волейболисток мезоморфного типа телосложения была толщина кожно-жировой складки под лопаткой. Можно сделать вывод, что в пределах одного соматотипа происходят значительные изменения антропометрических показателей, в частности тотальных размеров тела и продольных, поперечных, передне-задних размеров туловища под влиянием интенсивных нагрузок, которые испытывает организм современных волейболисток мезоморфного соматотипа.

Ключевые слова: *антропометрия, мезоморфный соматотип, волейболистки, юношеский возраст.*

DOI: 10.31393/morphology-journal-2018-24(3)-06 Reports of Morphology, Vol. 24, №3, Pages 37-42

ISSN 1818-1295 eISSN 2616-6194

REPORTS OF MORPHOLOGY

Official Journal of the Scientific Society of Anatomists, Histologists, Embryologists and Topographic Anatomists of Ukraine

journal homepage: https://morphology-journal.com

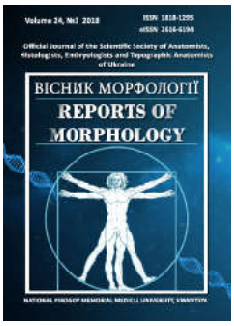

Features of the thyroid gland structural components remodeling in the toxemia stage after experimental thermal injury

Koritskiy V.G., Nebesna Z.M.

SHEI "I. Horbachevsky Ternopil State Medical University Ministry of Health of Ukraine", Ternopil, Ukraine

ARTICLE INFO

Received: 12 July, 2018

Accepted: 08 August, 2018

UDC: 616.441-003.93-02.616-001.17]-092.9

CORRESPONDING AUTHOR

e-mail: nebesna_zm@tdmu.edu.ua

Nebesna Z.M.

Thermal injury causes severe structural and metabolic disturbances not only of the skin itself, but also of all organs and systems of the affected organism, is a manifestation of a complex symptom complex - a burn disease. Of particular importance in patients with burns are changes in the endocrine system. The aim of the study was to establish the microscopic and electron-microscopic reorganization of the components of the thyroid gland of animals after thermal damage on 14 day after experimental thermal injury. A III degree burn was applied under ketamine anesthesia with copper plates heated in boiled water to a temperature of 97-100°C. The size of the lesion area was 18-20% of the epilated surface of the body of rats. An experimental study of the structural components of the thyroid gland after a burn injury was performed on laboratory white male rats weighing 160-180 g. Rats euthanasia was performed after ketamine anesthesia by decapitation. In the experiment, the study of the microscopic and submicroscopic state of the follicles and hemocapillaries of the thyroid gland after thermal injury of the III degree. It has been established that in the toxemia stage after the application of the burn injury on 14 day (late toxemia stage), significant destructive and degenerative changes are found in the thyrocytes of the wall of the follicles and hemocapillaries, the organ acquires a macrofollicular structure. The height of thyrocytes decreases, the nuclei and organelles of cytoplasm are significantly damaged, the number and height of microvilli on their apical surface decreases, which negatively affects the cell's secretory cycle and transcapillary organ metabolic processes. The established destructive changes in the blood capillaries and thyrocytes of the follicles are the morphological manifestation of the suppression of the secretory activity of the thyroid gland during thermal injury and corresponds to the hypofunctional state of the organ.

Keywords: *thyroid gland, microscopic and submicroscopic changes, thermal skin injury.*

Introduction

The study of the pathogenesis of organs in the composition of the body systems after severe thermal trauma is an urgent problem of combustiology [12, 15, 21]. Today, the frequency of burns in developed countries is 1: 1000 per year, and the mortality, despite the use of modern treatments, remains fairly high and ranges from 5.9% to 21.2% [12, 13, 15, 17, 21, 24, 25, 26]. In the case of severe thermal trauma, there are a number of factors that lead to sepsis and multiple organ failure: microcirculation disorder, presence of necrotic tissues inhabited by wounds, endogenous intoxication, activation of lipid peroxidation, development of syndrome of systemic inflammatory response, DIC, etc. [2, 3, 5, 6, 7, 10, 13, 14, 20]. It has been established that in the complicated and inadequately studied pathogenesis of burn disease one of the main places has endogenous intoxication, which is the result of proteolysis of damaged tissues and alteration of histo-hematological barriers. Hormonal changes are involved not only in triggering mechanisms of the pathogenesis of burn disease, but also in the development of compensatory-adaptive responses and the mobilization of protective functions of the organism [4, 11, 16, 19, 23]. Particularly important role in this complex process belongs to the systems of the pituitary gland - adrenal cortex, the pituitary gland - thyroid gland. They represent not only an intermediate link in the efferent pathways of the nerve regulation, but also are peripheral endocrine effector that provides a balance of metabolic and regenerative processes.

Today, we know about the ability of the thyroid gland to

morphofunctional reorganization under the influence of endo- and exogenous factors [1, 18, 19]. However, the status of this organ in the process of adaptation processes remains poorly understood.

The *aim* of the work was to establish microscopic and electron microscopic reorganization of the components of the thyroid gland of animals after thermal lesions in the stage of toxemia after an experimental thermal trauma.

Materials and methods

Experiments were conducted on 20 sexually mature white male rats. The animals were kept on a standard diet by the vivarium of the State Higher Educational Institution "I. Horbachevsky Ternopil State Medical University Ministry of Health of Ukraine". Animal care and all manipulations were conducted in accordance with the provisions of the "European Convention for the Protection of Vertebrate Animals Used for Experiments and for Other Scientific Purposes" (Strasbourg, 1986), as well as in accordance with the provisions of the "General Ethical Principles of Experiments on animals", adopted by the First National Congress on Bioethics (Kyiv, 2001).

Burns of the third degree were applied under ketamine anesthesia with copper plates heated in boiled water to a temperature of 97-100°C [7, 22]. The size of the lesions was 18-20% of the shaved surface of the body of rats. At daily inspection, we monitored their overall condition, the degree of manifestation of local changes in the area of burn wound, body weight and mortality. The object of the study was thyroid gland. To study micro and submicroscopic changes, animals were decapitated under ketamine anesthesia at 14 day, which, according to presentations, corresponds to the stage of late toxemia of burn disease [21].

Material for microscopic research was taken according to the generally accepted method [8]. Sections of the thyroid gland were fixed in a 10% neutral formalin solution, dehydrated in alcohols of increasing concentration, poured in paraffin blocks. The cut-offs of 5-6 microns thickness were stained with hematoxylin-eosin and methylene blue [8]. The histological preparations were studied using MIKROmed SEO SCAN light microscope and photo-documented with a Vision CCD Camera with a histologic image display system. For electron microscopic studies, we took pieces of the thyroid gland, fixed them in a 2.5% solution of glutaraldehyde, fixed with a 1% solution of osmium tetroxide on phosphate buffer. Further processing was carried out in accordance with the generally accepted method [8]. Ultra-thin sections made on ultramicrotome UMPT-7 were contrasted with uranyl acetate, lead citrate according to the Reynolds method and studied in an electron microscope of PEM-125K.

Results

According to conducted histological studies of experimental animals, after an experimental thermal trauma in the organ, there are heterogeneous in shape and size follicle. Prevailing large over-stretched with a dense, oxyphilic

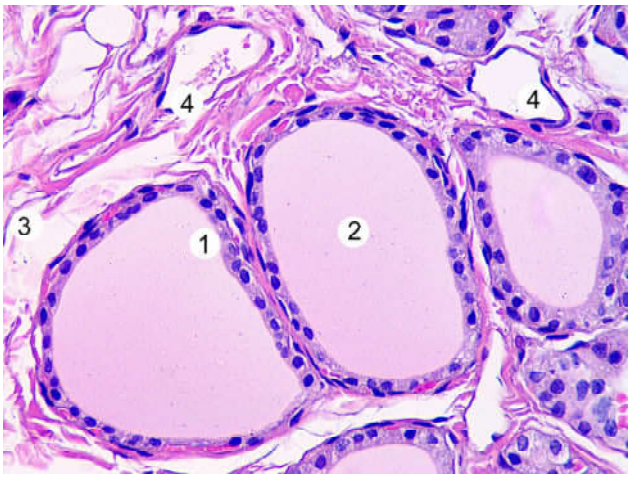

Fig. 1. Microscopic changes of the thyroid gland 14 days after the experimental thermal trauma. Large, over-stretched follicles (1), colloid (2), perifollicular edema of the connective tissue (3) of the vessel (4). Hematoxylin-eosin. x 200.

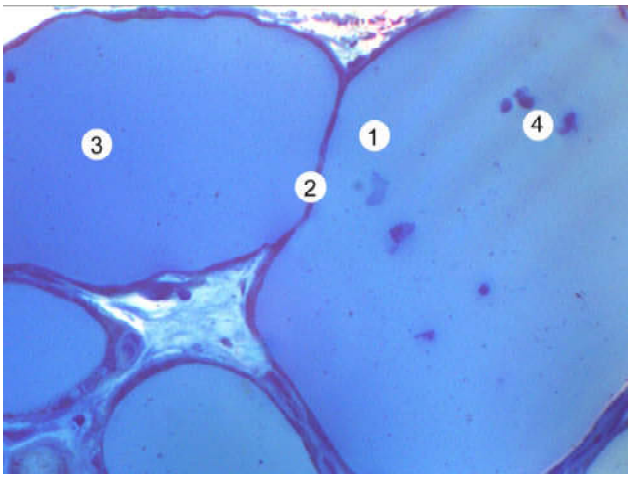

Fig. 2. Microscopic changes of the thyroid gland 14 days after the experimental thermal trauma. Large, over-stretched follicles (1) with flat thyrocytes in the wall (2), colloid (3), desquamated thyrocytes in the lumen of the follicle (4). Methylene blue. x200.

colloid, in which vacuole resorption is absent. Thyrocytes of such follicles have a flattened form and hyperchromic, picnotically altered nuclei. Desquamation of the thyroid gland epithelium is also revealed in the lumen of the follicle (Fig. 1, Fig. 2).

In the central parts of the lobules, also observed single deformed, medium and small follicles, in which the thyrocytes have cubic or prismatic form, light cytoplasm, normochromic, centrally located nuclei. The colloid in such follicles was not much, it was loose and acquired a disperse form, numerous and large vacuoles of resorption, which sometimes merged into illuminated strips, were found. Inter-follicular, interstitial of connective tissue is moderately swollen.

During this period of the experiment, changes in the organ vascular and microcirculatory system, manifested by plethora, stasis, are detected. The expansion capillaries are

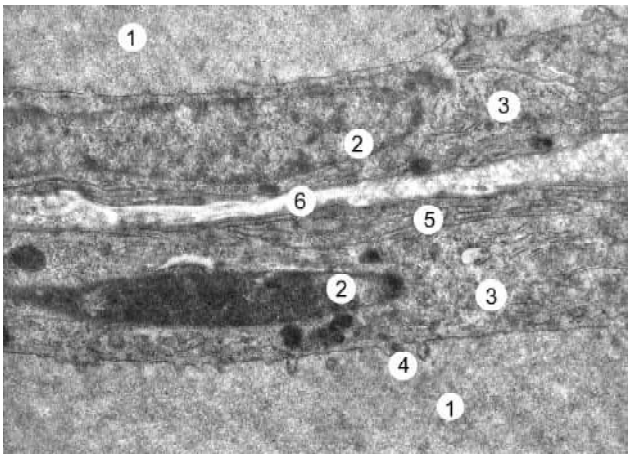

Fig. 3. Submicroscopic organization of the wall of the follicles of the thyroid gland 14 days after the experimental thermal trauma. Enlargement of the follicle with dense colloid (1), flat nucleus (2) and cytoplasm of thyrocyte (3), single microvilli on the apical surface of the cell (4), branching of the basal surface of the thyrocyte (5), basement membrane (6). x9000.

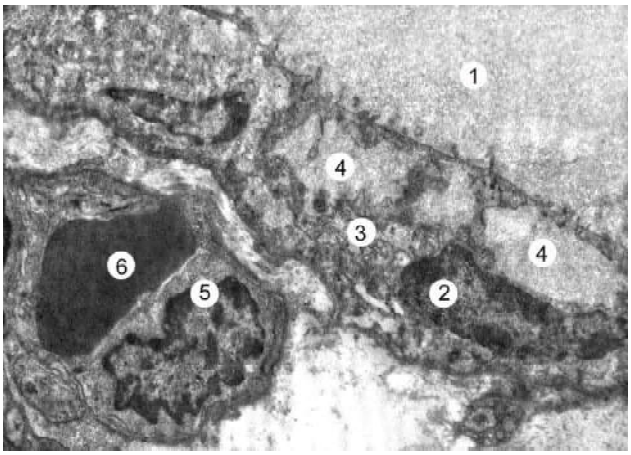

Fig. 4. Submicroscopic organization of the thyroid gland 14 days after the experimental thermal trauma. Enlargement of the follicle with colloid (1), osmophilic, fused nucleus (2) and cytoplasm (3) of the thyrocyte, large vacuolic structures (4), endothelial cell (5), erythrocyte in the lumen of the capillary (6). x7000.

densely surrounded by follicles and has expanded and narrowed areas of their lumens. In their wall there are hypertrophied, edematous endothelial cells, as well as densified, picnotic. Around the hemocapillaries there is significant perivascular space.

Submicroscopically in enlarged follicles, thyrocytes have a flattened form, poorly contoured borders between the cells. There are no microvilli on their luminal surface. In the swollen, enlightened cytoplasm, organelles are numb and significantly destructively altered. In the flat form of nuclei there is an electron-transparent karyoplasm, which includes small ectopic nucleoli. The outer membrane of nuclear membrane sometimes expands, increasing perinuclear space. Observed areas of a condensed osmophilic karyoplasm, which reduces the clarity of the nuclear membrane. Also decreases the number of nuclear pores. On the surface of the fragmented and thickened tubules, the granular endoplasmic net has little ribosomes, as well as free ribosomes and polysomes in the cell cytoplasm. Expansion and deformation of the granulosa endoplasmic mesh channels lead to the formation of large cavities of irregular shape, limited by unclearly contoured membranes (Fig. 3).

Circular vesicles of the Golgi complex sometimes expanding or vice versa considerably narrowing, their length extends. Available, primary and secondary lysosomes, which are freely located in the cytoplasm and near the Golgi complex. Damage to the mitochondria is accompanied by significant illumination of the matrix. A small number of cristae is contained in swollen electron-transparent mitochondria. Also, an irregular shape of the mitochondria with uneven contours of the outer membranes, which may be partially destroyed, is observed. Separate mitochondria have the appearance of large vacuoles. In the cytoplasm of the cells, an insignificant amount of apical grains is detected and large, irregularly shaped, vacuolic structures are filled with colloid (Fig. 4).

The need to intensify the metabolic processes of the affected organism causes the activation of the work of the synthetic apparatus of the thyrocytes: the tubules and circular vesicles of the granular endoplasmic net, which are concentrated at the basal pole, numerical polysomes, and the mitochondria have clearly contoured cristae, are expanding. The membranes of the basal part of the thyrocytes form a kind of labyrinth of branches, which are compensatory adapted changes to ensure the withdrawal of the hormone (Fig. 4).

It has been established that at separate sites in the follicles, the thyrocytes do not adhere tightly to the wall of the

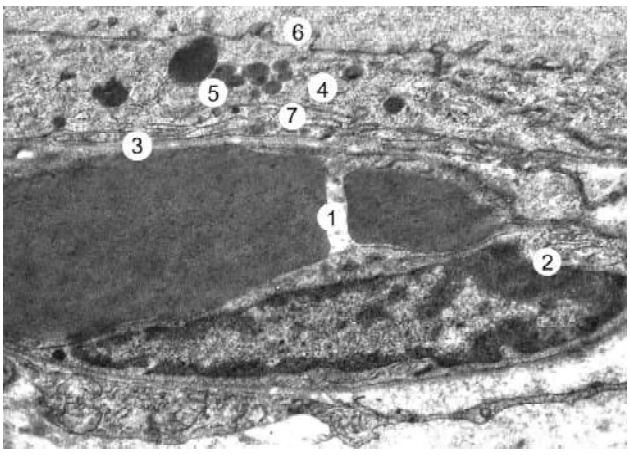

Fig. 5. Submicroscopic organization of the wall of the thyroid gland 14 days after the experimental thermal trauma. Enlargement of the capillary with erythrocytes (1), endothelial cell (2), capillary basement membrane (3), flat form of thyrocyte cytoplasm (4), primary and secondary lysosomes (5), microvilli on the apical surface of the cells (6), branching of the basal surface of the thyrocytes (7). x12000.

hemocapillaries, and separate from them by layers of connective tissue. Connective tissue strip looks edematous, has an electronically bright amorphous component and separate collagen fibrils.

The ultrastructure of blood capillaries is changing. Most of them have extensive erosions filled with erythrocytes. Endothelial cells are significantly altered, their nuclei are picnotically altered, they have elongated shape and deep invaginations of nuclear membrane. The perinuclear space between the membranes of the nuclear membrane is poorly expressed. The content of condensed heterochromatin increases, it forms large osmophilic clusters. In the cytoplasm there are few organelles and foamy cystic bubbles, their plasmalemma of the luminal surface is uneven and microvilli are single. In the cytoplasmic subtle areas, there is little fenestra. Such hemocapillaries are limited by narrow basal membranes (Fig. 4, Fig. 5).

Discussion

Histological studies have shown that changes in the structural components of the thyroid gland follicles during the experimental thermal trauma develop in the background of microcirculation disturbance, which is to some extent consistent with the studies [1, 7, 11, 21]. Significantly disturbed ultrastructure of the walls of perifollicular blood capillaries. Dystonia of blood vessels, which is detected on a burn injury on light optic and especially on submicroscopic levels, is manifested by enlargement, plethora, stasis and significant destructive changes in the walls of blood capillaries.

Activation of free-oxidation of lipids leads to the destruction of phospholipids of cell membranes. Such a statement about the mechanism of cellular membrane damage is consistent with the results of our research and [20, 21], which established a high level of toxic substances of lipid peroxidation in blood plasma of animals under investigation during thermal trauma. In this connection, it can be assumed that being in the blood, peroxides and free radicals primarily cause damage to the membranes of endothelial cells of the capillaries, and in the future, when they reach the bloodstream in the tissues, they lead to the destruction of the plasmalemma and organelles of the membranes of all organs of the affected organism, including thyroid gland.

It is known that the mechanisms of adaptation to hypoxia are realized on the principle of stress reactions with the participation of the hypothalamic-pituitary-adrenal system, the least explored is the role of the hypothalamic-pituitary-thyroid system [2, 3, 4, 10, 11, 23]. In the scientific literature, there is virtually no data on the participation of hormones in adapting to high temperatures. In the early stages of adaptation to hypoxia, hyperfunction of the thyroid gland and increased levels of thyroid hormones in the blood, which correlate with increased metabolism, is observed [1]. With prolonged action, hypofunction of the gland was noted under the conditions of "minimization" of metabolic functions and reduction of metabolism [1].

It is necessary to note the important role of thyroid hormones in the adaptation processes, since they have almost the widest spectrum of influence, since under their control are lipid, carbohydrate, protein and water-salt metabolism, as well as regeneration processes, permeability of cell membranes, etc.

In the scientific literature, the flow of compensatory and adaptive processes in the thyroid gland and its reorganization under conditions of stress, under the conditions of burn injury, have not been sufficiently studied. At morphological study of thyroid gland it is established that in the conditions of stress the volume of stromal elements of the organ increases, volume density of thyrocytes decreases, volume of colloid increases, the thyroid epithelium flings up. In some cases desquamation of thyrocytes occurs. If the stimulus is very strong or recurrent, then the resistance stage goes into the stage of exhaustion, there is a decrease in the function of the thyroid gland.

Thus, the results of histological studies correlate with the scientific data of other researchers [5, 14, 21] and indicate that in the stage of late toxemia after severe thermal trauma the destruction of membrane structural components of thyroid gland cells is significantly increased, which is necessarily accompanied by the development of dystrophic and necrobiotic processes in the body, a decrease in the secretory process.

In subsequent studies, it is planned to establish the degree of morphological changes in the structural components of the thyroid gland in the dynamics after the experimental thermal trauma under the use of corrective drugs.

Conclusions

In the stage of late toxemia after the thermal trauma in rats, deep irreversible destructive changes in thyrocytes in the follicles and hemocapillars of the thyroid gland develop, which are manifested by deep lesions of plasma, nuclear and intracellular membranes, leading to a decrease in secretion and excretion of hormones, a violation of transendothelial metabolism, and corresponds to the hypofunctional state of the organ.

References

[1] Boychuk, T. M., Khodorovskaya, A. A., Chala, K. M., Chernikova, G. M., & Khodorovsky, V. M. (2011). Morphometric indices of functional activity of the thyroid gland under stress reaction. *Bukovinsky medical bulletin*, 15(2), (58), 89-91.

[2] Cherkasov, V. G., Kovalchuk, A. I., Dzevulskaya, I. V., Malikov, A.V., Lakhtadyr, T.V., & Matkivskaya, R. M. (2015). Structural transformations in the internal organs with infusion therapy for burn disease. *Medical science of Ukraine*, 11(3-4), 4-11.

[3] Dzevulska, I. V., Kovalchuk, O. I., Cherkasov, E. V., Majewskyi, O. Ye., Shevchuk, Yu. G., Pastukhova, V. A. & Kyselova, T. M. (2018). Influence of lactoproteinum solution with sorbitol on dna content of cells of endocrine glands on the background of skin burn in rats. *World of Medicine and Biology*, 64(2), 033-039. doi: 10.26724/2079-8334-2018-2-64-33-39

[4] Dzevulska, I. V. (2015). Monthly rates of cell cycle of rat adrenal cells in administration of 0,9% NaCl solution, Lactoprotein with sorbitol or HAES-LX-5% during the first 7 day. *Biomedical and Biosocial Anthropology*, 25, 33-37.
[5] Evers, L. H. (2010). The biology of burn injury. Exp. Dermatol, 19(2), 9, 777-783 doi:10.1111/j.1600-0625.2010.01105.x
[6] Farina, Jr., J. A., Rosique, M. J., & Rosique, R. G. (2013). Curbing inflammation in burn patients. *International Journal of Inflammation,* 2013, 1-9. doi: 10.1155/2013/715645
[7] Galunko, G. M. (2017). Histological changes in the small intestine in the advanced stages of burn disease. *World of Medicine and Biology*, 3(61), 90-96. doi: 10.26724 / 2079-8334-2017-3-61-90-96
[8] Gunas, I., Dovgan, I., & Masur, O. (1997). *Method of thermal burn trauma correction by means of cryoinfluence.* Abstracts are presented in zusammen mit der Polish Anatomical Society with the participation of the Association des Anatomistes Verhandlungen der Anatomischen Gesellschaft, Olsztyn (p. 105). Jena - Munchen: Der Urban & Fischer Verlag.
[9] Goralskiy, L. P., Homich, V. T., & Kononskiy, O. I. (2011). *Fundamentals of histological technique and morphofunctional methods of research in norm and in pathology.* Zhitomir: Polissya.
[10] Gunas, I. V., Guminskiy, Yu. I., Ocheretna, N. P., Lysenko, D. A., Kovalchuk, O. I., Dzevulska, I. V., & Cherkasov, E. V. (2018). Indicators cell cycle and dna fragmentation of spleen cells in early terms after thermal burns of skin at the background of introduction 0.9% NaCl solution. *World of Medicine and Biology,* 1(63), 116-120. doi: 10.26.724/2079-8334-2018-1-63-116-120
[11] Gunas, I. V., Kovalchuk, O. I., Cherkasov, V. G., & Dzevulskaya, I. V. (2014). Structural aspects of the organs adaptive changes of the neuroimundocrine system in the treatment of burn disease with combined hyperosmolar solutions. *Galician Medical Herald,* 21(2), 21-26.
[12] Janak, J. C., Clemens, M. S., Howard, J. T., Le T. D., Cancio, L. C., Chung, K. K., & Stewart, Ian J. (2018). Using the injury severity score to adjust for comorbid trauma may be double counting burns: implications for burn research. *Burns*, 44, 8, 1920-1929. doi: 10.1016/j.burns.2018.03.012
[13] Jeschke, M. G., Pinto, R., & Kraft, R. (2015). Inflammation and the Host Response to Injury Collaborative Research Program. Morbidity and survival probability in burn patients in modern burn care. *Crit. Care. Med*, 43(2), 4, 808-815.
[14] Kallinen, O., Maisniemi, K., Bohling, T., Tukiainen, E., & Koljonen, V. (2012). Multiple organ failure as a cause of death in patients with severe burns. *J. Burn Care Res.*, 33(2), 206-211. doi: 10.1097/BCR.0b013e3182331e73
[15] Kearney, L., Francis, E. C., & Clover, A. J. (2018). New technologies in global burn care - a review of recent advances. *Int. J. Burns Trauma*, 8(4), 77-87. PMID: 30245912
[16] Kovalchuk, O. I. (2016). Features of cell cycle indices in the adenohypophysis at late terms post-burn skin injury in rats under separate infusion in the first 7 days of 0.9% solution of NaCl, lactobacillus solutions with sorbitol or HAES-LX-5%. *Ukrainian Scientific Medical Youth Journal*, 93(1), 24-31.
[17] Maden, M. (2018). Optimal skin regeneration after full thickness thermal burn injury in the spiny mouse. *Acomys cahirinus. Burns*, 44, 6, 1509-1520. doi: 10.1016/j.burns.2018.05.018
[18] Nurmetova, I. K., & Kuhar, I. D. (2012). Organometric parameters of thyroid gland in rats with acute burned toxemia on the background of treatment with infusion drugs. *Ukrainian Journal of Hematology and Transfusiology,* 15(4), 278-281.
[19] Nurmetova, I. K. (2012). Morphometric parameters of the thyroid gland during thermal trauma in the dynamics of its experimental treatment with combined hyperosmolar solutions on the 21st and 30th day of the experiment. *Reports of Morphology*, 18(2), 263-265.
[20] Nebesna, Z. M., Lisnichuk, N. Ye., & Demkiv, I. Ya. (2015). Dynamics of changes of oxidation-reduction reactions in the lung tissue in case of burn injury and its correction by lyophilized xenograft substrate. *Bulletin of Biology and Medicine,* 4(1), (124), 124-128.
[21] Netyukhailo, L. G., Kharchenko, A. G., & Kostenko, S. V. (2011). Pathogenesis of burn disease (in 2 parts). *World of Medicine and Biology,* 1, 127-131, 131-135.
[22] Regas, F. C., & Ehrlich, H. P. (1992). Elucidating the vascular response to burns with a new rat model. *J. Trauma*, 32, 5, 557-563.
[23] Strelchenko, Yu. I., Zyablytsev, S. V., & Yale, V. M. (2012). Pathophysiological relationships of pituitary-thyroid and pituitary-adrenal systems under the influence of polarized light in rats with dosed burns to open flames. *Clinical and Experimental Pathology*, 11(2), 3, 156-158.
[24] Swanson, J. W., Otto, A. M., Gibran, N. S., Klein, M. B., Kramer, C. B., Heimbach, D. M., & Pham, T. N. (2013). Trajectories to death in patients with burn injury. *J. Trauma Acute Care Surg.,* 74(1), 282-288. doi: 10.1097/TA.0b013e3182788a1c
[25] Takayuki, Y., Hayato, I., Timothy, W., King, H., Hara, D., & Cooper, K. (2018). Skin xenotransplantation: Historical review and clinical potential. *Burns,* 44(8), 1738-1749, doi: 10.1016/j.burns.2018.02.029
[26] Timmers, T. K., Verhofstad, M. H., & Leenen, L. P. (2015). Intensive care organisation: Should there be a separate intensive care unit for critically injured patients? *World Journal of Critical Care Medicine,* 4, 240-243. doi:10.5492/wjccm.v4.i3.240

ОСОБЛИВОСТІ РЕМОДЕЛЮВАННЯ СТРУКТУРНИХ КОМПОНЕНТІВ ЩИТОПОДІБНОЇ ЗАЛОЗИ В СТАДІЇ ТОКСЕМІЇ ПІСЛЯ ЕКСПЕРИМЕНТАЛЬНОЇ ТЕРМІЧНОЇ ТРАВМИ

Корицький В.Г., Небесна З.М.

Термічна травма спричиняє тяжкі структурно-метаболічні порушення не тільки безпосередньо шкірного покриву, але й усіх органів та систем ураженого організму, що є проявом складного симптомокомплексу - опікової хвороби. Особливе значення у хворих з опіками відіграють зміни органів ендокринної системи. Метою дослідження було встановлення мікроскопічної та електронно-мікроскопічної реорганізації компонентів щитоподібної залози тварин після термічного ураження на 14 добу після експериментальної термічної травми. Опік III ступеня наносили під кетаміновим наркозом мідними пластинами, нагрітими у киплячій воді до температури 97-100°С. Розміри ділянки ураження становили 18-20% епільованої поверхні тіла щурів. Експериментальне вивчення структурних компонентів щитоподібної залози після опікової травми було виконано на лабораторних білих щурах-самцях масою 160-180 г. Евтаназію щурів проводили після кетамінового наркозу шляхом декапітації. В експерименті вивчили мікроскопічний та субмікроскопічний стан фолікулів та гемокапілярів щитоподібної залози після термічної травми III ступеня. Встановлено, що в стадії токсемії після нанесення опікової травми - 14 доба (стадія пізньої токсемії) в тироцитах стінки фолікулів та гемокапілярах виявляються значні деструктивні

та дегенеративні зміни, орган набуває макрофолікулярної будови. Знижується висота тироцитів, значно пошкоджуються ядра і органели цитоплазми, зменшується кількість і висота мікроворсинок на їх апікальній поверхні, що негативно впливає на секреторний цикл клітин та транскапілярні обмінні процеси органу. Таким чином, встановлені деструктивні зміни кровоносних капілярів та тироцитів фолікулів є морфологічним проявом пригнічення секреторної активності щитоподібної залози при термічній травмі та відповідає гіпофункціональному стану органу.
Ключові слова: *щитоподібна залоза, мікроскопічні та субмікроскопічні зміни, термічна травма шкіри.*

ОСОБЕННОСТИ РЕМОДЕЛИРОВАНИЯ СТРУКТУРНЫХ КОМПОНЕНТОВ ЩИТОВИДНОЙ ЖЕЛЕЗЫ В СТАДИИ ТОКСЕМИИ ПОСЛЕ ЭКСПЕРИМЕНТАЛЬНОЙ ТЕРМИЧЕСКОЙ ТРАВМЫ

Корицкий В.Г., Небесная З.М.

Термическая травма вызывает тяжелые структурно-метаболические нарушения не только непосредственно кожного покрова, но и всех органов и систем пораженного организма, является проявлением сложного симптомокомплекса - ожоговой болезни. Особое значение у больных с ожогами играют изменения органов эндокринной системы. Целью исследования было установление микроскопической и электронно-микроскопической реорганизации компонентов щитовидной железы животных после термического поражения на 14 сутки после экспериментальной термической травмы. Ожог III степени наносили под кетаминовым наркозом медными пластинами, нагретыми в кипящей воде до температуры 97-100°С. Размеры участка поражения составляли 18-20% эпилированной поверхности тела крыс. Экспериментальное изучение структурных компонентов щитовидной железы после ожоговой травмы были выполнены на лабораторных белых крысах-самцах массой 160-180 г. Эвтаназию крыс проводили после кетаминового наркоза путем декапитации. В эксперименте изучили микроскопическое и субмикроскопическое состояния фолликулов и гемокапилляров щитовидной железы после термической травмы III степени. Установлено, что в стадии токсемии после нанесения ожоговой травмы на 14 сутки (стадия поздней токсемии) в тироцитах стенки фолликулов и гемокапиллярах обнаруживаются значительные деструктивные и дегенеративные изменения, орган приобретает макрофолликулярное строене. Снижается высота тироцитов, значительно повреждаются ядра и органеллы цитоплазмы, уменьшается количество и высота микроворсинок на их апикальной поверхности, что отрицательно влияет на секреторный цикл клеток и транскапиллярные обменные процессы органа. Таким образом, установленные деструктивные изменения кровеносных капилляров и тироцитов фолликулов являются морфологическим проявлением подавления секреторной активности щитовидной железы при термической травме и соответствует гипофункциональному состоянию органа.
Ключевые слова: *щитовидная железа, микроскопические и субмикроскопические изменения, термическая травма кожи.*

DOI: 10.31393/morphology-journal-2018-24(3)-07 Reports of Morphology, Vol. 24, №3, Pages 43-51

ISSN 1818-1295 eISSN 2616-6194

REPORTS OF MORPHOLOGY

Official Journal of the Scientific Society of Anatomists, Histologists, Embryologists and Topographic Anatomists of Ukraine

journal homepage: https://morphology-journal.com

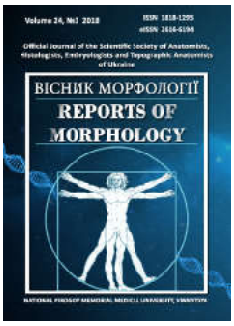

Morphological state of the mucous membrane of the esophagus of patients with postresection manifestations of reflux esophagitis depending on the method of the formation of mechanical esophagus-gastric anastomosis

Usenko O.U., Sidyuk A.V., Klimas A.S., Sidyuk O.E., Savenko G.U.

State Enterprise "Shalimov's National Institute of Surgery and Transplantology NAMS of Ukraine", Kyiv, Ukraine

ARTICLE INFO

Received: 19 July, 2018

Accepted: 14 August, 2018

UDC: 616.329:611.018.73:616-089.86

CORRESPONDING AUTHOR

e-mail: klimas.andrew@gmail.com

Klimas A.S.

The formation of mechanical gastrointestinal anastomosis after esophagectomy is often accompanied by the development in patients various degrees of reflux esophagitis. The aim of the study - to evaluate the pathogistological changes of the esophagus mucosa associated with gastro-esophageal reflux in patients with esophageal cancer and gastroesophageal, junction cancer after surgical treatment, depending on the technique of forming the esophagus-gastric anastomosis. The study included 30 patients who developed a mechanical invagination of the esophagus-gastric anastomosis developed by the Ukrainian patent (study group) and 30 patients who formed the end-to-end mechanical circulatory esophagus-gastric anastomosis (comparison group). At 12 months of observation all patients were given fibroesophagogastroduodenoscopy. Endoscopic diagnosis of esophagitis was performed according to a modified Los Angeles classification. To assess the morphological state of the esophageal mucosa, the esophageal mucosal biopsy was performed on the site of anastomosis and morphologically evaluated the severity of the reflux esophagitis. Reflux-associated changes in squamous epithelium of the esophagus were evaluated according to the consensus recommendations of the Esohisto Project. Statistical data analysis was performed using the EZR v statistical analysis package. 1.35 (Saitama Medical Center, Jichi Medical University, Saitama, Japan), a graphical interface to R (The R Foundation for Statistical Computing, Vienna, Austria). In a comparative analysis of frequency characteristics between different groups of patients, the 2 criterion was used; for tables 2 2 (in the case of a small number of patients (<5 cases), in the study subgroups) Fisher's exact test was used. The differences in the results obtained were considered statistically significant at p<0.05, which ensures a 95% level of probability. It has been established that the frequency with which the microscopic signs of reflux esophagitis are fixed are almost 2 times lower in the group of patients who were formed mechanical invagination esophagus-gastric anastomosis in comparison with the mechanical circular (46.7% vs. 83.3%, p<0.05), since invagination simulates the reproduction of antireflux properties of the lost gastrointestinal transition. Endoscopically diagnosed cases of reflux esophagitis are additionally supplemented by microscopically detected from 5.9% of subjects in the study group to 28.6% of subjects (p<0.05) in the comparison group, which indicates a higher sensitivity histological diagnosis. The signs that are consistently associated with post-resection reflux esophagitis include hyperplasia of the basal layer at both the frequency (86.7% vs. 100%) and the severity of the severity (6.7% vs. 23.3%, p<0.05), as well as moderate prolongation of papillae (30.0% vs. 66,6%, p<0.01), according to which the best results were obtained in the group of patients that formed the invagination mechanical esophagus-gastric anastomosis. According to the Esohisto Project criteria, the frequency of both "mild" and "severe" esophagitis in the group of patients that formed the invagination mechanical esophagus-gastric anastomosis was lower compared to the group with mechanical circulatory esophagus-gastric anastomosis (36.7% and 10.0% vs. 63.3% and 20.0%, p<0.01,

respectively).
Keywords: *proximal gastrectomy with esophageal resection, esophagus-gastric anastomosis, post-resection reflux esophagitis, Esohisto Project criteria, Histology; Histopathology.*

Introduction

Analysis of the literature on these issues suggests that that most surgeons around the world use mechanical techniques to form thoracic anastomosis [3, 4, 21].

However, along with convincing benefits, the use of stapling devices somewhat impairs the functional results of operations due to the high level of development of late complications from anastomoses: inflammatory complications (anastomositis, reflux esophagitis) and benign strictures [7, 10, 15, 17, 22]. Therefore, the key to success, as S.Y. Law [16] notes, is not only a thorough formation of anastomosis, but also the development of new methods aimed at improving the quality of intrathoracic anastomosis after esophagectomy in terms of reducing the level of development of late complications from the anastomosis [21].

Despite the fact that clinical symptoms, endoscopy and pH monitoring are the most important diagnostic tools for diagnosing reflux esophagitis, however, these tests may give controversial conclusions [1]. Diagnostic difficulties are greatest when symptoms of reflux occur without apparent damage to the esophageal mucosa during normal endoscopy [8]. Recent studies suggest that esophageal biopsy in such cases may play an additional role [27]. Currently published several reports on histological findings in patients with reflux esophagitis, but similar changes were found in patients without signs of reflux esophagitis [12]. That is, individual histological markers showed low diagnostic value, which led to the application of histological scores in the diagnosis of reflux esophagitis. Estimates that take into account the combination of histological parameters associated with extensive acid reflux revealed new perspectives on the role of the esophagus biopsy [27]. That is why research is promising to establish a correlation between endoscopic findings and histological changes in the esophagus [12].

The *aim* of the study - to evaluate the pathogistological changes of the esophagus mucosa associated with gastro-esophageal reflux in patients with esophageal cancer and gastroesophageal, junction cancer after surgical treatment, depending on the technique of forming the esophagus-gastric anastomosis.

Materials and methods

Under observation were 60 patients with esophageal cancer and gastroesophageal junction cancer who were on examination and in-patient treatment at the department of gastrointestinal surgery of the Shalimov's National Institute of Surgery and Transplantation for the period from 2015 to 2018 with overall survival not less than a year. All patients underwent proximal gastrectomy with subtotal esophagectomy by accesses of Lewis, or Osawa-Garlock. The study included 30 patients who were formed mechanical invagination esophagus-gastric anastomosis that was developed and protected by the Ukrainian patent [28] (study group) and 30 patients who formed the circular mechanical esophagus-gastric anastomosis end-to-side (comparison group).

At 12 months of observation all patients performed esophagogastroscopy. Endoscopic examination was performed by video gastroscope Olympus GIF-H180. In doubtful cases, the virtual chromoscopy of NBI was used. Endoscopic diagnosis of esophagitis was performed according to a modified Los Angeles classification. All patients performed a biopsy of the mucous membrane of the esophagus over the place of anastomosis. For histological analysis of biopsy material after routine placement, the dyes were stained with hematoxylin-eosin. The preparations were studied on a light microscope of Olympus BH-2 (lens x10, eyepiece x10; lens x40, eyepiece x10). The photos were taken using the DIGITAL Camera for Microscope ScienseLab DCM520 (USB 2.0) digital camera.

Esophageal mucus preparations of the study group and the comparison group were analyzed for the presence of histological signs of reflux esophagitis: hyperplasia of the basal cell layer, papillary prolongation, expansion of intercellular spaces and the presence of intraepithelial eosinophils, neutrophils and mononuclear cells, since these four features are considered the most informative elemental lesions [23]. The combined assessment of microscopic lesions in patients conducted under standardized criteria established Esohisto project, introducing assessment of severity for each parameter in the range of 0 to 2 [8, 26, 31]. In this case:

- basal layer thickness (basal cell layer in μm, expressed as a fraction of the total thickness of the epithelium (x10) - 0 (absent)<15%, 1 - 15-30%, 2 - >30%;

- the length of the papillae (the length of the papillae in μm, expressed as the percentage (%) of the thickness of the general epithelium (x10) - 0 (absent)<50%, 1 - 50-75%, 2 - >75%;

- expansion of intercellular spaces (Identify as irregular round dilations or diffuse widening of intercellular space (x40), small intercellular space = diameter <1 lymphocyte, large intercellular space = diameter $\geq$1 lymphocyte): 0 (absent or $\leq$5 small intercellular spaces), 1 (1 lymphocyte or $\geq$6 small and $\leq$5 large intercellular spaces), 2 ($\geq$1 lymphocyte or $\geq$6 large intercellular spaces);

- intraepithelial eosinophils (count the cells in the most damaged field (x40)): 0 (absent) 1 - (1-2 cells), 2 (>2 cells);

- intraepithelial neutrophils (count the cells in the most

damaged field (x40)): 0 (absent) 1 - (1-2 cells), 2 (>2 cells);

- intraepithelial mononuclear cells (count the cells in the most damaged field (x40)): 0 (0-9 cells), 1 (10-30 cells), 2 (>30 cells).

The total figure severity estimates calculated by summing the severity of lesions divided by the estimated lesion types (exclude intraepithelial mononuclear cells and neutrophils, erosion/erosion healed). Scores 0-0.25 were considered normal, values ≥0.35 were positive for microscopic esophagitis, scores 0.5-0.75 were qualified for the diagnosis of "mild" esophagitis, and scores ≥1 for the diagnosis of "severe" esophagitis respectively [23, 31].

Statistical analysis of the data was performed using the statistical analysis package EZR v.1.35 (Saitama Medical Center, Jichi Medical University, Saitama, Japan), Graphic interface to R (The R Fund for Statistical Computing, Vienna, Austria). A comparative analysis of the frequency characteristics between different groups of patients using the criterion χ^2, for tables 2x2 (in the case of a small number of patients (<5 cases) in the study subgroups) used the Fisher exact test [9, 13]. Differences in the results obtained were statistically significant at $p<0.05$, which provides 95% probability level.

Results

At 12 months of follow up of operated patients, endoscopic changes in the esophagus mucosa were not detected in 24 (40%) patients: in 17 (56.7%) - in the study group and in 7 (23.3%) - in comparison groups; morphological confirmation of absence of signs of reflux esophagitis was obtained in 21 (35%) patients: in 16 (53.3%) and 5 (16.7%) patients respectively (Table 1).

Figure 1 illustrates the absence of signs of postreaction reflux esophagitis: the papillary length is less than half (<50%) of the total thickness of the epithelium, the basal layer is only a small percentage (<15%) of the total thickness of the epithelium, intercellular spaces are not significantly dilated (≤5 small). Intraepithelial eosinophils are absent.

Endoscopic signs of reflux esophagitis detected in 36 (60.0%) patients, 13 (43.3%) patients in the study group and 23 (76.7%) patients comparison groups. In addition to endoscopically identified patients with symptoms of reflux esophagitis identified individuals with histological changes and the lack of visible lesions endoscopically: the study group - 1 in the comparison group - 2 patients. Thus, morphologically confirmed reflux esophagitis was detected in 39 (65.0%) patients: in 14 (46.67%) patients in the study group and 25 (83.33%) patients in the comparison group (Table 1).

For histological characteristics of patients found violations of the esophageal mucosa varying degrees regardless of the method of forming esophagus-gastric anastomosis.

Postresection reflux-associated microscopic changes in the esophageal epithelium are given in Table 2.

Multilayer epithelium was detected in 26 (86.7%) persons in the study group and in 30 (100%) persons - groups of comparison, extension of the papillae - respectively in 14 (46.7%) and 25 (83.3%) persons, enlargement intercellular spaces and intraepithelial eosinophils were detected in 3 (10.0%) persons in the study group and in 6 (20.0%) persons in the comparison group (Table 2). That is, the most common reflux-associated histological signs, according to Table 2, include an increase in the thickness of the basal layer, which is 15-30% relative to the total thickness of the epithelium (1) and papilla extension, which is 50-75% relative to the total thickness of the epithelium (1). Less dilatation of small intercellular spaces (1) and the presence of intraepithelial eosinophil in one field (1) are observed. However, the degree of histological changes in the mucous membrane of the esophagus, according to which the study groups differed 3 times, ranged as 2 - were inherent in only hyperplasia of the basal layer. In assessing the degree of change as 1 - elongation of the papillae, according to which the study groups differed 2 times, as well as - dilatation of intercellular spaces and the presence of intraepithelial eosinophils, however, in the last two cases, the number of persons having such changes was insignificant (Table 2). Figure 2 illustrates the signs of postreaction reflux esophagitis, which is accompanied by an increase in the thickness of the basal layer, prolongation of the papillae (<75%), and the dilatation of the intercellular spaces.

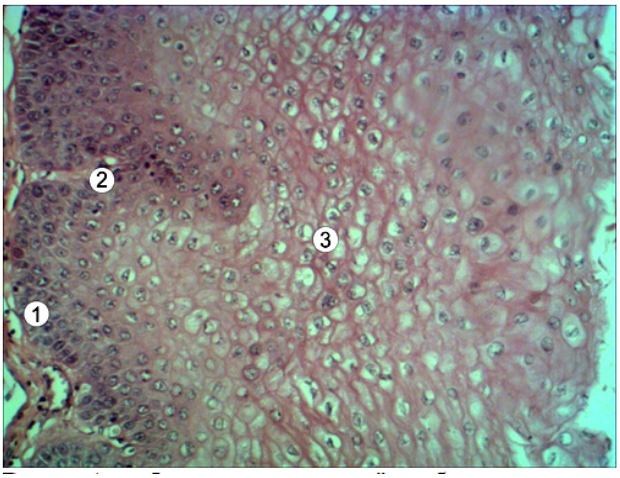

Fig. 1. A fragment of the esophageal mucosa over the place of esophago-gastric anastomosis with no pathological changes. 1 - basal layer; 2 - papillae; 3 - intercellular spaces. Hematoxylin-eosin. Lens x10. Ocular x10.

Table 1. Frequency of endoscopic and morphologically confirmed manifestation of reflux esophagitis after 12 months of follow up.

Reflux esophagitis	Research group, (n=30) (%)		Comparison Group, (n=30) (%)		Level of significance of difference between groups, p
	Not found	Detected	Not found	Detected	
Endoscopically detected	17 (56.7)	13 (43.3)	7 (23.3)	23 (76.7)	<0.05
Morphologically verified	16 (53.3)	14 (46.7)	5 (16.7)	25 (83.3)	<0.01

Table 2. Degree of severity of reflux esophagitis by microscopic diagnosis of Esohisto Project.

Criterion	Severity	Research group, n (%)	Comparison Group, n (%)	Level of significance of difference between groups, p
Hyperplasia of the basal layer	0 1 2	4 (13.3) 24 (80.0) 2 (6.7)	0 (0.0) 23 (76.7) 7 (23.3)	**<0.05**
Papillary elongation	0 1 2	16 (53.3)9 (30.0)5 (16.7)	5 (16.7) 20 (66.6) 5 (16.7)	**<0.01**
Expansion of intercellular spaces	0 1 2	27 (90.0) 2 (6.7) 1 (3.3)	24 (80.0) 5 (16.7) 1 (3.3)	>0.05
Intraepithelial eosinophils	0 1 2	27 (90.0) 2 (6.7) 1 (3.3)	24 (80.0) 5 (16.7) 1 (3.3)	>0.05

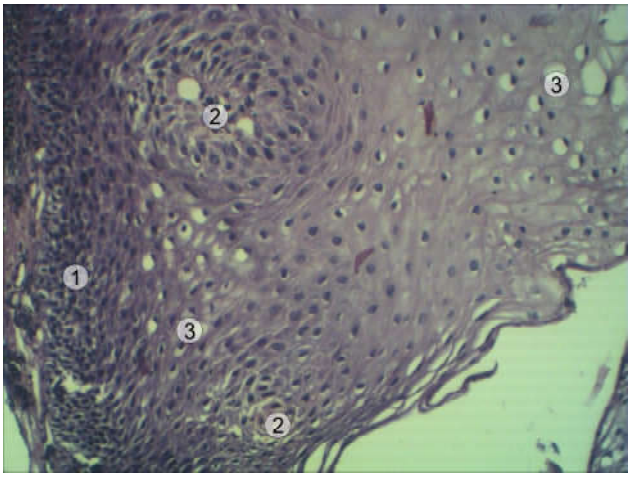

Fig. 2. A fragment of the esophageal mucosa over the place of esophago-gastric anastomosis with pathological changes. 1 - basal layer; 2 - elongated papillae; 3 - dilated intercellular spaces. Hematoxylin-eosin. Lens x10. Ocular x10.

Table 3. Distribution of ballroom characteristics of patients and aggregate indicator of severity of histological changes of the mucous membrane.

Severity	Score	Research group. n (%)	Comparison Group. n (%)
Norm	<0.5	16 (53.4)	5 (16.7)
"Mild" esophagitis	0.5	7 (23.3)	12 (40.0)
	0.75	4 (13.4)	7 (23.3)
"Severe" esophagitis	1	1 (3.3)	1 (3.3)
	1.25	1 (3.3)	4 (13.4)
	2	1 (3.3)	1 (3.3)

Based on detected reflux-associated microscopic changes in the epithelium of the esophagus, the distribution of patients according to the degree of severity of histological changes in the mucous membrane was further analyzed (Table 3).

In the group in which patients were formed invagination mechanical esophagus-gastric anastomosis, reflux esophagitis was detected in 14 (46.7%) patients versus 25 (83.3%) in patients who had circular mechanical esophagus-gastric anastomosis (Table 1, 3). Histological "mild" esophagitis was found in 11 patients (36.7%) in the study group and in 19 patients (63.3%) of the comparison group, "severe" esophagitis - in 3 (10%) and 6 (20%) of patients respectively, the difference between the groups is statistically significant (p=0.03 according to the 2 criterion) (Table 3). At the same time, the vast majority of patients whose esophagitis were classified as "mild", were scored by 0.5 points in both groups. Among patients with esophagitis are classified as "severe", attracts comparison group in which the majority of patients met the 1.25 point scale characterization, while in the comparison group points evenly distributed (Table. 3).

The results of the comparison of the severity of the reflux esophagitis associated with the endoscopic diagnosis of esophagitis, evaluated according to the Los Angeles classification and evaluated according to the histological criteria of Esohisto Project, are presented in Table 4.

The reflux esophagitis according to the Los Angeles Classification of Grade A was found in 10 (33.3%) patients, grade B - in 3 (10.0%) patients in the study group and accordingly in 18 (60.0%) and 5 (16.7%) of the patients in the comparison group. At the same time, according to the histological criteria, Esohisto's "mild" esophagitis was detected in 11 (36.7%) patients, and severe in 3 (10.0%) patients in the study group and 19 (63.3%), respectively, and 6 (20.0%) patients in the comparison group (Table 4). That is, endoscopically diagnosed cases of reflux esophagitis were

Table 4. Compliance with the severity of the reflux esophagitis associated with the endoscopic diagnosis of esophagitis. evaluated according to the Los Angeles classification and evaluated according to the histological criteria of the Esohisto Project.

Category	Research group, n (%)	Comparison Group, n (%)	Level of significance of difference between groups
Los Angeles Classification			
N	17 (56.7)	7 (23.3)	**<0.05**
LA-A	10 (33.3)	18 (60.0)	
LA-B	3 (10.0)	5 (16.7)	
LA-C	0 (0.0)	0 (0.0)	
Detected changes in general	13 (43.3)	23 (76.7)	**<0.05**
Esohisto Project			
Mucus without changes	16 (53.3)	5 (16.7)	**<0.01**
"Mild" esophagitis	11 (36.7)	19 (63.3)	
"Severe" esophagitis	3 (10.0)	6 (20.0)	
Detected changes in general	14 (46.7)	25 (83.3)	**<0.01**

Fig. 3. A fragment of the esophageal mucosa over the place of esophago-gastric anastomosis with pathological changes that correspond to the "mild" reflux esophagitis. 1 - basal layer; 2 - elongated papillae; 3 - slightly enlarged intercellular spaces. Hematoxylin-eosin. Lens x10. Ocular x10.

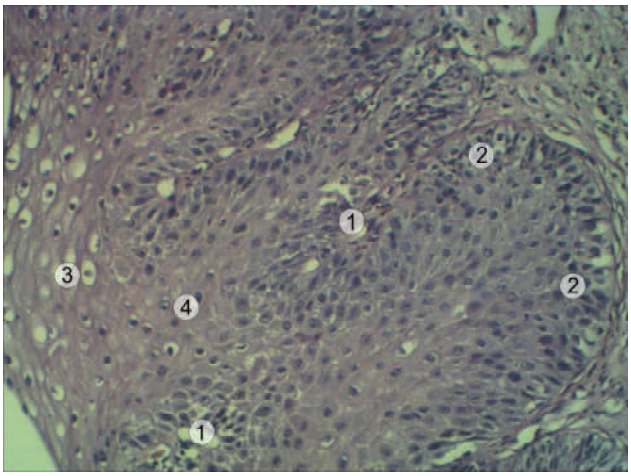

Fig. 4. A fragment of the esophageal mucosa over the place of esophago-gastric anastomosis with pathological changes that correspond to "severe" reflux esophagitis. 1 - elongated papillae; 2 - thickened basal layer; 3 - extended intercellular spaces; 4 - intraepithelial eosinophils. Hematoxylin-eosin. Lens x10. Ocular x10.

additionally supplemented by microscopically detected from 5.9% of the subjects in the study group to 28.6% of the subjects in the comparison group with the normal mucous membrane of the esophagus in the category N classification of Los Angeles (Table 4). It should be noted that in the invagination mechanical method of forming the esophagus-gastric anastomosis, the ratio of "mild"/"severe" esophagitis in the group was almost 4/1, and at the circular - 3/1. That is, regardless of the method of forming the esophagus-gastric anastomosis, the "mild" esophagitis was more often compared to "severe" (Table 4). At the same time, the combined evaluation of microscopic lesions Esohisto Project, the frequency of reflux esophagitis generally in the study group was significantly lower compared to the comparison group (14 (46.7%) compared to 25 (83.3%), $p<0.01$). In this case, the frequency of both "mild" and "severe" esophagitis in the group of patients who formed the invagination mechanical esophagus-gastric anastomosis, was lower compared to the group with circular mechanical esophagus-gastric anastomosis (36.7% and 10.0% vs. 63.3% and 20.0%, $p<0.01$ respectively). Histology esophageal mucosa, corresponding to the degree of reflux esophagitis A is characterized by increased length of papillae, representing 50-75% of the total thickness of the epithelium. Basal layer is increased in thickness and is 15-30% of the total thickness of the epithelium. Intercellular spaces are slightly extended. There are no intra-epithelial eosinophils (Fig. 3).

Histology esophageal mucosa of patients that meets reflux esophagitis stage B, characterized by elongation of papillae, representing >75% of the total thickness of the epithelium, increased basal layer in thickness, representing >30% of the total thickness of the epithelium, intercellular spaces greatly expanded. Presence of intraepithelial eosinophils (Fig. 4).

Discussion

In normal esophageal lumen lays out a squamous epithelium, consisting of four layers: basal, parabasal, intermediate and superficial. Epitheliocytes are connected by adhesive, slit, dense and desmosomic contacts, that are located in the intermediate layer [24]. Reactive squamous epithelium changes in response to the action of acid, form the basis of histological diagnostics of reflux esophagitis.

Analyzing the obtained data, it should be noted that the endoscopically normal mucosa of the esophagus of patients after esophagectomy for 12 months of observation was almost 2.5 times more frequent (56.7% vs. 23.3%, $p<0.05$), and the frequency with which fixed the microscopic signs of reflux esophagitis, was almost 2 times lower (46,67% vs. 83,33%, $p<0,05$) in patients who were formed by invagination mechanical esophagus-gastric anastomosis in comparison with the circular mechanical esophagus-gastric anastomosis, since the invagination modeled the reproduction of antireflux properties of the lost of gastroesophageal junction (see Table. 1, 4).

It should be noted that in addition to endoscopically diagnosed, microscopic changes with signs of reflux esophagitis were found in 1 out of 17 (5.9%) subjects in the study group and in 2 out of 7 (28.6%) persons in the comparison group with normal mucous membrane esophagus according to the Los Angeles Class N classification, which indicates a higher ($p<0.05$) sensitivity to the histological diagnosis (see Table 4). About the absence of endoscopic visible lesions, but the presence of histological changes of squamous epithelium in non-aerosive reflux disease is reported by a number of researchers [8, 19, 29].

According to the histological study conducted by us, hyperplasia of the basal layer can be considered a feature that is consistently associated with post-resection reflux esophagitis both in frequency and severity. Normally, the basal layer of the esophagus consists of 2-6 layers of basal

cells, which is<15% of the total thickness of the epithelium [2, 8, 26, 31]. The multilayer squamous epithelium was detected in the vast majority of patients in the study group (86.67%) and in all patients in the comparison group (100%). However, the number of patients with more severe severity (2) was 3 times less (p<0.05) among patients who were formed by invagination mechanical esophagus-gastric anastomosis in comparison with the circular mechanical esophagus-gastric anastomosis (Table 2). In healthy individuals, the papilla's length is less than 50% of the total thickness of the epithelium [23, 26, 31]. Papillary elongation, accounting for 50-75% and 75% relative to the total thickness of the epithelium was found in 14 (46.7%) patients in group study and 25 (83.3%) patients comparison group (difference between groups is statistically significant, p<0.01). In addition, the number of patients with a more moderate degree of severity (1) was 2 times lower (p<0.05) among patients who were formed by invagination mechanical esophagus-gastric anastomosis in comparison with the circular mechanical esophagus-gastric anastomosis, indicating its benefits (Table 2). The good diagnostic value of these two parameters in the GERD is indicated by M. Vieth [30]. According to some researchers, hyperplasia of the basal layer and extension of the stromal papillae represent a regenerative reaction to damage to the mucous membrane caused by reflux ("hyperregeneration") [6, 11, 18, 26]. However, for normal esophageal epithelium characterized by low regenerative property: moving cells from the basal layer to the surface proceeds 30 days [20]. Expansion of intercellular spaces and the presence of intraepithelial eosinophils occurred occasionally: 10.0% in the study group and 20.0% in the comparison group (p>0.05), with the number of patients with a more moderate degree of severity (1) was almost 2 times less (but did not achieve a significant difference) among patients who were formed by invagination mechanical esophagus-gastric anastomosis (Table 2). According to literature in the epithelium of the esophagus in patients with non-erosive reflux disease, expanded intercellular spaces are detected, the mean diameter of which in the distal esophagus is three times higher compared to control [5].

We found that the ratio of the frequency of "mild" and "severe" esophagitis does not depend on the method of forming esophagus-gastric anastomosis: the histologically "mild" esophagitis is found in 3 times more often than in the "severe". However, the frequency of both "mild" and "severe" esophagitis according to the criteria of Esohisto Project in the study group was 2 times lower compared with the comparison group (36.7% and 10.0% vs. 63.3% and 20.0%, respectively. p<0.01) (Table 4). In conclusion, it should be noted that recent studies have shown that histological evaluation based on a combination of histological parameters may be largely due to patient symptoms and esophageal acid exposure and thus can contribute not only to the diagnosis of non-erosive reflux disease, but and differential diagnosis between patients with non-erosive reflux disease and patients with functional heartburn [14, 25] and play a role in the comparative evaluation of various therapies [23]. Thus, the results of the study indicate that the formation invagination mechanical esophagus-gastric anastomosis significantly reduces histological signs of reflux esophagitis compared to the mechanical method of forming a circular mechanical esophagus-gastric anastomosis, and the use of histological severity ratings showed promising results when assessing the quality of new ways of forming esophagus-gastric anastomosis.

Conclusions

1. Histologically normal mucosa of the esophagus of patients after esophagectomy for 12 months of follow up was found more than 2 times more often in the group of patients who were formed mechanical invagination esophagus-gastric anastomosis compared with circular mechanical esophagus-gastric anastomosis (53.3% vs. 16.7%, p<0.05 in accordance).

2. According to the histological study, the frequency of reflux esophagitis is almost 2 times lower in the group of patients who were formed mechanical invagination esophagus-gastric anastomosis compared with circular mechanical esophagus-gastric anastomosis (46.7% vs. 83.3%, p<0.05), since invasion models the reproduction of antireflux properties of lost gastroesophageal junction.

3. The combination of histological parameters in patients with morphologically confirmed post-resection reflux esophagitis appears to be in the vast majority of cases, such as hyperplasia of the basal layer and elongation of the papillae of predominantly moderate severity, occasionally supplemented by the dilation of small intercellular spaces and single intraepithelial eosinophils.

4. Among patients with mechanical invagination esophagus-gastric anastomosis, the number of patients with hyperplasia of the basal layer of severe severity (2) was 3 times smaller (6.7% vs. 23.3%, p<0.05), and the number of patients with papillary elongation (30.0% vs. 66.6%, p<0.01), the expansion of intercellular spaces and the presence of intraepithelial eosinophils of moderate severity (1) (6.7% versus 16.7%, p>0.05) was in 2 times less, compared with patients who formed a circular mechanical esophagogastro-anastomosis, which confirms the advantages of mechanical invagination esophagus-gastric anastomosis.

5. The degree of severity of esophagitis evaluated according to the Esohisto Project criteria, the frequency of both "mild" and "severe" esophagitis in the group of patients who was formed mechanical invagination esophagus-gastric anastomosis was 2 times lower compared with the group with circular mechanical esophagus-gastric anastomosis (36,7% and 10.0% vs. 63.3% and 20.0%, p<0.01 respectively).

6. The histological diagnosis of reflux esophagitis in post-resection patients is more sensitive than endoscopic, since it allows individuals with a lack of endoscopic visible lesions of the esophagus mucosa to detect individuals with microscopic signs of reflux esophagitis.

References

[1] Allende, D. S., & Yerian, L. M. (2009). Diagnosing gastroesophageal reflux disease: the pathologist's perspective. *Adv. Anat. Pathol.,* 16(3), 161-165. doi: 10.1097/PAP.0b013e3181a186a3.

[2] Behar, J., & Sheahan, D. (1975). Histologic abnormalities in reflux esophagitis. *Arch. Pathol.,* 99(7), 387-391. Retrieved from: https://www.ncbi.nlm.nih.gov/pubmed/238497.

[3] Biere, S. S., Maas, K. W., Cuesta, M. A., & van der Peet, D. L. (2011). Cervical or Thoracic Anastomosis after Esophagectomy for Cancer: a systematic review and meta-analysis. *Dig. Surg.*, 28 (1), 29-35. doi: 10.1159/000322014.

[4] Bogopolsky, P. M., Balalykin, D. A., & Chernousov, F. A. (2012). To the history of the development and use of sewing apparatuses in the surgery of the esophagus in Russia. *Bulletin of Surgical Gastroenterology*, 1, 66-71. ISSN: 2072-7984.

[5] Caviglia, R., Ribolsi, M., Gentile, M., Rabitti, C., Emerenziani, S., Guarino, M. P. … Cicala, M. (2007). Dilated intercellular spaces and acid reflux at the distal and proximal oesophagus in patients with non-erosive gastro-oesophageal reflux disease. *Aliment. Pharmacol. Ther.*, 25(5), 629-636. DOI: 10.1111/j.1365-2036.2006.03237.x.

[6] Dent, J. (2007). Microscopic esophageal mucosal injury in nonerosive reflux disease. *Clin. Gastroenterol. Hepatol.*, 5(1), 4-16. DOI: 10.1016/j.cgh.2006.08.006.

[7] Dong Zhou, Quan-Xing Liu, Xu-Feng Deng, Jia-Xin Min, & Ji-Gang Dai (2015). Comparison of two different mechanical esophagogastric anastomosis in esophageal cancer patients: a meta-analysis. *J. Cardiothorac. Surg.,* 10, 67. https://doi.org/10.1186/s13019-015-0271-4.

[8] Fiocca, R., Mastracci, L., Riddell, R., Takubo, K., Vieth, M., Yerian, L. … Ruth, M. (2010). Development of consensus guidelines for the histologic recognition of microscopic esophagitis in patients with gastroesophageal reflux disease: the Esohisto project. *Hum. Pathol.*, 41(2), 223-231. doi: 10.1016/j.humpath.2009.07.016.

[9] Guryanov, V. G., Lyakh, Yu. E., Pari, V. D., Korotkyy, O. V., Chaly, O. V., Chaly, K. O., & Tsekhmyster, Ya. V. (2018). *Biostatistics guide. Analysis of the results of medical research in the EZR package (R-statistics): tutorial*. K.: Vistka.

[10] Honda, M., Kuriyama, A., Noma, H., Nunobe, S., & Furukawa, T. A. (2013). Hand-sewn versus mechanical esophagogastric anastomosis after esophagectomy: a systematic review and meta-analysis. *Ann. Surg.*, 257(2), 238-248. DOI:10.1097/SLA.0b013e31826d4723.

[11] Ismail-Beigi, F., Horton, P. F., & Pope, C. E. 2nd (1970). Histological consequences of gastroesophageal reflux in man. *Gastroenterology,* 58(2), 163-174. Retrieved from: https://www.ncbi.nlm.nih.gov/pubmed/5413015.

[12] Kaiyo Takubo, Naoko Honma, Gopi Aryal, Motoji Sawabe, Tomio Arai, Yasuo Tanaka … Katsuhiko Iwakiri (2005). Is There a Set of Histologic Changes That Are Invariably Reflux Associated? *Arch. Pathol. Lab. Med.,* 129(2), 159-163. DOI: 10.1043/1543-2165(2005)129<159:ITASOH>2.0.CO;2.

[13] Kanda, Y. (2013). Investigation of the freely available easy-to-use software 'EZR' for medical statistics. *Bone Marrow Transplant.*, 48, 452-458.

[14] Kandulski, A., Jechorek, D., Caro, C., Weigt, J., Wex, T., M?nkem?ller, K., & Malfertheiner, P. (2013). Histomorphological differentiation of non-erosive reflux disease and functional heartburn in patients with PPI-refractory heartburn. *Aliment. Pharmacol. Ther.,* 38(6), 643-651. doi: 10.1111/apt.12428.

[15] Kovalchuk, A. V. (2004). *The choice of a method for the formation of anastomosis in the surgical treatment of patients with esophageal and stomach cancer with the transition to the esophagus.* (Dis. cand. med. sci.). AMS of Ukraine. Institute of Oncology, Kyiv.

[16] Law, S. Y. (2012). The Art and Science of Esophageal Anastomosis. I*n Innovation in Esophageal Surgery,* 95-102. doi: 10.1007/978-88-470-2469-4_12.

[17] Liu, Q. X., Min, J. X., Deng, X. F., & Dai, J. G. (2014). Is hand sewing comparable with stapling for anastomotic leakage after esophagectomy? A meta-analysis. *World J. Gastroenterol.,* 20(45), 17218-26. doi: 10.3748/wjg.v20.i45.17218.

[18] Livstone, E. M., Sheahan, D. G., & Behar, J. (1977). Studies of esophageal epithelial cell proliferation in patients with reflux esophagitis. Gastroenterology, 73, 1315-1319. PMID: 913973.

[19] Lundell, L., Dent, J., & Bennett, J. (1999). Endoscopic assessment of esophagitis: clinical and functional correlates and further validation of Los Angeles classification. *Gut*, 45, 172-180. PMID:10403727; PMCID:PMC1727604.

[20] Lutsik, O., Ivanova-Sogomonyan, A., Kabak, K., & Tchaikovsky, Yu. (2018). *Human histology.* (3rd ed.). Kyiv: The book plus. http://chtyvo.org.ua/authors/Lutsyk_Oleksandr/Histolohiia_liudyny/

[21] Maas, K. W., Biere, S. S. A. Y., Scheepers, J. J. G., Gisbertz, S. S., Turrado Rodriguez, V., van der Peet, D. L., & Cuesta, M. A. (2012). Minimally invasive intrathoracic anastomosis after Ivor Lewis esophagectomy for cancer: a review of transoral or transthoracic use of staplers. *Surg. Endosc.*, 26(7), 1795-1802. doi: 10.1007/s00464-012-2149-z.

[22] Markar, S. R., Karthikesalingam, A., Vyas, S., Hashemi, M., & Winslet, M. (2011). Hand-Sewn Versus Stapled Oesophagogastric Anastomosis: Systematic Review and Meta-analysis. *Journal of Gastrointestinal Surgery,* 15(5), 876-884. doi: 10.1007/s11605-011-1426-9.

[23] Mastracci, L., Spaggiari, P., Grillo, F., Zentilin, P., Dulbecco, P., Ceppa, P. … Fiocca, R. (2009). Microscopic esophagitis in gastro-esophageal reflux disease: individual lesions, biopsy sampling, and clinical correlations. *Virchows Arch.,* 454(1), 31-39. doi: 10.1007/s00428-008-0704-8.

[24] Orlando, R. C. (2010). The integrity of the esophageal mucosa. Balance between offensive and defensive mechanisms. *Best Pract. Res. Clin. Gastroenterol.,* 24(6), 873-882. doi: 10.1016/j.bpg.2010.08.008.

[25] Savarino, E., Zentilin, P., Mastracci, L., Dulbecco, P., Marabotto, E., Gemignani, L. … Savarino, V. (2013). Microscopic esophagitis distinguishes patients with non-erosive reflux disease from those with functional heartburn. *J. Gastroenterol.,* 48(4), 473-482. doi: 10.1007/s00535-012-0672-2.

[26] Schneider, N. I., & Langner, C. (2015) The Status of Histopathology in the Diagnosis of Gastroesophageal Reflux Disease - Time for Reappraisal? *J. Gastrointest. Dig. Syst.,* 5, 355. doi:10.4172/2161-069X.1000355.

[27] Triantos Ch., Koukias N., Karamanolis G., & Thomopoulos K. (2015). Changes in the esophageal mucosa of patients with non erosive reflux disease: How far have we gone? *World J. Gastroenterol.,* 21(19), 5762-5767. doi: 10.3748/wjg.v21.i19.5762.

[28] Usenko, O. Yu., Sidyuk, A. V., & Klimas, A. S. (2016). Method

of performing esophagectomy. Patent of Ukraine №107325, IPC: A61B 17/00 A61B 17/115. Kyiv: State Patent Office.
[29] Vakil, N., van Zanten, S. V., Kahrilas, P., Dent, J., & Jones, R. (2006). The Montreal definition and classification of gastroesophageal reflux disease: a global evidence-based consensus. *Am. J. Gastroenterol.,* 101(8), 1900-1920. DOI:10.1111/j.1572-0241.2006.00630.x.
[30] Vieth, M., Peitz, U., Labenz, J., Kulig, M., Nauclér, E., Jaspersen, D. … Stolte, M. (2004). What parameters are relevant for the histological diagnosis of gastroesophageal reflux disease without Barrett's mucosa? *Dig. Dis*., 22(2), 196-201. DOI:10.1159/000080319.
[31] Yerian, L., Fiocca, R., Mastracci, L., Riddell, R., Vieth, M., Sharma, P. … Ruth, M. (2011). Refinement and reproducibility of histologic criteria for the assessment of microscopic lesions in patients with gastroesophageal reflux disease: the Esohisto Project. *Dig. Dis. Sci.*, 56(9), 2656-2665. doi: 10.1007/s10620-011-1624-z.

МОРФОЛОГІЧНИЙ СТАН СЛИЗОВОЇ ОБОЛОНКИ СТРАВОХОДУ ХВОРИХ З ПОСТРЕЗЕКЦІЙНИМИ ПРОЯВАМИ РЕФЛЮКС-ЕЗОФАГІТУ ЗАЛЕЖНО ВІД СПОСОБУ ФОРМУВАННЯ МЕХАНІЧНОГО СТРАВОХІДНО-ШЛУНКОВОГО АНАСТОМОЗУ

Усенко О.Ю., Сидюк А.В., Клімас А.С., Сидюк О.Є., Савенко Г.Ю.

Формування механічних стравохідно-шлункових анастомозів після езофагектомії нерідко супроводжується розвитком у пацієнтів рефлюкс-езофагіту різного ступеня. Мета роботи - оцінити патогістологічні зміни слизової оболонки стравоходу, пов'язані з шлунково-стравохідним рефлюксом, хворих на рак стравоходу та кардіоезофагіальний рак після радикального оперативного втручання залежно від варіанту сформованого езофагогастроанастомозу. До дослідження включені 30 пацієнтів, котрим було сформовано розроблений і захищений патентом України механічний інвагінаційний езофагогастроанастомоз (група дослідження) і 30 хворих, котрим було сформовано механічний циркулярний езофагогастроанастомоз кінець в бік (група порівняння). На 12 місяць спостереження усім хворим проведена фіброезофагогастродуоденоскопія. Ендоскопічну діагностику езофагіту проводили відповідно до модифікованої Лос-Анджелеської класифікації. Для оцінки морфологічного стану слизової оболонки стравоходу виконували біопсію слизової оболонки стравоходу над місцем анастомозу та морфологічно оцінювали вираженість рефлюкс-езофагіту. Рефлюкс-асоційовані зміни плоского епітелію стравоходу оцінювали згідно із консенсусними рекомендаціями Esohisto Project. Статистичний аналіз даних проведений з використанням пакету статистичного аналізу EZR v.1.35 (Saitama Medical Center, Jichi Medical University, Saitama, Japan), графічний інтерфейс до R (The R Foundation for Statistical Computing, Vienna, Austria). При порівняльному аналізі частотних характеристик між різними групами пацієнтів використовували критерій 2, для таблиць 2 2 (у випадку малої кількості пацієнтів (<5 випадків) у підгрупах дослідження) використано точний критерій Фішера. Розбіжності отриманих результатів вважали статистично значущими при p<0,05, що забезпечує 95% рівень ймовірності. Встановлено, що, частота, з якою фіксуються мікроскопічні ознаки рефлюкс-езофагіту, майже у 2 рази нижча у групі хворих, яким було сформовано механічний інвагінаційний езофагогастроанастомоз порівняно з механічним циркулярним (46,7% проти 83,3%, p<0,05), оскільки інвагінація моделює відтворення антирефлюксних властивостей втраченого стравохідно-шлункового переходу. Ендоскопічно діагностовані випадки рефлюкс-езофагіту додатково доповнюються мікроскопічно виявленими від 5,9% осіб у групі дослідження до 28,6% осіб (p<0,05) у групі порівняння, що свідчить про більш високу чутливість гістологічного діагнозу. До ознак, які стійко пов'язані з пострезекційним рефлюкс-езофагітом віднесено гіперплазію базального шару як за частотою (86,7% проти 100%), так і за більш тяжким ступенем вираженості (6,7% проти 23,3%, p<0,05), а також помірне видовження сосочків (30,0% проти 66,6%, p<0,01), за якими кращі результати отримані в групі хворих, котрим сформували інвагінаційний механічний езофагогастроанастомоз. За критеріями Esohisto Project частота як "м'якого", так і "важкого" езофагіту в групі хворих, котрим сформований інвагінаційний механічний езофагогастроанастомоз, була нижчою порівняно з групою з механічним циркулярним езофагогастроанастомозом (36,7% і 10,0% проти 63,3% і 20,0%, p<0,01 відповідно). Таким чином, формування інвагінаційного механічного езофагогастроанастомозу дозволяє достовірно зменшити частоту гістологічних проявів рефлюкс-езофагіту порівняно зі способом формування циркулярного механічного анастомозу.

Ключові слова: *проксимальна резекція шлунку з резекцією стравоходу, езофагогастроанастомоз, пострезекційний рефлюкс-езофагіт, критерії Esohisto Project, гістологія, гістопатологія.*

МОРФОЛОГИЧЕСКОЕ СОСТОЯНИЕ СЛИЗИСТОЙ ОБОЛОЧКИ ПИЩЕВОДА БОЛЬНЫХ С ПОСТРЕЗЕКЦИОННЫМИ ПРОЯВЛЕНИЯМИ РЕФЛЮКС-ЭЗОФАГИТА В ЗАВИСИМОСТИ ОТ СПОСОБА ФОРМИРОВАНИЯ МЕХАНИЧЕСКОГО ПИЩЕВОДНО-ЖЕЛУДОЧНОГО АНАСТОМОЗА

Усенко А.Ю., Сидюк А.В., Климас А.С., Сидюк Е.Е., Савенко Г.Ю.

Формирование механических пищеводно-желудочных анастомозов после эзофагэктомии нередко сопровождается развитием у пациентов рефлюкс-эзофагита разной степени. Цель работы - оценить патогистологические изменения слизистой оболочки пищевода, связанные с желудочно-пищеводным рефлюксом, больных раком пищевода и кардиоэзофагиальным раком, после радикального оперативного вмешательства в зависимости от варианта сформированного эзофагогастроанастомоза. В исследование включены 30 пациентов, которым был сформирован разработанный и защищенный патентом Украины механический инвагинационный эзофагогастроанастомоз (группа исследования) и 30 больных, которым был сформирован механический циркулярный эзофагогастроанастомоз конец в бок (группа сравнения). На 12 месяц наблюдения всем больным проведена фиброэзофагогастродуоденоскопия. Эндоскопическую диагностику рефлюкс-эзофагита проводили в соответствии с модифицированной Лос-Анджелесской классификацией. Для оценки морфологического состояния слизистой оболочки пищевода выполняли биопсию слизистой оболочки пищевода над местом анастомоза и морфологически оценивали выраженность рефлюкс-эзофагита. Рефлюкс-ассоциированные изменения плоского эпителия пищевода оценивали согласно консенсусным рекомендациям Esohisto Project. Статистический анализ данных проведен с использованием пакета статистического анализа EZR v.1.35 (Saitama Medical Center, Jichi Medical University, Saitama, Japan), графический интерфейс к R (The R Foundation for Statistical Computing, Vienna, Austria). При сравнительном

анализе частотных характеристик между различными группами пациентов использовали критерий 2, для таблиц 2 2 (в случае малого количества пациентов (<5 случаев) в подгруппах исследования) использован точный критерий Фишера. Различия полученных результатов считали статистически значимыми при p<0,05, что обеспечивает 95% уровень вероятности. Установлено, что частота, с которой фиксируются микроскопические признаки рефлюкс-эзофагита, почти в 2 раза ниже в группе больных, которым был сформирован механический инвагинационный эзофагогастроанастомоз по сравнению с механическим циркулярным (46,7% против 83,3%, p<0,05), поскольку инвагинация моделирует воспроизведение антирефлюксных свойств утраченного пищеводно-желудочного перехода. Эндоскопически диагностированные случаи рефлюкс-эзофагита дополнительно дополняются микроскопически обнаруженными от 5,9% лиц в группе исследования до 28,6% лиц (p<0,05) в группе сравнения, что свидетельствует о более высокой чувствительности гистологического диагноза. К признакам, которые устойчиво связаны с пострезекционным рефлюкс-эзофагитом отнесено гиперплазию базального слоя как по частоте (86,7% против 100%), так и по более тяжелой степени выраженности (6,7% против 23,3%, p<0,05), а также умеренное удлинение сосочков (30,0% против 66,6%, p<0,01), по которым лучшие результаты получены в группе больных, которым сформировали инвагинационный механический эзофагогастроанастомоз. По критериям Esohisto Project, частота как "мягкого", так и "тяжелого" эзофагита в группе больных, которым сформирован инвагинационный механический эзофагогастроанастомоз, была ниже по сравнению с группой с механическим циркулярным эзофагогастроанастомозом (36,7% и 10,0% против 63,3% и 20,0%, p<0,01 соответственно). Таким образом, формирование инвагинационного механического эзофагогастроанастомоза позволяет достоверно уменьшить частоту гистологических проявлений рефлюкс-эзофагита по сравнению со способом формирования циркулярного механического анастомоза.

Ключевые слова: *проксимальная резекция желудка с резекцией пищевода, эзофагогастроанастомоз, пострезекционный рефлюкс-эзофагит, критерии Esohisto Project, гистология, гистопатология.*

DOI: 10.31393/morphology-journal-2018-24(3)-08 Reports of Morphology, Vol. 24, №3, Pages 52-57

ISSN 1818-1295 eISSN 2616-6194

REPORTS OF MORPHOLOGY

Official Journal of the Scientific Society of Anatomists, Histologists, Embryologists and Topographic Anatomists of Ukraine

journal homepage: https://morphology-journal.com

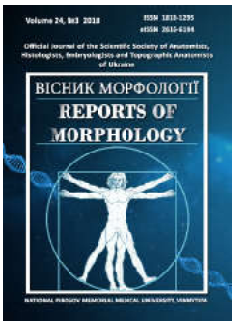

Changes in the sizes of the kidney after contralateral nephrectomy in the experiment

Monastyrskyi V.M.
National Pirogov Memorial Medical University, Vinnytsya, Ukraine

ARTICLE INFO
Received: 12 July, 2018
Accepted: 06 August, 2018

UDC: 611.611:611.061:611.068:
616.61-089.87

CORRESPONDING AUTHOR
e-mail: vova.monastirskiy@gmail.com
Monastyrskyi V.M.

The evaluation of renal measurements such as length, width and thickness, volume is important in the diagnosis and treatment of many renal disorders, since there is a close relationship between the sizes of the kidneys and its function. The purpose of the study was to establish and compare during the postoperative period changes in the mass and sizes of the kidney left after nephrectomy in the sexually mature male rats. An experimental study was carried out on 84 sexually mature white male rats weighing 178-194 grams. Animals were divided into two groups: control (42 rats) and experimental (42 rats). In the control group, the animals under ketamine anesthesia were followed by an abdominal cavity dilution, after which the abdominal wall was applied in a row. All animals of the experimental group performed surgical intervention - nephrectomy of the left kidney. The animals were withdrawn from the trial by intra-pleural administration of thiopental-sodium 50 mg/kg after 7, 14, 21, 30, 90 days after nephrectomy. Macroscopic evaluation and description of the kidneys of animals was performed after their removal. Their weight was determined on the laboratory scale of HLR-200 up to 0.1 mg, and the length, width and thickness of the organ were measured with the help of a caliper to an accuracy of 0.05 mm. Calculated the volume of the kidney. The statistical analysis of the obtained results was carried out using the program STATISTICA 5.5 using parametric methods for evaluating the results. It was established that the mass, length, width, thickness and volume of the kidney of animals in the experimental group, as compared with the control group, were statistically significantly higher in all terms of observation. The fraction of the growth of the width and thickness of the single kidney of animals in the experimental group compared with the control animals in the animals was statistically significantly greater than the proportion of kidney growth during the postoperative period. It was found that the largest increase in the mass and thickness of the kidney, as compared with the control group, was observed after 30 days of the postoperative period, and the greatest increase in the length and width of the kidney, as compared with the control group, was observed after 14 days of the postoperative period.

Keywords: *single kidney, nephrectomy, kidney sizes, experiment, sexually grown rats.*

Introduction

Despite recent developments in systemic therapy, nephrectomy is still considered the only reliable treatment for kidney cancer, and as a result, the number of performed nephrectomies will increase [25, 28].

The question of the compensation of structure and function in the loss of one of the paired organs is of interest to clinical practice, in this connection, the attention of researchers to the experimental study of the kidneys remaining after the removal of contralateral.

Several studies have found that body weight and body mass index are independent predictors of the development of chronic kidney disease after nephrectomy [23, 29]. The risk of chronic kidney disease following nephrectomy with regard to kidney cancer has been confirmed in several retrospective studies of populations [5, 24]. The risk of terminal renal dysfunction in renal donor increases with age [17]. It is established that the larger the mass of the kidneys, the greater the predictability of survival after nephrectomy in the elderly [26].

The evaluation of renal measurements, such as length, width and thickness, is important in the diagnosis and treatment of many renal disorders, since there is a close relationship between the size of the kidney and its function [22]. According to researchers after nephrectomy, renal

function of the contralateral kidney decreases in patients regardless of the choice of access (open, laparoscopic) [11] and depends on the volume of loss of renal parenchyma [2]. The volume of kidneys is considered to be the most accurate indicator of the size of the kidneys. Recent studies have shown that kidney volume is an optimal parameter for predicting renal function [8, 12]. Changing the size of the kidneys from one survey to another can be an important indicator of the presence or progression of the disease. The increase in the volume of the kidneys was observed to a greater extent after nephrectomy than after renal resection [19].

We have established the patterns of possible displacements of a single kidney with an increase in its mass after the removal of contralateral using mathematical modeling [13]. The study of the angles of inclination of a single kidney remaining after contralateral nephrectomy, in the frontal, sagittal, and horizontal planes, reveals certain patterns with magnetic resonance imaging depending on somatotypes [21].

According to scientists, the mean values of length, width and thickness of the kidneys should be determined for each population [1, 16]. It is especially important to know the volume of the kidney, the accuracy of which depends on the technique of morphometry, the use of magnetic resonance imaging [15].

Changes in the size of kidney after nephrectomy, direction, size, speed and duration are of value for predicting the change of position, function and possible pathology of the kidney.

The *aim* of the study - to establish and compare changes in organometric parameters of the kidney left after nephrectomy in sexually mature male rats during the postoperative period.

Materials and methods

Experimental study was performed on 84 sexually mature white male rats weighing 178-194 grams, which were kept on the standard diet in vivarium of National Pirogov Memorial Medical University.

Animal retention and manipulation were conducted in accordance with the "General Ethical Principles of Animal Experiments" adopted by the First National Congress on Bioethics (Kyiv, 2001), and were guided by the recommendations of the "European Convention for the Protection of Vertebrate Animals Used for Experimental and Other Scientific Purposes" (Strasbourg, 1985) and the provisions of the "Rules for Preclinical Safety Assessment of Pharmacological Products (GLP)".

All animals were divided into two groups: control (42 rats) and experimental (42 rats). In the control group all animals were performed abdominal section, followed by sewn up of abdominal wall layers under anesthesia by ketamine.

All animals of the experimental group were performed surgical intervention - nephrectomy of the left kidney. Rats under general intra-muscle anesthesia (aminazine 10 mg/kg and ketamine 20 mg/kg) were treated with left-sided nephrectomy by crossing the renal leg between two ligatures and then removing the organ. The operation was carried out as follows. The animal was inserted and fixed with soft straps for the limbs in the position on the back to the operating table. Pararectal incision was done in the length up to 3-5 cm in layers for opening an abdominal cavity. The small intestine with a gauze napkin was pulled down and medially. Left kidney and its vessels were isolated from the surrounding tissues. The kidney was molded into the wound and isolated from the fatty tissue of the upper third of the ureter. A clamping device was applied to the ureter, under which it was tied with a catgut ligation and then crossed under a clamp. In a droop way, they isolated the renal artery and vein and imposed two clips, between which they were crossed. The kidney was removed, and the stump of the blood vessels were tied together by catgut ligatures. The layer of the wound was tightly sewn.

The animals were withdrawn from the trial by intra-pleural administration of thiopental-sodium 50 mg/kg after 7, 14, 21, 30, 90 days after nephrectomy.

Macroscopic evaluation and description of the kidneys of animals was performed after their removal. Their weight was determined on the laboratory scale of HLR-200 up to 0.1 mg, and the length, width and thickness of the organ were measured with the help of a caliper to an accuracy of 0.05 mm. The volume of the kidney [4] was calculated according to the formula: V=0.523?a?b?c, where a is length, b is width, c is the thickness of the kidney. It is believed that the method for assessing the volume of the kidney after its hypertrophy using the ellipsoid volume formula is the most accurate and useful for predicting the functional status of the kidney [18].

The kidney mass index was calculated by obtaining a percentage relationship between the weight of the kidney and the weight of the body of the rat being examined. In the investigated animals of the experimental group, the index of hypertrophy of the kidney was calculated. It was calculated by obtaining a percentage correlation between the weight of a single kidney and the weight of the two kidneys of the control group rats at the given time of the study.

Statistical analysis of the obtained results was carried out using the program STATISTICA 5.5 using parametric and non-parametric methods for evaluating the obtained results.

Results

First of all, it is necessary to note changes in the body weight of the animals of the control and experimental groups. At the beginning of the study, no statistically significant change in body mass was detected. After 7 days, the body weight of the experimental group animal was 4.01% lower than the control group animal. Subsequently, the comparison of body mass data showed a lower body weight of experimental group animals in 14 days by 3.67%, in 21 days - by 4.36%, after 30 days - by 5.02%, after 60 days - by 3.18%,

Table 1. Weight of the body and the right kidney of the mature rat of the control and experimental groups.

The term of the postoperative period	Control group (n=42)			Experimental group (n=42)		
	Animal weight (g)	Kidney mass (g)	Kidney Mass Index (%)	Animal weight (g)	Kidney mass (g)	Kidney Mass Index (%)
1 day	184.8±2.9	0.892±0.028	0.483±0.007	185.6±3.2		
7 days	202.4±4.6*	0.975±0.008*	0.493±0.005	194.3±3.2*#	1.027±0.026#	0.532±0.013#
14 days	218.5±3.5*	1.077±0.017*	0.501±0.003	210.5±3.6*#	1.250±0.020*#	0.596±0.011*#
21 days	231.0±4.9*	1.165±0.037*	0.505±0.008	220.9±4.9*#	1.662±0.072*#	0.656±0.031*#
30 days	245.6±4.7*	1.268±0.026*	0.510±0.008	233.3±5.9*#	1.710±0.060#	0.721±0.018*#
60 days	262.4±3.7*	1.352±0.022*	0.510±0.002	254.1±3.8*#	1.757±0.010*#	0.700±0.005#
90 days	274.7±4.7*	1.497±0.023*	0.545±0.002*	265.5±3.7*#	1.858±0.013*#	0.700±0.013#

Note: * - statistically significant differences ($p<0.05$) according to the Mana-Whitney criterion between the corresponding indicators in comparison with the indicators of the previous term of research; # Are statistically significant differences ($p<0.05$) according to the Mana-Whitney criterion between the respective indices compared with the control animals.

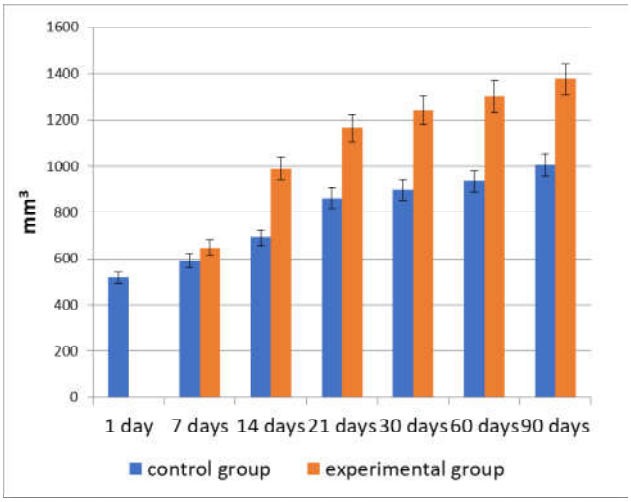

Fig. 1. Volume of the right kidney of the sexually mature rats in different terms after the operation of the control and experimental groups.

after 90 days - by 3.34% compared with similar terms in the control animals. The weight of the kidney increased both in the control and in the experimental groups. However, in the experimental group, the mass of the right kidney was greater compared to the weight of the kidney of the control group in the similar term: after 7 days - 4.85%, 14 days - by 13.6%, in 21 days - by 25.52%, through 30 days - by 25.73%, 60 days - by 24.58%, after 90 days - by 19.35%. Thus, the peak growth rate of the kidney mass in the experimental group relative to the control group data was observed after 30 days (Table 1).

The kidney mass index of the experimental group significantly differed from that of the control group. Thus, in the control group it ranged from 0,49% to 0,54%, and in the experimental group - from 0,53% to 0,72%. The peak in the control group in the 90th day of the experiment, in the experimental group - at 30 days.

The integral index of kidney size - volume, compared with the data at the beginning of the experiment, changed as follows: after 7 days, it increased by 12.43% in the control group and by 19.87% in the experimental group, after 14 days, it increased by 24.78% and by 47.69%, respectively, in 21 days - by 39.90% and 55.48% respectively, after 30 days - by 42.22% and 58.33% respectively, after 60 days - by 44.54 % and 60.23% respectively, after 90 days - by 48.40% and 62.39% respectively (Fig. 1).

The length of the right kidney compared with the same indicator of animals in the control group was greater after 7 days after nephrectomy by 2.87%, after 14 days - by 6.21%, 21 days - by 3.86%, 30 days later - by 2, 65%, after 60 days - by 4.62%, after 90 days - by 5.34%. The width of the right kidney was greater after 7 days after nephrectomy by 3.38%, after 14 days - by 13.99%, after 21 days - by 12.16%, after 30 days - by 13.24%, after 60 days - by 12,88%, after 90 days - by 11,69%. The thickness of the right kidney was greater after 7 days after nephrectomy by 2.51%, after 14 days - by 13.76%, in 21 days - by 12.32%, after 30 days - by 14.57%, after 60 days - by 13,68%, after 90 days - by 12,74% (Fig. 2).

Discussion

Compensatory and adaptive reactions of a single kidney after removal from the body of the contralateral form part of the general system of adaptation of the body in cases of its damage. We have established an increase in the mass of the right kidney of rats after the removal of the left kidney, which reached its peak after 30 days, consistent with the data of other authors [7]. By comparing the mass of a single kidney remaining after contralateral nephrectomy, with the weight of two kidneys of the control group in a given experiment period, we found that the index of hypertrophy of the kidney during the postoperative period ranged from 52.35% to 65.22The maximum index of kidney hypertrophy was observed in the period of 30 days. In the future there was a decrease in the index. Several authors note that the maximum hypertrophy of a single kidney, after removal of contralateral, is 77% of the sum of volumes of two kidneys in the control group [10].

The fraction of the growth of the width and thickness of the single kidney of animals in the experimental group

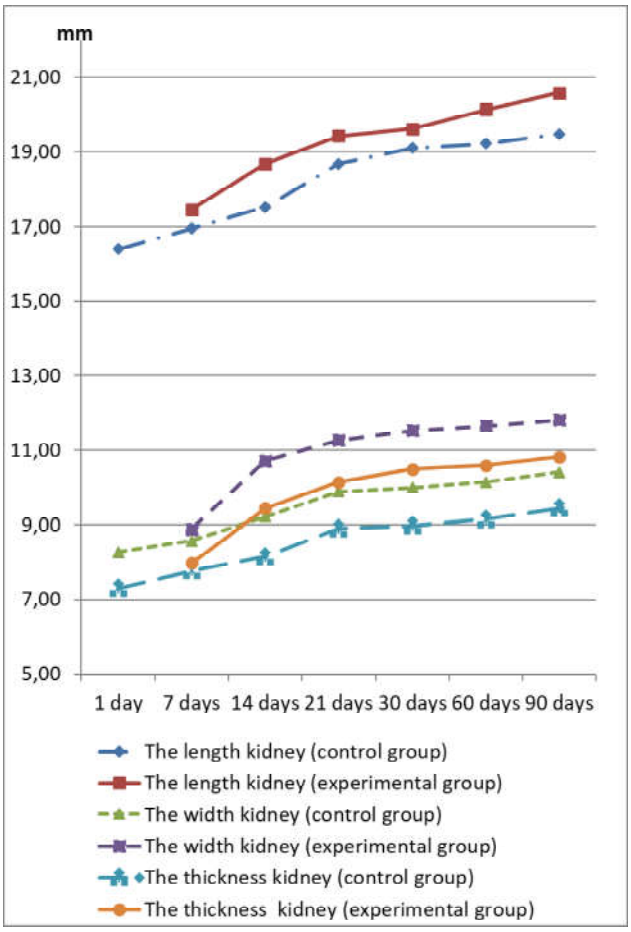

Fig. 2. Length. width and thickness of the right kidney of the control and experimental groups during the experiment.

compared with the control animals in the animals was statistically significantly greater than the proportion of kidney growth during the postoperative period. According to scientific literature, the length of the kidneys directly correlates with the clearance of creatinine [6], and the width of the kidneys better reflects the influence of environmental factors than the length of the kidneys. The results of the research show that the width of the kidney, and not the length, is a predictor of renal insufficiency [27].

Adjustment-compensatory changes after the performed nephrectomy were manifested in the early stages of the experiment by compensatory hypertrophy of the area of the renal cortex and the reorganization of the vascular bed. In the later stages of the experiment, part of the nephrons develop morpho-functional changes of a destructive nature [14]. We have found that at the 7th and 14th day after nephrectomy in the vascular glomeruli of the renal corpuscles hemocapillaries have blood-filling enlightenment. On the 21st day after the experimental nephrectomy there are significant changes in the vessels and structural components of the nephrons. There is swelling of the stroma, focal infiltration. On the 30th and 60th day organelles are destructively altered and poorly detected against the background of osmophilic hyaloplasm. Membrane folds in the basal region of these cells and microvilli on the apical surface are affected [20].

The significance of damage to podocytes and swelling of the kidneys as a universal mechanism of development of renal failure [3] has been confirmed today. The relevance of the study of the dependence of the renal function on its size is established [9].

Conclusions

1. The weight, length, width, thickness and volume of the kidneys of animals in the experimental group were statistically significantly higher in all terms of observation compared with the control group ($p < 0.05$).

2. The increase in the width and thickness of the single kidney of animals in the experimental group compared with the control animals was statistically significantly greater than the proportion of kidney growth during the postoperative period.

3. The largest increase in the mass and thickness of the kidney, as compared to the control group, was observed after 30 days of the postoperative period.

4. The largest increase in the length and width of the kidney, as compared to the control group, was observed after 14 days of the postoperative period.

In the future, it is planned to compare changes in organometric parameters of the kidney, remaining after nephrectomy, in non-sexually mature and mature animals.

References

[1] Adedeji, E. (2014). Need for a nomogram of renal sizes in the Indian population. *Indian J. Med. Res*., 139(5), 663-665. http://www.ijmr.org.in/text.asp?2014/139/5/663/136461

[2] Antoniewicz, A. A., Poletajew, S., Boro'wka, A., Pasierski, T., Rostek, M., & Pietkiewicz, W. P. (2012). Renal function and adaptive changes in patients after radical or partial nephrectomy. *Int. Urol. Nephrol.*, 44(3), 745-751. doi: 10.1007/s11255-011-0058-z

[3] Bobkova, I., Chebotareva, N., Kozlovskaya, L., & Shilov, E. (2016). Edema in renal diseases - current view on pathogenesis. *Nephrology and Point of Care*, 2(1), 47-55. doi: doi.org/10.5301/pocj.5000204

[4] Breau, R., Clark, E., Bruner, B., Cervini, P., Atwell, T., Knoll, G., & Leibovich, B. (2013). A simple method to estimate renal volume from computed tomography. *Canadian Urological Association Journal,* 7(5-6), 189-192. doi: doi.org/10.5489/cuaj.1338

[5] Choi, S.-K., & Song, Ch. (2014). Risk of Chronic Kidney Disease After Nephrectomy for Renal Cell Carcinoma. *Korean. J. Urol.,* 55(10), 636-642. doi: 10.4111/kju.2014.55.10.636

[6] Di Zazzo, G., Stringini, G., Matteucci, M. C., Muraca, M., Malena, S., & Emma, F. (2011) Serum creatinine levels are significantly influenced by renal size in the normal pediatric population. *Clin. J. Am. Soc. Nephrol.,* 6(1), 107-113. doi: 10.2215/CJN.00580110

[7] Eladl, M. A., Elsaed, W. M., Atef, H., & El-Sherbiny, M. (2017). Ultrastructural changes and nestin expression accompanying compensatory renal growth after unilateral nephrectomy in adult rats. *Int. J. Nephrol. Renovasc*. Dis., 10, 61-76. doi:

10.2147 / IJNRD.S121473

[8] Jeon, H. G., Gong, I. H., Hwang, J. H., Choi, D. K., Lee, S. R., & Park, D. S. (2012). Prognostic significance of preoperative kidney volume for predicting renal function in renal cell carcinoma patients receiving a radical or partial nephrectomy. *BJU Int.,* 109(10), 1468-1473. doi: 10,1111 / j.1464-410X.2011.10531.x

[9] Kishore, S. S., Oberoi, S., Bhattacharya, A., Prasad, R., Trehan, A., Bansal, D., & Marwaha, R. K. (2015). Function and size of the residual kidney after treatment of Wilms tumor. *Pediatr. Hematol. Oncol.,* 32(1), 11-17. doi:10.3109/08880018.2014.887804

[10] Kosiak, M., Stefanowicz, J., Adamkiewicz-Dro?y?ska, E., Balcerska, A., Kurylak, A., & Demidowicz, E. (2018). Sonographic Image of Solitary Kidney in Wilms Tumour Survivors. *Kidney Blood Press Res.,* 43(4), 1363-1363. https://doi.org/10.1159/000492951

[11] Krebs, R. K., Andreoni, C., & Ortiz, V. (2014). Impact of Radical and Partial Nephrectomy on Renal Function in Patients with Renal Cancer. *Urol. Int.*, 92(4), 449-454. doi.org/10.1159/000355609

[12] Lange, D., Helck, A., Rominger, A., Crispin, A., Meiser, B., Werner, J. … Habicht, A. (2018). Renal volume assessed by magnetic resonance imaging volumetry correlates with renal function in living kidney donors pre- and postdonation: a retrospective cohort study. *Transplant International,* 31(7), 773-780. doi.org/10.1111/tri.13150

[13] Monastirskiy, V. M., Pivtorak, V. I., & Fedotov, V. A. (2017). Modeling of possible movements of a single human kidney. *Deutscher Wissenschaftsherold.*, 5, 31-33. doi: 10.19221/201759.

[14] Monastirskiy, V. M., Pivtorak, V. I., & Kozak I.O. (2015). The remaining morphology of the kidney after removal of the contralateral. *Reports of Morphology*, 21(1), 37-41.

[15] Moorthy, H. K., & Venugopal, P. (2011). Measurement of renal dimensions in vivo: A critical appraisal. I*ndian J. Urol.*, 27(2), 169-175. doi: 10,4103/0970-1591.82832

[16] Muthusami, P., Ananthakrishnan, R., & Santosh, P. (2014). Need for a nomogram of renal sizes in the Indian population-findings from a single centre sonographic study. Indian J. Med. Res., 139(5), 686-693.

[17] Muzaale, A. D., Massie, A. B., Wang, M-Ch., Montgomery R. A., McBride, M. A., Wainright, J. L., & Segev, D. L. (2014). Risk of End-Stage Renal Disease Following Live Kidney Donation. JAMA, 311(6), 579-586. doi: 10.1001/jama.2013.285141

[18] Park, B. H., Kang, S. H., Jung, J. S., Bae, S. R., Lee, Yo. S., & Han, Ch. H. (2017). A useful method for assessing differences of compensatory hypertrophy in the contralateral kidney before and after radical nephrectomy in patients with renal cell carcinoma: ellipsoid formula on computed tomography. The Journal of Urology, 197(4S), e785-e786. doi.org/10.1016/j.juro.2017.02.1829

[19] Park, D. S., Hong, Y.K., Lee, S. R., Hwang, J. H., Kang, M. H., & Oh, J. J. (2016). Three-dimensional reconstructive kidney volume analyses according to the endophytic degree of tumors during open partial or radical nephrectomy. Int. Braz. J. Urol., 42(1), 37-46. doi: 10.1590/S1677-5538.IBJU.2014.0417

[20] Pivtorak, V. I., & Monastirskiy, V. M. (2015). Ultrastructural changes of podocytes of the single kidney after removal of the contralateral one. Clinical Anatomy and Operative Surgery, 14(2), 33-37.

[21] Pivtorak, V. I., & Monastyrskyi, V. M. (2018). Features of the topography of a single kidney after removal of contralateral one. Pathologia, (2), 236-241. doi: 10.14739/2310-1237.2018.2.141369

[22] Rathore, R. S., Mehta, N., Pillai, B. S., Sam, M. P., Upendran, B., & Krishnamoorthy, H. (2016). Variations in renal morphometry: A hospital-based Indian study. Indian J. Urol., 32(1), 61-64. doi: 10.4103/0970-1591.173115

[23] Reinstatler, L., Klaassen, Z., Barrett, B., Terris, M. K., & Moses, K. A. (2015). Body mass index and comorbidity are associated with postoperative renal function after nephrectomy. Int. Braz. J. Urol., 41(4), 697-706. doi: 10.1590 / S1677-5538.IBJU.2014.0383

[24] Sun, M., Bianchi, M., Hansen, J., Trinh, Q. D., Abdollah, F., Tian, Z. … Karakiewicz, P. I. (2012). Chronic kidney disease after nephrectomy in patients with small renal masses: a retrospective observational analysis. *Eur. Urol.,* 62(4), 696-703. Doi: 10.1016/j.eururo.2012.03.051

[25] Tan, H.-J., Norton, E. C., Ye, Z., Hafez, K. S., Gore, J. L., & Miller, D. C. (2012). Long-term survival following partial versus radical nephrectomy among older patients with early-stage kidney cancer. *JAMA,* 307(5), 1629-1635. doi: 10.1001/jama.2012.475

[26] Tang, D. H., Nawlo, J., Chipollini, J., Gilbert, S. M., Poch, M., Pow-Sang, J. M., Sexton, W. J., & Spiess, Ph. E. (2017). Management of Renal Masses in an Octogenarian Cohort: Is There a Right Approach? *Clin. Genitourin. Cancer,* 15(6), 696-703. doi: 10,1016/j.clgc.2017.05.011

[27] Tarnoki, D. L., Tarnoki, A. D., Bata, P., Littvay, L., Garami, Z., Berczi, V., & Karlinger, K. (2015). Different genetic impact in the development of renal length and width: a twin study. *Internal Medicine Journal,* 45(1), 63-67. doi.org/10.1111/imj.12631

[28] Van Poppel, H., Da Pozzo, L., Albrecht, W., Matveev, V., Bono, A., Borkowski, A. … Sylvester R. (2011). A Prospective, Randomised EORTC Intergroup Phase 3 Study Comparing the Oncologic Outcome of Elective Nephron-Sparing Surgery and Radical Nephrectomy for Low-Stage Renal Cell Carcinoma. *Eur. Urol.,* 59(4), 543-552. doi:10,1016 / j.eururo.2010.12.013

[29] Verhoest, G., Patard, J. J., Oger, E., Rioux-Leclercq, N., Peyronnet, B., Bessede, T. … Bensalah, K. (2014). Predictive factors of chronic kidney disease stage V after partial nephrectomy in a solitary kidney: a multi-institutional study. *Urol. Oncol.,* 32(1), 28. doi: 10,1016 / j.urolonc.2012.10.003

ЗМІНИ РОЗМІРІВ НИРКИ ПІСЛЯ НЕФРЕКТОМІЇ КОНТРАЛАТЕРАЛЬНОЇ В ЕКСПЕРИМЕНТІ

Монастирський В.М.

Оцінка ниркових вимірювань, таких як довжина, ширина і товщина, об'єм важлива при діагностиці і лікуванні багатьох ниркових розладів, оскільки існує тісний зв'язок між розміром нирок і їх функцією. Мета дослідження - встановити та порівняти протягом післяопераційного періоду зміни маси та розмірів нирки, що залишилась після нефректомії, у статевозрілих щурів-самців. Експериментальне дослідження виконано на 84 статевозрілих білих щурах-самцях масою 178-194 грамів. Тварин розподілили на дві групи: контрольну (42 щури) та дослідну (42 щури). У контрольній групі тваринам під кетаміновим знеболенням проводили розтин черевної порожнини, після чого пошарово ушивали черевну стінку. Усім тваринам дослідної групи виконували оперативне втручання - нефректомію лівої нирки. Тварин виводили з досліду шляхом

внутрішньоплеврального введення тіопенталу-натрію 50 мг/кг через 7, 14, 21, 30, 90 діб після нефректомії. Макроскопічну оцінку та описання нирок тварин проводили після їх вилучення. Масу нирок визначали на лабораторних вагах ВЛР-200 з точністю до 0,1 мг, довжину, ширину і товщину - за допомогою штангенциркуля з точністю до 0,05 мм. Розраховували об'єм нирки. Статистичний аналіз отриманих результатів проведений із застосуванням програми "STATISTICA 5.5" з використанням параметричних методів оцінки отриманих результатів. Встановлено, що маса, довжина, ширина, товщина та об'єм нирки тварин дослідної групи, порівняно з контрольною групою, були статистично значуще більшими у всі терміни спостереження. Частка зростання ширини та товщини єдиної нирки тварин дослідної групи у порівнянні з показниками у тварин контрольної групи була статистично значуще більше, ніж частка зростання довжини нирки під час післяопераційного періоду. Встановлено, що найбільша величина приросту маси та товщини нирки, порівняно із показниками контрольної групи, спостерігалася через 30 діб післяопераційного періоду, а найбільша величина приросту довжини та ширини нирки, порівняно з показниками контрольної групи, спостерігалася через 14 діб післяопераційного періоду.
Ключові слова: *єдина нирка, нефректомія, розміри нирки, експеримент, статевозрілі щури.*

ИЗМЕНЕНИЯ РАЗМЕРОВ ПОЧКИ ПОСЛЕ НЕФРЭКТОМИИ КОНТРАЛАТЕРАЛЬНОЙ В ЭКСПЕРИМЕНТЕ

Монастырский В.Н.

Оценка почечных измерений, таких как длина, ширина и толщина, объем важна при диагностике и лечении многих почечных расстройств, поскольку существует тесная связь между размерами почек и их функций. Цель исследования - установить и сравнить в течение послеоперационного периода изменения массы и размеров почки, оставшейся после нефрэктомии, у половозрелых крыс-самцов. Экспериментальное исследование выполнено на 84 половозрелых белых крысах-самцах массой 178-194 граммов. Животных разделили на две группы: контрольную (42 крысы) и опытную (42 крысы). В контрольной группе животным под кетаминовым обезболиванием проводили вскрытие брюшной полости, после чего послойно ушивали брюшную стенку. Всем животным опытной группы выполняли оперативное вмешательство - нефрэктомию левой почки. Животных выводили из опыта путем внутриплеврального введения тиопентала натрия 50 мг/кг через 7, 14, 21, 30, 90 суток после нефрэктомии. Макроскопическую оценку и описание почек животных проводили после их удаления. Определяли их массу на лабораторных весах ВЛР-200 с точностью до 0,1 мг, измеряли длину, ширину и толщину с помощью штангенциркуля с точностью до 0,05 мм. Рассчитывали объем почки. Статистический анализ полученных результатов проведен с применением программы "STATISTICA 5.5" с использованием параметрических методов оценки полученных результатов. Установлено, что масса, длина, ширина, толщина и объем почки животных опытной группы по сравнению с контрольной группой, были статистически значимо больше на всех сроках наблюдения. Доля роста ширины и толщины единственной почки животных опытной группы по сравнению с показателями у животных контрольной группы была статистически значимо больше, чем доля роста длины почки в течение послеоперационного периода. Установлено, что наибольшая величина прироста массы и толщины почки по сравнению с показателями контрольной группы, наблюдалась через 30 суток послеоперационного периода, а наибольшая величина прироста длины и ширины почки по сравнению с показателями контрольной группы, наблюдалась через 14 дней послеоперационного периода.
Ключевые слова: *единственная почка, нефрэктомия, размеры почки, эксперимент, половозрелые крысы.*

DOI: 10.31393/morphology-journal-2018-24(3)-09 Reports of Morphology, Vol. 24, №3, Pages 58-64

ISSN 1818-1295 eISSN 2616-6194

REPORTS OF MORPHOLOGY

Official Journal of the Scientific Society of Anatomists, Histologists, Embryologists and Topographic Anatomists of Ukraine

journal homepage: https://morphology-journal.com

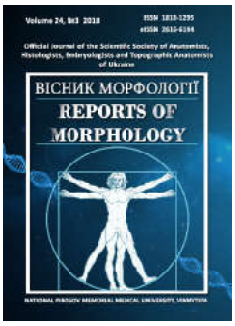

Characteristics of nervous tissue after modeling of focal cerebral ischemia in rats at different periods of reperfusion

Savchuk O.I., Skibo G.G.

Bohomoletz Institute of Physiology National Academy of Sciences of Ukraine, Kyiv, Ukraine

ARTICLE INFO

Received: 20 July, 2018

Accepted: 23 August, 2018

UDC: 591.481.1: 616-005.4: 612.825

CORRESPONDING AUTHOR

e-mail: floweringbowl@ukr.net

Savchuk O.I.

The stroke-causing problems are extremely important in Ukraine. This makes a heavy burden not only on the health care system, but also on the whole society as a whole. That's why we've studied structural and ultrastructural changes of cortical neurons and striatum of the brain and the development of delayed death of nerve cells after the modeling of the middle cerebral artery occlusion (MCAO) and post ischemic period in rats. We've analyzed the data at different terms after modeling of MCAO. The purpose of the study was to investigate the changes in the nervous tissue in the modeling of focal cerebral ischemia by monofilament occlusion of MCAO in rats at different periods of reperfusion. The statistical processing of primary digital experimental data was carried out using the software Statistica 6.0. It was confirmed that the 60-minute occlusion of the MCAO is an adequate model of focal ischemic brain damage in rats. Changes of locomotor activity and a tactile sensitivity were determined in rats after occlusion and after reperfusion during the post-period period. It was found that in the experimental group with a reperfusion period of 72 hours, a clear increase of the volume of the ischemic area of the brain, accompanied by significant neurological deficiency, was observed. Reduced research activity of the rats was revealed, which was shown in the decrease of the number of squares they crossed, the number of racks, the increase of acts of grooming and the duration of acts of frizings. Following ischemic brain damage, there was also a disbalance of somato-sensory functions, as evidenced by an increase in the time during which the animal took a test stimulus ("Sticky tape") from both the anterior paws when tested for tactile sensitivity (adhesive removal test). An electron microscopic study of the cortex showed that dark wrinkled neurons and enlightened swollen neurons were observed at 72 hours of post-occlusion period, indicating different ways of death of these cells. Changes in striatum were similar to changes in the cortex, which progressed with an increase in the post-occlusion period. The protocol of the serial evaluation of neurological disorders used after MCAO modeling allowed detecting long-term stable functional disorders in laboratory rats. The obtained data indicate significant changes in the structure of the cortex and striatum in the post-ischemic period and the progressive nature of these changes.

Key words: *ischemic stroke, focal cerebral ischemia, monofilament occlusion.*

Introduction

Ischemic stroke (IS) is one of the most important causes of morbidity, disability and mortality in developed countries.

According to indicators of morbidity and mortality caused by stroke Ukraine occupies one of the first places in Europe. Every year from 100 to 110 thousand Ukrainians first get ill with cerebral stroke [5]. Every third stroke affects people of working age. From 40 to 43 thousand inhabitants die after stroke in Ukraine annually. According to the World Health Organization (WHO), stroke is the second only among world death factors, and the third is in developed countries and is a major factor in disabling the population [3, 23].

Modeling of ischemic brain damage is an indispensable step for approbation of treatment methods for patients with IS. The models of IS are the basis for determining the mechanisms of cell death in neuronal repair in vivo.

The disclosure of the pathophysiological mechanisms underlying the cell death in the area of brain infarction is a

prerequisite for the development of new methods and therapeutic methods for IS.

The *aim* of the study was to analyze neural tissue changes after the modeling of focal cerebral ischemia by monofilament occlusion of MCA in rats at different periods of reperfusion and behavioral responses.

Materials and methods

Experimental studies were performed on 63 males of the Wistar line with body weight 280-320 g in age from 4 to 6 months.

Animals received from the vivarium of Bohomoletz Institute of Physiology National Academy of Sciences of Ukraine, where they were kept on a standard diet and in general were in similar conditions. All experiments were conducted in accordance with the "Rules for the implementation of works using experimental animals", approved by the Ministry of Health of Ukraine. Experimental procedures were carried out in the cytology department of Bohomoletz Institute of Physiology in the first half of the day, which coincided with the circadian rhythms of animals.

Animals were divided into 3 experimental groups ("Sham-operated" - an operating control in which all surgical manipulations were performed, except for the introduction of monofilament (n = 21), animals of the two following groups were modeled focal cerebral ischemia by monofilament occlusion of the middle cerebral artery by the method of J. Koizumi et al. (1986) using monofilaments with a silicone coating: "Short-term MCAO" - lasting 2 minutes (n=21) , "Long-term MCAO" - lasting 60 minutes (n=21) [8, 17, 18].

To assess the presence of ischemic brain damage before the ischemia was simulated, and after 6, 24 and 72 hours of reperfusion, an "open field" test was performed that evaluated locomotor activity and a tactile sensitivity test [2, 13, 21].

Sticky tape test is one of the most sensitive tests for identifying sensory disorders in rats with OCMA [9, 15]. For this, the animal was removed from the cage and labeled with a 3x1 cm Leofix adhesive tape on the distal part of the front paw, deprived of wool, in a circle of 360°, so that both ends of the tape protruded and glued together, and the front paw protruded somewhat forward of the formed cuffs Immediately after the adhesion of the tape, the animal was placed back into the cage and began observation. The rats use their teeth and, to a lesser extent, the opposite limb to remove the tape. Before the start of the observation, two timers were triggered: one timer was switched on constantly, and the other one - during the attempts of the animal to remove the tape. Each attempt lasted 30 seconds. The desired ratio is the number of seconds the animal responds to the stimulus, divided by 30 seconds. This test was repeated with an opposite limb. Each session consisted of 5 attempts at each end. Of the 5 attempts, two best results were chosen. After each test, the tape was removed using warm water and soap.

The final result was expressed in a formula:

$x=[(x1+x2)/30)]-2/[(y1+y2)/30)]-2$

where x - is the end result, x1 and x2 - are the number of seconds spent by the animal to remove the tape from the affected (left) extremity in the best attempts; in 1 and 2 - the number of seconds spent by the animal on removing the tape from the intact (right) limb, 30 - duration of the attempt (30s), 2 - two attempts with the best result.

When properly executed, this test clearly reflects the focal nature of the damage, demonstrating the pronounced difference in the score of the affected and intact limbs throughout the observation time.

The improved experimental model of ischemic stroke with the help of monofilament occlusion of the middle cerebral artery in rats allowed to reproduce the focal point of focal ischemic brain damage mainly in the cortex and striped body of rats, to a lesser extent, in adjacent brain structures, which was accompanied by the emergence of a stable and long-term neurological deficiency in the experimental animals.

To determine the ischemic volume, we calculated the area of the infarct area and multiplied it by the thickness of the sections (Fig. 1).

To determine the size of the cerebral infarction, in vivo experiments, we chose a commonly used method that allows the macroscopic level to separate the damaged (necrotized) region of the brain from the brain tissue that retained viability and was substantiated by the staining of TTC brain sections. The slices of the brain were placed in a 2% solution of TTC, which paints a viable tissue in a bright red color. Incubation sections were performed for 15 minutes at 37°C.

According to the literature, on the 3rd day after MCAO there is a clearly defined zone of ischemic injury, with the area of perifocal edema less pronounced than on 1st - 2nd day [1, 6, 16, 22]. In these studies, we conducted a

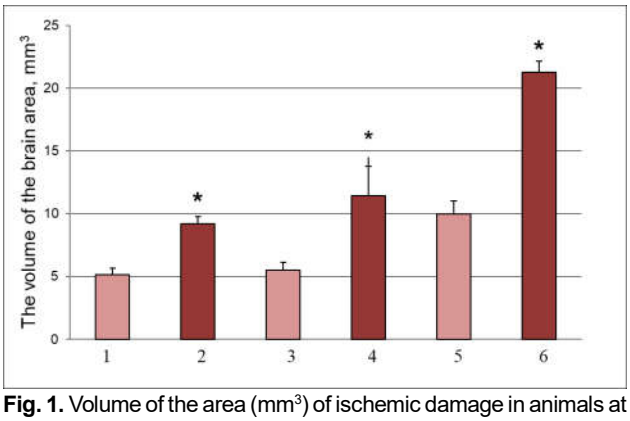

Fig. 1. Volume of the area (mm^3) of ischemic damage in animals at different periods of reperfusion after MCAO. 1 - 6 hour reperfusion group of short-term MCAO; 2 - 6 hour reperfusion of long-term MCAO; 3 - 24 hour reperfusion group of short-term MCAO; 4 - 24 hour reperfusion group of long-term MCAO; 5 - 72 hour reperfusion of short-term MCAO; 6 - 72 hour reperfusion group of long-term MCAO; * - $p<0.05$.

morphometric evaluation of lesions within 6 hours, 24 hours and 72 hours from the time of occlusion.

It is known that after ischemic brain damage there are changes of neurological functions in experimental animals [3, 10]. Therefore, in addition to the study of morphological changes occurring in the ischemic brain, we determined locomotor activity and conducted a test for tactile sensitivity in rats before occlusion and after reperfusion during the post-ischemic period. We conducted behavioral reactions in animals of different groups in 6, 24 and 72 hours after the modeling of focal ischemia. The main indicators were evaluated: motor activity, research activity and degree of anxiety, which was evaluated by grooming (all varieties of this reaction, which manifested themselves in licking and scratching), frizings (fading).

Another indicator, which was analyzed during the "open field" test, was the measurement of the number of racks (vertical motor activity) that demonstrated the research activity.

Structural characteristics of cortical nerve cells and striatum of the brain in the post-lateral period were investigated using light and electron microscopy methods.

Analysis and statistical processing of the results were carried out using the following software: ImageJ, Exel, Origin 8.0, SPSS ver., 20.0.

Results

In the sham-operated animals, histological damage to the brain was not observed.

In the group of animals of short-term occlusion of MCA after 6, 24, 72 hours the amount of damage was 5.110±1.250 mm^3; 5.520±1.470 mm^3; 10.01±2.340 mm^3, respectively, and in animals of the group of long-term occlusion of MCA in the similar terms of the experiment - 9.180±1.430 mm^3, 11.47±5.41 mm^3, 21.27±2.07 mm^3, ($p<0.05$).

It was found that in the experimental group with a reperfusion period of 72 hours, a clear increase in the volume of the ischemia of the brain. This indicates that the process of damaging the brain is dynamic with a gradual increase in the area of damage with an increase in the period of reperfusion.

6 hours after the carotid occlusion of the carotid artery in rats there was a weakened locomotor activity, which gradually increased with the duration of the post-ischemic period; single spontaneous movements were rotational.

A group of pseudo-operated animals showed a high percentage of research activity and averaged 86% of the total number of racks. Rats with ischemic brain damage, in the first day after occlusion, this percentage was significantly lower (19%) than in control animals and gradually decreased during the post occlusive period.

After the operation, all animals had a reduction in research activity, which was manifested in the reduction of the number of squares they crossed (Table 1), the number of racks, the increase in the acts of grooming and the duration of acts of frizings (Table 2).

Table 1. Counting the number of squares (N), crossed by the rats when testing locomotor activity ("open field" test): in the control group (Pseudo-operated animals) and after 6, 24 and 72 hours after ischemia. (* - $p<0.01$).

Time of reperfusion	N	Pseudo-operated animals	Short-term MCAO	Long-term MCAO
6 hours	7	41.20±6.94	22.60±1.20*	16.01±1.73*
24 hours	7	43.80±1.32	23.50±1.05*	19.80±2.85*
72 hours	7	45.20±1.90	28.20±3.44*	24.40±1.86*

Table 2. Indicator of increased level of stress and freezing by the open field test: in the control group (Pseudo-operated animals), and after 6, 24 and 72 hours after ischemia with an occlusion duration of 2 minutes (Short-term MCAO) and 60 minutes (Long-term MCAO) expressed in seconds (* - $p<0.01$).

Time of reperfusion	Pseudo-operated animals	Short-term MCAO	Long-term MCAO
6 hours	5.001±2.110	9.001±1.490*	18.80±4.49*
24 hours	6.000±2.490	18.00±4.81*	28.60±5.79*
72 hours	7.810±2.040	19.80±3.49*	31.20±5.30*

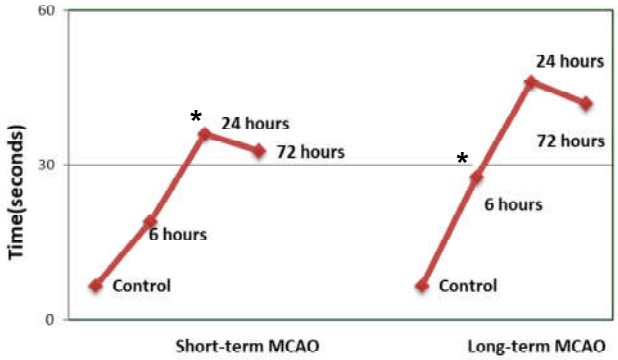

Fig. 2. Duration of rats removing the test stimulus when tested for adhesion removal to ischemia (Control) and after 6, 24 and 72 hours after ischemia. * - $p<0.01$.

There was also a violation of somatosensory functions following an ischemic injury in the brain, as evidenced by an increase in the time during which the animal took a test stimulus ("Sticks") from both front paws when tested for tactile sensitivity (adhesive removal test) (Fig. 2).

In a microscopic study, it was found that the zone of ischemic lesion anatomically covers areas of the somatosensory (parietal region) and, in part, the motor cortex (the frontal and prefrontal areas), the corpus callosum, the lateral and, partially, the medial parts of the striped body, and reaches the wall of the right side Ventricle, which corresponds to the basin of the blood supply of the right MCA.

In the cortex of the contralateral hemisphere (control) we observed the normal structure of the neuropile, the synapses had clearly defined presynaptic vesicles, synaptic cleft and postsynaptic density (Fig. 3A).

Microglial cells, microglia and astrocytes, were the first to respond to ischemic injury. Already after 6 hours we observed edema of astrocyte processes (Fig. 3B).

With the increase of the post-occlusion period, destructive

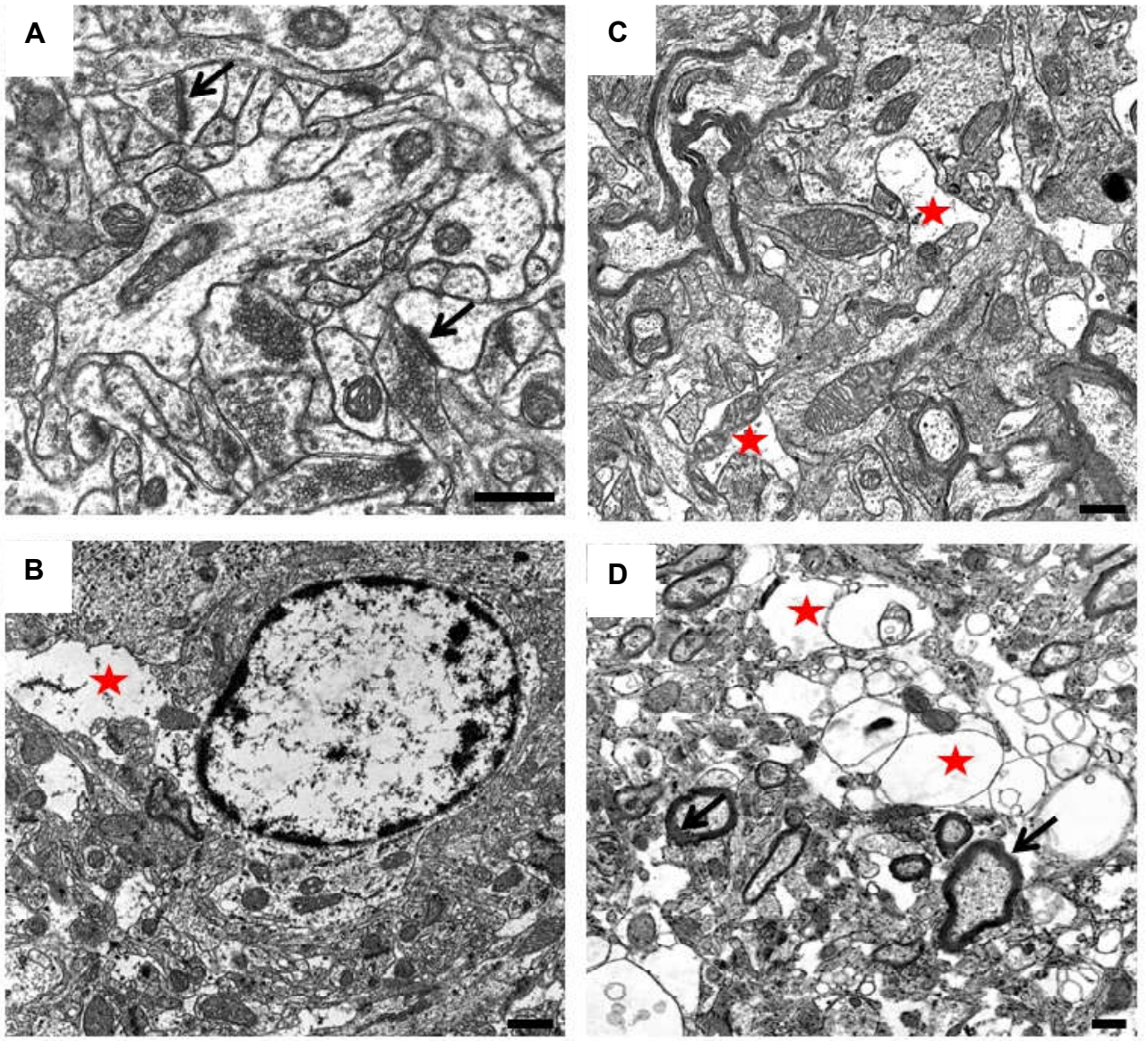

Fig. 3. Electronic microphotography of cortex after ischemic injury in animals at different reperfusion periods after MCAO: A - control; B - after 6 hours the structural changes of the neuropile are expressed in a vague way; C - after 24 hours there are more pronounced destructive changes, swelling of not only appendages, but also somas of astrocytes (indicated by a star); D - after 72 hours there were clear signs of degenerative changes of neuropile, manifested in the devastation and edema of dendrites and astrocytes (indicated by a star), pathological changes in myelin fibers (indicated by an arrow). The large line A, B, D - 0.4 microns, C - 0.8 microns.

changes in the cortex were increasing. After 24 hours we observed a swelling of not only astrocyte processes, but also of astrocytes (indicated by an asterisk, Fig. 3C).

An electron microscopic study of the cortex showed that 72 hours of post-occlusion period were observed as dark wrinkled neurons and enlightened swollen, indicating different ways of death of these cells. At this period of reperfusion, we showed clear signs of degenerative neuropile changes, manifested in the devastation and edema of dendrites and astrocytes (indicated by asterisks), pathological changes in myelin fibers (indicated by an arrow, Fig. 3D).

In the group of animals with ischemia for 72 hours post-occlusion period, both necrotic and apoptotic altered neurons were observed, neuropile of the cortex was strongly vacuated.

In the microvessels of the cortex there was a progressive, perivascular edema of the structures over time, of which the blood-brain barrier, mainly astrocytic processes, is formed.

Changes in striatum were similar to changes in the cortex, which progressed with an increase in the post-occlusion period. On the electronogram of the striatum site, we observed bundles of the myelin sheath, the destruction of microtubules in dendrites, and the presence of degenerative changes in synaptic terminals.

In the striatum of the contralateral hemisphere (control), the neuron bodies had a large, light rounded nucleus with

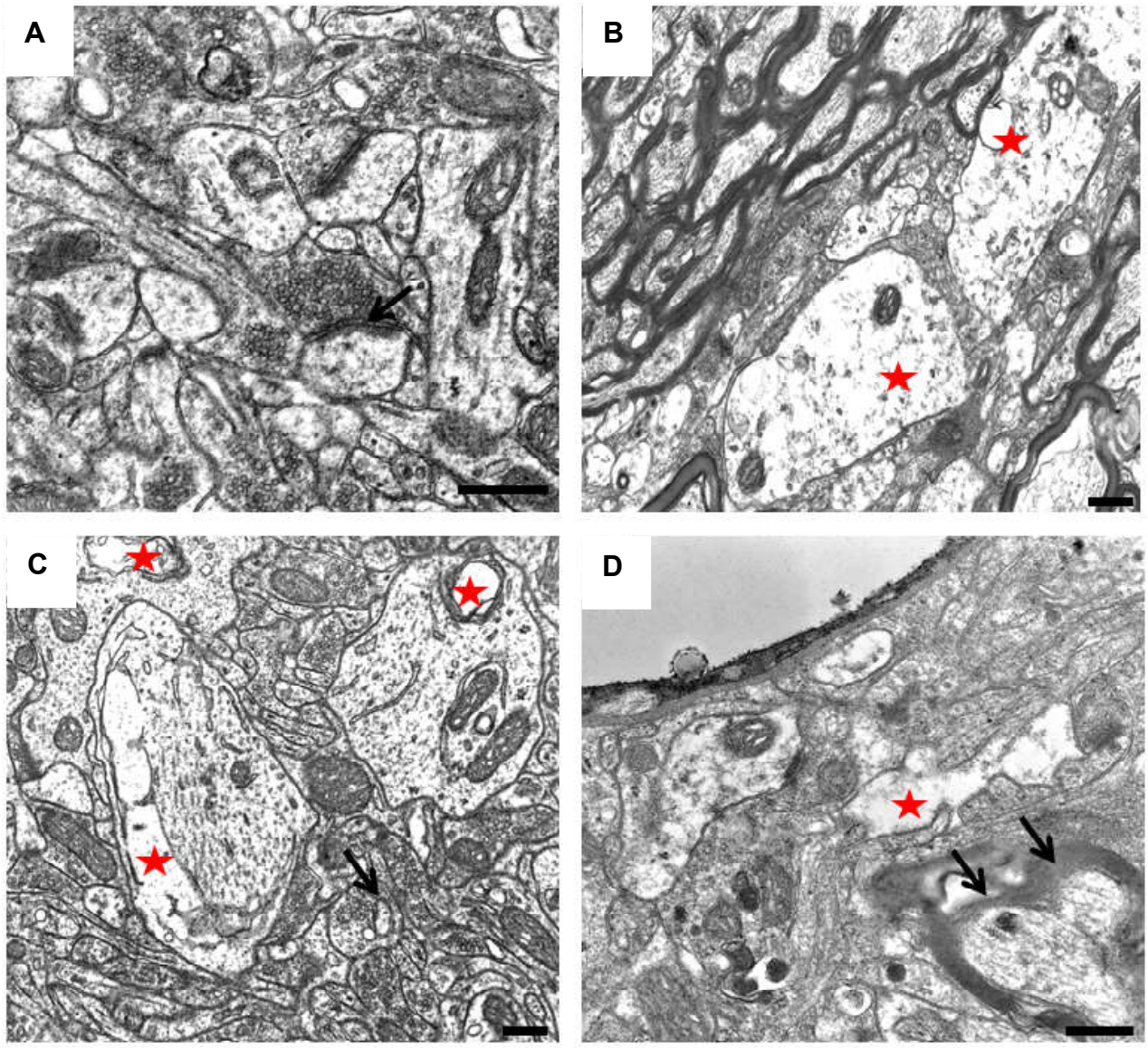

Fig. 4. Electron micrographs of striatum after ischemic injury in animals at different periods of reperfusion after MCAO: A - control; B - after 6 hours there are minor changes of neuropile, which are manifested in the enlightenment of astrocyte processes; C - after 24 hours destructive changes became more pronounced, destruction of mitochondria (indicated by a star), violation of the structure of synapses (indicated by an arrow); D - after 72 hours, swelling of the sprouts (indicated by a star), myelin bundle (indicated by the arrows) is observed. The large ruler is 0.4 microns.

well-differentiated one or two nucleoli and a narrow strip of slightly darker cytoplasm around the nucleus. In the control group, synapses can be visualized with well-defined presynaptic vesicles, synaptic cleft and postsynaptic density (Fig. 4A).

MCAO after 6 hours of reperfusion led to minor structural changes in neuropile, which manifested in enlightened astrocyte processes (Fig. 4B).

After 24 hours destructive changes became more pronounced, destruction of mitochondria (indicated by asterisks), destruction of the structure of synapses (indicated by an arrow, figure 4C).

The most striking were changes in striatum for 72 hours after occlusion of the carotid artery. Significant destructive changes in neuropile are observed, edema of the processes (indicated by an asterisk), myelin bundle (indicated by the arrowheads, Fig. 4D).

Discussion

A detailed assessment of neurological functions and behavioral reactions may require a large set of tests, each of which meets a certain aspect of animal behavior. The optimal set of tests should meet the requirements and objectives of a particular experiment and be sensitive to the type and severity of the deficit predicted after simulation of neurological damage. Since the effects of ischemic stroke

in humans are mainly sensory, motor and cognitive impairments, experimental post- MCAO tests in animals should be aimed at quantifying these violations and independent of compensatory behavior, due to repeated repetition of the procedure and training [7, 20].

Behavioral testing also allows to monitor changes in the neurological functions under the influence of new regenerative technologies (cell and gene therapy, growth factors, etc.). The need for statistically significant results requires the availability of an experimental model that can reproduce the mechanisms of the IS observed in humans [14].

In the majority of cases, as a result of MCAO, the centers of ischemic damage are formed in large sizes and the volume of the area of the damage in the acute period of the stroke (24 hours) is used as the final value for assessing the effectiveness of therapy [6, 13]. However, according to some researchers, the area of the damage after a 60-minute MCAO gradually increases for 6 weeks to its stabilization [13]. Expert recommendations and protocols of preclinical studies indicate the need to evaluate the effectiveness of new treatment methods IS based on behavioral responses and functional changes in experimental animals for a long observation time (11 months) [12].

The one-way MCAO leads to contralateral neurological deficits, which manifests itself primarily asymmetry of sensory and motor functions [4, 7, 12, 19].

Thus, the data obtained indicate significant changes in the structure of cerebral cortex and striatum in the postischemic period and the progressive nature of these changes.

The obtained results will be used in the future to study the participation of proteasome proteolysis and its role in the processes of ischemic brain damage, as well as to create opportunities for its influence on the prevention and treatment of cerebral diseases in general and ischemic stroke in particular.

Conclusions

1. It is confirmed that 60-minute occlusion of MCA is an adequate model of focal ischemic brain damage in rats.

2. The protocol of serial evaluation of neurological disorders that we've proposed after the modeling of MCAO allowed to detect long-term stable functional disorders in laboratory rats.

3. It was shown that at transient occlusion of the middle cerebral artery, there were structural and ultrastructural changes in the zone of damage to the brain tissues of rats and had a progressive nature with an increase in the post-occlusion period.

References

[1] Apple, D. M., Solano-Fonseca, R., & Kokovay, E. (2017). Neurogenesis in the aging brain. *Biochem Pharmacol,* 141, 77-85, doi:10.1016/j.bcp.2017.06.116.

[2] Belayev, L., Endres, M., & Prinz, V. (2010). *Focal cerebral ischemia in the mouse and rat using the intraluminal suture-filament model. Neuromethods*. Ed. by Ulrich Dirnagl. - Berlin: Humana Press, 286.

[3] Benjamin, E. J., Blaha, M. J., Chiuve, S. E., Cushman, M., Das, S. R., Deo R, de Ferranti. … Muntner, P. (2017). American Heart Association Statistics Committee and Stroke Statistics Subcommittee. Heart Disease and Stroke Statistics. Update: A Report From the American Heart Association. *Circulation,* 135(10), 146-603, doi: 10.1161/CIR.0000000000000485.

[4] Freret, T. (2009). Improvements of the Stroke Model Guidelines. Animal body weight and long-term functional concerns. *J. Exp. Stroke Transl. Med.*, 2(2), 28-31, doi: 10.1038/jcbfm.2012.185.

[5] Gandzjuk, V. A. (2014). The dynamics of morbidity and prevalence of circulatory system diseases among the population of Ukraine at the present stage: national and regional aspects. *Bulletin of Social Hygiene and Health Care Organizations of Ukraine,* 60(2), 74-78.

[6] Jander, S., Schroeter, M., Saleh, A. doi:10.1002/nbm.881 (2007). Imaging inflammation in acute brain ischemia. *Stroke,* 38(2), 642-645.

[7] Kojima, T., Hirota, Y., Ema, M., Takahashi, S., Miyoshi, I., Okano, H., & Sawamoto, K. (2010). Subventricular zone-derived neural progenitor cells migrate along a blood vessel scaffold toward the post-stroke striatum. *Stem Cells,* 28(3), 545-548, doi:10.1002/stem.306.

[8] Koizumi, J., Yoshid, Y., Nakazama, T., & Genju, O. (1986). Experimental studies of ischemic brain edema:1. A new experimental model of cerebral embolism in rats in which recirculation can be introduced in the ischemic area. *Stroke J.*, 8, 1-8.

[9] Komotar, R. J., Kim, G. H., & Sughrue, M. E. (2007). Neurologic assessment of somatosensory dysfunction following an experimental rodent model of cerebral ischemia. *Nature Protocols*, 2(10), 2345-2347, doi:10.1038/nprot.2007.359.

[10] Lindner, M. D., Gribkoff, V. K., & Donlan, N. A. (2003). Long-lasting functional disabilities in middle-aged rats with small cerebral infarcts. *The Journal of Neuroscience,* 23(34), 10913-10922.

[11] Meloni, B. P., Zhu, H., & Knuckey, N. W. (2006). Is magnesium neuroprotective following global and focal cerebral ischaemia? A review of published studies. *Magnes Res.,* 19(2), 123-137.

[12] Modo, M. (2009). Long-term survival and serial assessment of stroke damage and recovery-practical and methodological considerations. *J. Exp. Stroke Transl.* Med., 22(2), 52-68, doi:10.6030/1939-067X-2.2.52.

[13] Modo, M., Stroemer, R. P., & Tang, E. (2000). Neurological sequelae and long-term behavioural assessment of rats with transient middle cerebral artery occlusion. *Journal of Neuroscience Methods,* 194, 99-109, doi: 10.1016/S0165-0270(00)00329-0.

[14] Schaar, K. L. (2010). Functional assessments in the rodent stroke. *Experimental & Translational Stroke Medicine,* 2(13), 1-11, doi: 10.1186/2040-7378-2-13.

[15] Schallert, T., Woodlee, M. T., & Fleming, S. M. (2002). Disentangling multiple types of recovery from brain injury. *Pharmacology of Cerebral Ischemia,* 201-217.

[16] Skibo, G. G., Kovalenko, T. M., Osadchenko, I. O., Tsupikov, O. M., & Pivneva, T. A. (2006). Structural changes in the hippocampus in experimental brain ischemia. *Ukrainian Neurological Journal,* 1, 86-92.

[17] Tamura, A., Graham, D.I., McCulloch, J., & Teasdale, G. M.

(1981). Focal cerebral ischemia in the rat: 1. Description of technique and early neuropathological consequences following middle cerebral artery occlusion. *J. Cereb. Blood Flow Metab.*, 1, 53-60.

[18] Traystman, R. (2003). Animal models of focal and global cerebral ischemia. *ILAR Journal.*, 44(2), 85-95.

[19] Tsimbalyuk, V. I., & Yarmolyuk, Ye. S. (2012). Modified model of experimental ischemic stroke in rats using monophlates with silicone coating. *Ukrainian Neurological Journal*, 4, 97-105.

[20] Tsupikov, O., Kirik, V., Smozhanik, E., Rybachuk, O., Butenko, G., Pivneva, T., & Skibo, G. (2014). Long-term fate of grafted hippocampal neural progenitor cells following ischemic injury. *J. Neurosci. Res.,* 92(8), 964-974.

[21] Tsupikov, O., Kirik, V., Yatsenko, K., Butenko, G., & Skibo, G. (2017). Influence of transplanted neural progenitors on proliferation of hippocampal cells after ischemic brain damage. *ScienceRise. Medical Science,* 14(6), 32-36.

[22] Zhang, F., Liu, C. L., & Hu, B. R. (2006). Irreversible aggregation of protein synthesis machinery after focal brain ischemia. *J. Neurochem,* 98, 102-112.

[23] Zozulya, I. S. (2011). Epidemiology of cerebrovascular diseases in Ukraine. *Ukrainian Medical Journal,* 85(5), 38-41.

ХАРАКТЕРИСТИКА НЕРВОВОЇ ТКАНИНИ ПРИ МОДЕЛЮВАННІ ФОКАЛЬНОЇ ЦЕРЕБРАЛЬНОЇ ІШЕМІЇ У ЩУРІВ У РІЗНІ ПЕРІОДИ РЕПЕРФУЗІЇ

Савчук О.І., Скибо Г.Г.

Проблеми, які спричиняє інсульт, є надзвичайно актуальними в Україні, тому нами були вивчені структурні та ультраструктурні зміни нейронів кори та стріатума головного мозку при моделюванні порушення кровопостачання в різні строки оклюзії середньої мозкової артерії (ОСМА) та постішемічного періоду у щурів. Мета дослідження - аналіз змін нервової тканини при моделюванні фокальної церебральної ішемії шляхом монофіламентної оклюзії СМА у щурів у різні періоди реперфузії та зміни поведінкових реакцій. Статистичну обробку первинних цифрових експериментальних даних здійснювали за допомогою програмного забезпечення Statistica 6.0. Підтверджено, що 60-хвилинна ОСМА є адекватною моделлю фокального ішемічного пошкодження головного мозку щурів. Використовуючи поведінкові тести, виявлено зміни локомоторної активності та тактильної чутливості у щурів після оклюзії та після реперфузії протягом постішемічного періоду. Виявлено, що в дослідній групі з періодом реперфузії 72 години спостерігається чітке збільшення об'єму ішемізованої ділянки мозку, що супроводжується значним неврологічним дефіцитом. Виявлено зниження дослідницької активності щурів, що проявлялось в зменшенні кількості квадратів, які вони перетинали, кількості стійок, збільшенні актів грумінгу та тривалості актів фризінгу. Після ішемічного ушкодження мозку спостерігалось також порушення сомато-сенсорних функцій, про що свідчило збільшення часу, протягом якого тварина знімала тестовий стимул ("липучку") з обох передніх лап при тестуванні на тактильну чутливість (adhesive removal test). Електронно-мікроскопічне дослідження кори показало, що на 72 годину постоклюзійного періоду спостерігалися як темні зморщені нейрони, так і просвітлені набухлі, що свідчило про різні шляхи загибелі цих клітин. Зміни в стріатумі були аналогічними змінам в корі, які прогресували зі збільшенням постоклюзійного періоду. Запропонований нами протокол серійної оцінки неврологічних порушень при моделюванні ОСМА дозволив виявити довготривалі стійкі функціональні порушення у лабораторних щурів. Отримані дані свідчать про суттєві зміни структури кори та стріатума в постішемічному періоді і про прогресуючий характер цих змін.

Ключові слова: *ішемічний інсульт, фокальна церебральна ішемія, монофіламентна оклюзія.*

ХАРАКТЕРИСТИКА НЕРВНОЙ ТКАНИ ПРИ МОДЕЛИРОВАНИИ ФОКАЛЬНОЙ ЦЕРЕБРАЛЬНОЙ ИШЕМИИ У КРЫС В РАЗНЫЕ ПЕРИОДЫ РЕПЕРФУЗИИ

Савчук Е.И., Скибо Г.Г.

Проблемы, которые вызывает инсульт, являются чрезвычайно актуальными в Украине, поэтому нами были изучены структурные и ультраструктурные изменения нейронов коры и стриатума мозга при моделировании нарушения кровоснабжения в разные сроки окклюзии средней мозговой артерии (ОСМА) и в постишемическом периоде у крыс. Цель исследования - анализ изменений нервной ткани при моделировании фокальной церебральной ишемии путем монофиламентной окклюзии СМА у крыс в разные периоды реперфузии и изменении поведенческих реакций. Статистическую обработку первичных цифровых экспериментальных данных осуществляли с помощью программного обеспечения Statistica 6.0. Подтверждено, что 60-минутная окклюзия СМА является адекватной моделью фокального ишемического повреждения головного мозга крыс. Используя поведенческие тесты, выявлены изменения локомоторной активности и тактильной чувствительности у крыс после окклюзии и после реперфузии в течение постишемического периода. Выявлено, что в экспериментальной группе с периодом реперфузии 72 часа наблюдается четкое увеличение объема ишемизированного участка мозга, сопровождающегося значительным неврологическим дефицитом. Выявлено снижение исследовательской активности крыс, что проявлялось в уменьшении количества квадратов, которые они пересекали, количества стоек, увеличении актов груминга и продолжительности актов фризинга. После ишемического повреждения мозга наблюдалось также нарушение сомато-сенсорных функций, о чем свидетельствовало увеличение времени, в течение которого животное снимало тестовый стимул ("липучку") с обеих передних лап при тестировании на тактильную чувствительность (adhesive removal test). Электронно-микроскопическое исследование коры показало, что на 72 часу постокклюзионного периода наблюдались как темные сморщенные нейроны, так и просветленные набухшие, что свидетельствовало о различных путях гибели этих клеток. Изменения в стриатуме были аналогичными изменениям в коре, которые прогрессировали с увеличением постокклюзионного периода. Предложенный нами протокол серийной оценки неврологических нарушений при моделировании ОСМА позволил выявить долговременные устойчивые функциональные нарушения у лабораторных крыс. Полученные данные свидетельствуют о существенных изменениях структуры коры и стриатума в постишемическом периоде и о прогрессирующем характере этих изменений.

Ключевые слова: *ишемический инсульт, фокальная церебральная ишемия, монофиламентная окклюзия.*

DOI: 10.31393/morphology-journal-2018-24(3)-10 Reports of Morphology, Vol. 24, №3, Pages 65-72

ISSN 1818-1295 eISSN 2616-6194

REPORTS OF MORPHOLOGY

Official Journal of the Scientific Society of Anatomists, Histologists, Embryologists and Topographic Anatomists of Ukraine

journal homepage: https://morphology-journal.com

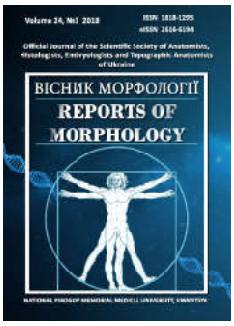

Proliferative features of diffuse astrocytic tumors Grade III-IV and their impact on the prognosis

Yakovtsova I.I.[1], Gavriliyuk A.O.[2], Chertenko T.M.[1]

[1]Kharkiv medical academy of postgraduate education, Kharkiv, Ukraine
[2]National Pirogov Memorial Medical University, Vinnytsya, Ukraine

ARTICLE INFO

Received: 30 July, 2018
Accepted: 29 August, 2018

UDC: 616-006.484.03-091.8-092.18

CORRESPONDING AUTHOR

e-mail: taisiachertenko@gmail.com
Chertenko T. M.

Anaplastic astrocytoma and glioblastoma are malignant brain tumors with a poor prognosis. The aim of our study was the complex investigation of the factors, those influence their aggressive behavior and proliferation (Ki-67, EGFR, MMP-9, PR, p53, vascular network formation), and the evaluation of their prognostic impact. These data could be used for optimization of target therapy in different groups of patients with diffuse astrocytic tumors Grade III-IV. Our study included 30 patients who were put through brain surgery for the first time and were divided into two equal groups: 15 patients who experienced a recurrence within 1 year after the surgery (1st group) and 15 patients without recurrence within 1 year after the surgery (2nd group). Postoperative tumor materials were obtained in formalin-fixed, paraffin-embedded blocks. In addition, we investigated the case histories of these patients. The expression of Ki-67, EGFR, MMP-9, PR, p53, VEGF, and CD34 was evaluated with immunohistochemical testing. Chi-squared test, Mann-Whitney U and Kruskal-Wallis H tests were performed for comparison of quantitative parameters between groups. Spearman's rank correlation coefficient was used for the measure of rank correlation between quantitative variables. Results of our study showed, that there was a tendency (U_{emp}=75,00; p>0.05) to higher proliferative index in the 1st group (18,29±3,44) compared to the 2nd group (16,57±3,09). EGFR expression was significantly higher in the 1st group (U_{emp}=70.50; p<0.05). Moreover, the higher EGFR expression was associated with higher MMP-9 expression (U_{emp}=7.500; p<0.01) and lower p53 expression (r_s= -0.62, p<0.001). The higher MMP-9 expression was also associated with higher vascularization index (MVD(VEGF)/ MVD(CD34)) (r_s=0.43; p<0.05). Our data confirm the close connections of different factors of tumor aggressiveness and the presence of molecule-biological discrepancy in homogenous histologically, but heterogenous prognostically groups of tumors. This evidence may be used in future for better-personalized therapy of patients with diffuse astrocytic tumors Grade III-IV.

Keywords: *glioblastoma, anaplastic astrocytoma, proliferation, tumor aggressiveness, prognosis, EGFR.*

Introduction

Diffuse astrocytic tumors Grade III-IV is the most common malignant neoplasms of the brain [15, 17]. Glioblastoma accounted for 46,6% of all malignant tumors of the central nervous system (CNS) [17]. Due to a numerous mutations in anaplastic astrocytomas and glioblastomas the individual prognosis of relapse-free survival and overall survival for different patients can vary significantly and the study of these mutations will allow selecting the most effective targeted therapy for each patient [24]. According to the 2016 WHO classification of tumors of the CNS, it was proved, that patients with IDH1 mutant glioblastomas have better overall survival than patients with glioblastoma IDH-wild type (31 and 15 months respectively) [14, 17]. The immunohistochemical markers, that give information about activity of oncogenesis, are promising in terms of prognosis and open up broad possibilities for the selection of targeted therapy. The family of tyrosine kinase receptors (RTKs) is a good example of such promising markers. The most important members of this family are the epidermal growth factor receptor (EGFR) and the vascular endothelial growth factor receptor (VEGF) [19, 20]. EGFR belongs to the crucial receptors influencing to the tumor progression [3, 18]. VEGF

is an angiogenic protein and malignant transformation has been shown to induce its expression [5, 6, 19, 22]. According to some scientific reports the VEGF expression in tumor cells of diffuse astrocytic neoplasms is a poor prognostic factor [6, 9, 13]. Glial tumor cells rarely show the progesterone receptor (RP) expression in cytoplasm, nuclei and also in endothelium of blood vessels [11, 25]. But the causes of this phenomenon are still unclear and insufficiently studied.

There is data, that RP can increase EGFR and VEGF expression in tumor cells [8]. On the other hand, the tumor with no or low EGFR expression show the higher levels of p53 tumor protein, that respond of apoptosis [6, 13]. The numerous reports show that anaplastic astrocytomas and glioblastomas with p53 expression grow slower and give a good response to temozolomide and as a result the patients with such tumors have better overall survival prognosis [13, 16].

Matrix metalloproteinase-9 (MMP-9) expression plays an important role in facilitating cancer invasion. According to different research reports, the high MMP-9 expression is a sign of aggressive tumor behavior [1, 4, 6], so the level of MMP-9 expression theoretically can be an important predictive factor of tumor progression.

The gold standard in investigation of proliferative activity of any tumor is the evaluation of Ki-67 proliferative index (PI). Nevertheless, there are no exact levels of Ki-67 PI, those can definitely confirm the worse prognosis for patients with anaplastic astrocytoma or glioblastoma [13, 23].

Contemporary data about the role of expression of each of above-mentioned markers in glioblastomas are inconsistent and need to be specified [10, 21, 27, 28]. There is no complex investigation of the role of Ki-67, EGFR, MMP-9, p53, PR expression and the vascular network development in diffuse astrocytic tumors Grade III-IV, which would be aimed to find the optimal criteria for prognosis. It is caused the short lifespan the patients with diffuse astrocytic tumors Grade III-IV and numerous difficulties due to selection good-quality observation groups.

The *aim* of our study is the clarification the correlations between expression a number of markers, that describe the oncogenesis (Ki-67, EGFR, MMP-9, p53) and the development of tumor vascular network (VEGF, CD34) in anaplastic astrocytomas and glioblastomas. Moreover, we are tried to find the prognostic value of the expression of these markers by the patients with high-grade diffuse astrocytomas.

Materials and methods

We formed two groups of patients to investigate the proliferative features, aggressive behavior of diffuse astrocytic tumors Grade III-IV and also to find predictive criteria of long-term survival of patients with these tumors. The first group included 15 tumor samples collected from 15 patients, who were primarily diagnosed with a high-grade astrocytic tumor, were treated with surgery and had a recurrence for a year after surgery. The second group included 15 tumor samples collected from 15 patients, who were primarily diagnosed with a high-grade astrocytic tumor, were treated with surgery and did not have a recurrence for a year after surgery. Postoperative tumor material was obtained from pathology departments of Kharkiv Regional Clinical Hospital and Kharkiv City Clinical Hospital №7. All surgical resections were performed between 2011 and 2016. Parts of the tumors were formalin fixed and paraffin embedded (FFPE). All tumors had the supratentorial location and were resected as much as possible (at least 95% of tumor tissue were resected). All patients had a standard course of chemo and radiotherapy. Eligibility criteria included the availability of follow-up data at least for a year after surgical resection, good quality and sufficient quantity of tumor material for immunohistochemical analysis. The details are presented in Table 1.

The histological investigation performed with the light microscope Primo Star (Carl Zeiss), magnification x40, 100, 400, 1000. Results were photographed with ZEISS Axiocam ERc5. The immunohistochemical study was performed with 7 primary antibodies, those are presented in Table 2.

We used a semiquantitative approach for assessment of the results. The expression of EGFR, VEGF, RP scored in such a scale:

"-" - no expression;

"+" - low expression;

Table 1. The clinical and morphological features of observed tumor samples in two groups.

Feature		Group	
		1	2
Sex	M	9 (60%)	9 (60%)
	F	6 (40%)	6 (40%)
Age	(M±m)	50.13±10,86	56.20±12.29
Tumor location	Frontal lobe	5 (33%)	9 (60%)
	Other supratentorial location	10 (67%)	6 (40%)
Grade	Ⅲ	1 (7%)	3 (20%)
	Ⅳ	14 (93%)	12 (80%)

Table 2. The primary antibodies panel.

Name	Clon	Dilution	Manufacturer
EGFR	SP84	1:100	ThermoScentific, USA
MMP-9	Ab-1 GE-213	1:200	ThermoScentific, USA
Ki-67	SP6	1:400	ThermoScentific, USA
P53	SP5	1:200	ThermoScentific, USA
VEGF	JH121	1:20	ThermoScentific, USA
anti-CD34 antibody Class Ⅱ	QBEnd 10	1:50	Dako, Denmark
progesterone receptor (RP) antibody	polyclon	1:200	ThermoScientific, USA

"++" - moderate expression;

"+++" - high expression.

For MMP-9 evaluation we counted the percentage of tumor cells that show positive expression. The evaluation was performed in hot spot areas (the foci, where the MMP-9 expression was very prominent).

The proliferative index was evaluated due to the count of the percentage of tumor cells that show positive Ki-67 expression. We considered such levels as 0-4%, under 15% and more than 15% of tumor cells [13].

The index of p53 expression was counted as the ratio of tumor cells with p53 expression multiplied by 100% to the total number of tumor cells in field of view.

The vascularization features were studied due to evaluation of CD34 expression in endothelial cells. VEGF expression helped to value the neoangiogenesis. For the complex investigation of the vascular network in studied tumors, we used such a term as a vascularization index, that can be defined as a ratio of microvascular density (MVD) by VEGF to MVD by CD34.

Vascularization index = MVD(VEGF)/MVD(CD34).

All statistical analyses were performed with the "Microsoft Exel 2010" and the "Statistica 10.0". The significant result was $p<0.05$. We were used methods of parametric and non-parametric statistics for analysis of immunohistochemical data. In our study we used such criteria as Mann-Whitney U-test, Kruskal-Wallis test, Pearson's chi-squared test (χ^2). The correlation was evaluated with Spearman's rank correlation coefficient. Cheddok scale correlation was also used.

Results

We had evaluated proliferative activity of tumors that relapsed during a year and tumors that didn't. In order to do this, we determined PI based on evaluation of a nuclear expression of Ki-67 in tumor tissue (an example of expression of a marker is shown on figure 1). The average value of PI was higher in a group of tumors which have relapsed during a year (18,29±3,44), against a group of tumors that didn't relapse (16,57±3,09). Observations reveal that average IP of a first group was higher than second's even if anaplastic astrocytomas are excluded from comparison (18,79±2,94) versus (18,00±0,98), although evaluating significance of this difference by Mann-Whitney test did not show reliable difference of IP value between two groups (U_{emp}=75,00; $p>0.05$).

We had also evaluated expression of p53 marker in a group of tumors that relapsed during a year after the surgery and in a group without such relapse. An average percentage of tumor cells that expressed p53 was insignificantly higher in a second group (13,85±4,08) than in a first one (12,73±3,84). Verifying significance of observed results by Mann-Whitney test did not reveal reliable difference in p53 expression values between the tested groups (U_{emp}=88,50; p=0,336). Some scientists say about direct link between IP and p53 expression by tumor cells but in our research such

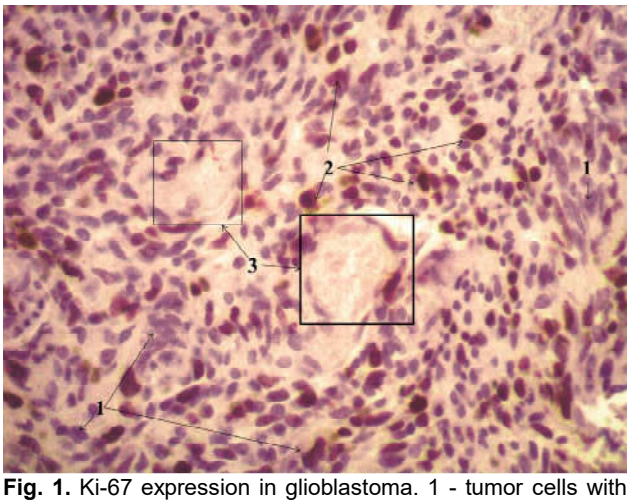

Fig. 1. Ki-67 expression in glioblastoma. 1 - tumor cells with hyperchromic nuclei, different shape of tumor cells, 2 - nuclear Ki-67 expression (the cells with brown nuclei), 3 - vessels. The additional staining with Mayer's hematoxylin, magnification x400.

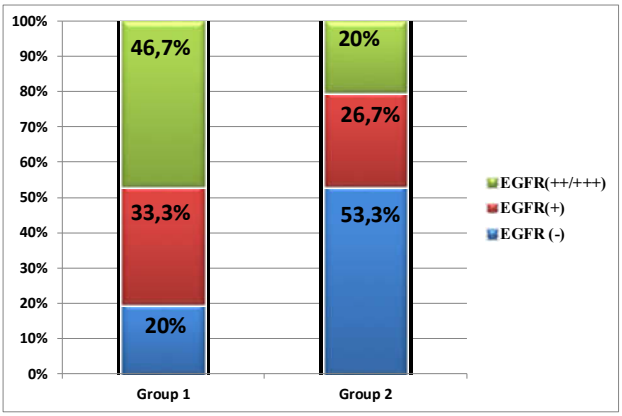

Fig. 2. The comparison of EGFR expression in the group with a recurrence within 1 year (group 1) and in the group without a recurrence (group 2).

link was not observed (r_s=0,08, $p>0.05$).

Expression of EGFR was also evaluated. For this evaluation tumors were classified by 2 groups: 1) ones that have no or have weak expression of EGFR by tumor tissue; 2) ones that have moderate or high expression. 46,7% of patients that had relapse during a year appeared in a group with moderate or high expression of EGFR against only 20% of patients that had no relapse. Mann-Whitney test confirms statistically significant difference of EGFR expression between the groups (U_{emp}=70,50; $p<0.05$) (see fig. 2).

Data from literature suggests that EGFR marker is one of the main markers that point to aggressive potential of a tumor so it was important to establish if there is a connection of this marker with clinical and morphological characteristics of tumors being researched. As can be seen from table 3, statistically significant connections were only established with MMP-9 and p53 markers as well as with vascularization index. Further in our study we researched these connections in deeper detail.

Evaluating expression of MMP-9 as a possible

Table 3. The correlation of main immunohistochemical features with the level of EGFR expression.

Feature	Number of cases		EGFR (-)		EGFR (+)		EGFR (++/+++)		p
	N	%	N	%	N	%	N	%	
The total number of patients	30	100	**11**	36,70	**9**	30	**10**	33,30	
MMP-9									**<0,01**
<33%	24	80	**11**	100	**9**	100	**4**	40	
>33%	6	20	**0**	0	**0**	0	**6**	60	
Ki 67									**>0,05**
< 17,4	12	40	**6**	54,50	**5**	55,60	**1**	10	
>17,4	18	60	**5**	45,50	**4**	44,40	**9**	90	
Vascularization index									**<0,05**
<0,67	18	60	**9**	81,800	**6**	66,70	**3**	30	
>0,67	12	40	**2**	18,20	**3**	33,30	**7**	70	
P53									**<0,05**
<13,29	14	46,70	**2**	18,20	**5**	55,60	**7**	70	
>13,29	16	53,30	**9**	81,80	**4**	44,40	**3**	30	

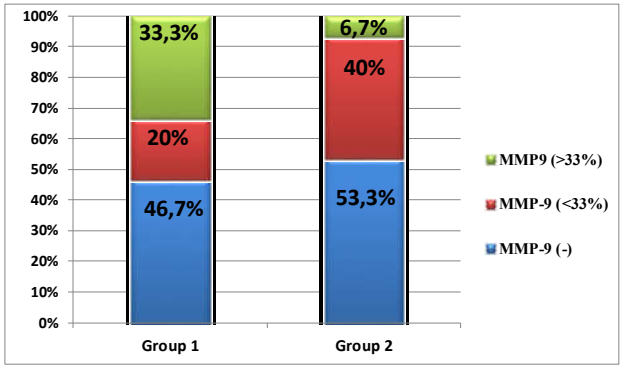

Fig. 3. The comparison of MMP-9 expression in the group with a recurrence within 1 year (group 1) and in the group without a recurrence (group 2).

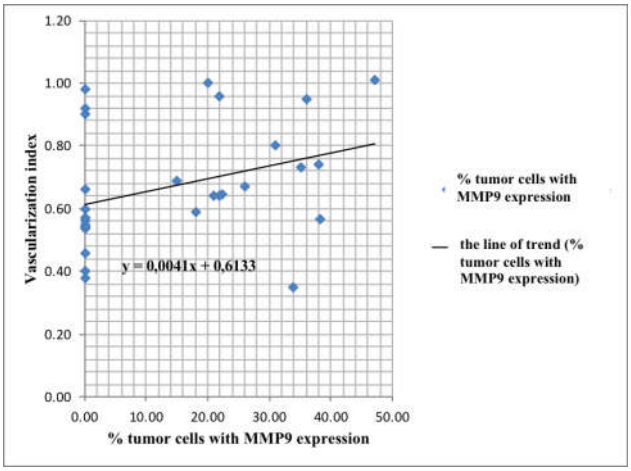

Fig. 4. The field of correlation and the regression analysis between the levels of MMP-9 expression and vascularization index.

independent factor that affects prognosis did not reveal statistically significant differences between groups (p>0.05), although tumors that didn't relapse during a year have in general shown a tendency towards lower MMP-9 that those that did relapse (see fig. 3).

It was revealed that in many cases when expression of EGFR was absent an expression of MMP 9 was also absent. Comparing groups with low and moderate or high EGFR expression had revealed that higher MMP-9 expression is more common for the latter group (Mann-Whitney test: U_{emp}=7,500; U_{cr}=16; p<0.01).

A connection has been revealed between EGFR expression level and vascularization index (Kruskal-Wallis test H (3, N=30) = 10,66 p<0.05) and a moderately strong link between MMP-9 expression and vascularization index (r_s=0,43; p<0.05) (see fig. 4).

In addition we have verified a theory about presence of an inverse relationship between expression level of EGFR and expression of p53. It is believed that EGFR expression is often related with more aggressive tumors and is more common among primary glioblastomas while p53 expression is more common in secondary glioblastomas and is related to slower development of a tumor. Kruskal-Wallis test in our research shows significance of p53 expression in groups with various EGFR expression indicators (neg, +, ++, +++). The result of a test is H (3, N=30) = 12.46 p<0.01. In order to find presence of a correlation we have computed a Spearman rank correlation coefficient which appeared to be r_s= -0,62, p<0,001, which points to moderately strong inverse relationship between expression level of EGFR and expression of p53 by tumor cells: higher the expression of EGFR, the lower is the expression of p53 (see fig. 5).

In three cases of tumors that have relapsed during a year there was an expression of progesterone in tissues of a tumor (fig. 6). Cells that expressed progesterone were

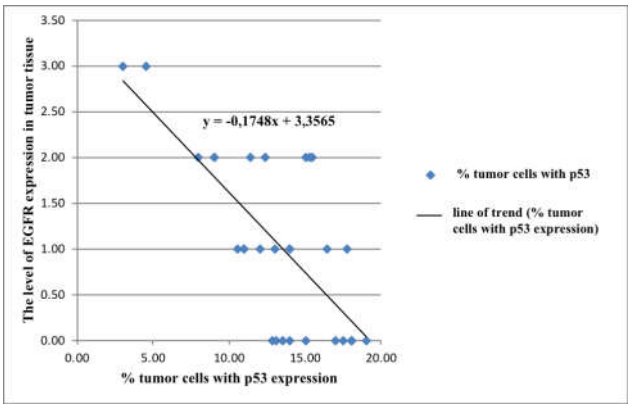

Fig. 5. The field of correlation and the regression analysis between the levels of p53 expression and EGFR expression.

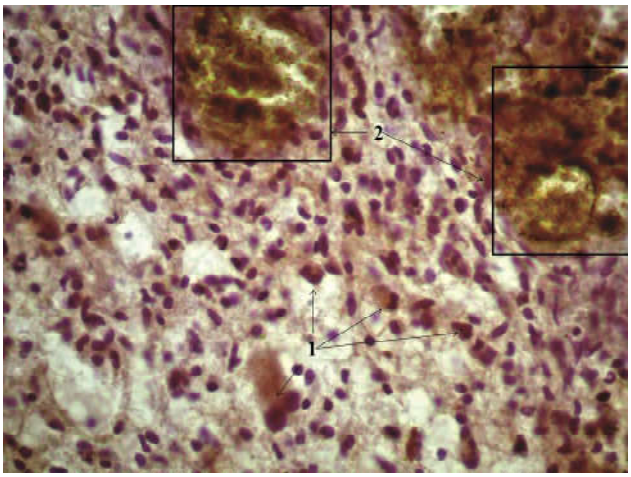

Fig. 6. Progesterone receptor expression in glioblastoma that predominantly built of small cells. 1 - nuclear and cytoplasmic expression (brown color), 2 - big vessels. The additional staining with Mayer's hematoxylin, magnification x400.

located close to necrosis zones. All three tumors had quite high vascularization index (1,170±0,610). It should be noted that these tumors had moderate or high expression of EGFR and a high expression of MMP-9 (the number of tumor cells that express MMP-9, was 41% and higher). This phenomenon was not statistically analyzed due to low number of observations. In biopsies taken from peripheral areas of some tumors with high expression of EGFR there was a clearly observed expression of MMP-9 and VEGF markers in tumor cells.

Discussion

The levels of proliferative index by Ki-67 in high grade astrocytic tumors are the same to WHO data for these tumor histotypes [13,14]. It was not found any influence of PI to the prognosis ($p>0.05$). Although, there was found a tendency to higher PI in a group with a recurrence within 1 year after the surgery in comparison to group without a recurrence.

The investigation of aggressive behavior of tumors showed that tumors with a recurrence within 1year after the surgery had moderate or high EGFR expression in 46.7% of cases compared to 20% of cases in group of tumors without a recurrence. Mann-Whitney U-test confirmed the significant difference between EGFR expression in these two groups ($U=70.50$; $p<0.05$). Our data about the prevalence of tumors with high EGFR expression in the group with adverse prognosis are similar to data of meta-analysis, that was based on 17 research reports and included 1458 tumor samples. According to the data of meta-analysis, the high EGFR expression in the tumor tissue can be used as a significant predictive factor of adverse prognosis and shorter relapse-free survival for patients [12].

There are a lot of data about the presence of some associations between different features of aggressive tumor behavior. The immunohistochemical study presents the activity of different oncogenetical processes due to several criteria, for instance, the level of EGFR expression, the number of MMP-9-positive tumor cells and the level of angiogenesis activity (vascularization index (MVD(VEGF)/ MVD(CD34); VEGF expression in tumor cells. It was caused the fact of the stimulating effect of EGFR to the MMP-9 and VEGF synthesis [6, 13, 19, 20]. Our research also confirmed the presence of such association. We found the significant correlation between EGFR expression (++/+++) and the higher percentage of MMP9-positive tumor cells ($U_{emp}=7,50$; U critical=16; $p<0.01$), and the correlation between EGFR expression (++/+++) and higher value of vascularization index (Kruskal-Wallis H-test (2, N=45)=34.19 ($p<0.0001$)). There is also a direct moderate correlation between vascularization index and the percentage of MMP9-positive tumor cells ($rs=0.43$; $p<0.05$).

It should be also mentioned the VEGF and MMP9 expression in the samples obtained from the peripheral tumor regions. The high EGFR expression was also observed in these areas. According to the data of WHO and numerous studies, the VEGF expression in tumor cells is a sign of adverse prognosis [6, 9, 13]. The fact that this expression was better observed in the peripheral tumor regions pointed out the active tumor growth, so pathologists should carefully investigate besides central tumor regions also its peripheral zones to understand totally the level of tumor aggressive potential [5, 6, 9]. The high VEGF expression in tumor cells may serve as a direct indication for bevacizumab prescription [5, 7].

It was found the significant difference among p53 expression in groups with different levels of EGFR expression (neg, +, ++, +++) (Kruskal-Wallis H-test (3, N=30) = 12.46, $p<0.01$) and the presence of the moderate inverse correlation between EGFR expression and p53 expression ($r_s= -0.62$, $p<0.001$). Our data are similar to scientific data, that confirmed that the level of EGFR expression was opposite to the level of p53 expression. It is explained by the fact that tumors with high EGFR expression usually belong to primary glioblastomas and tend to progress faster than the tumors with high p53 expression that grow slower and usually associated with secondary glioblastomas [2, 6, 13, 26].

Worth to be mentioned also such an observation as 3

cases of PR expression in tumors with a recurrence within 1 year after the surgery. These observations were not statistically analyzed, because the number of cases was insufficient, but some researchers mentioned, that RP was able to influence to the proliferation due to increasing the EGFR and VEGF synthesis in tumor cells. This mechanism is caused by Ser345-phosphorylation of RP-β, that in its turn is associated with Sp-1 transcription factor, that regulated EGFR expression [8].

In the future, it will be planned to investigate the proliferative features of high grade diffuse astrocytic tumors and their aggressive potential in larger groups of patients with not only immunohystochemical, but also molecule-genetical methods. In addition, it will be tracked the 3-year and 5-year survival among groups of patients with initially different prognosis and to figure out if the trends that we found in this research are constant with the length of time. We are also going to deeply investigate the molecular features of early and remote relapses of high grade diffuse astrocytic tumors. The obtained result may be used for development of the more effective chemotherapy and may be interesting for oncologists when they choosing the most effective treatment strategy for patients.

Conclusion

1. A tendency toward higher PI value was found in tumors that relapsed during a year (18.29±3.44) in comparison to a group of similar tumors that didn't relapse (16.57±3.09), but statistically significant differences of PI value between groups were not found (U_{emp}=75.00; p>0.05).

2. Statistically significant difference was found in expression of EGFR between primary tumors with different outcomes (U^{emp}=70.50; p<0.05). High and moderate expression of EGFR was found in 46,7% of primary tumors that relapsed within a year after surgery.

3. Higher expression of EGFR was related to higher expression of MMP-9 (Mann-Whitney test: U_{emp}=7.500; U_{cr}=16.00; p<0.01).

4. Significant differences were found in expression of p53 in groups of primary tumors with different indicators of expression of EGFR (neg, +, ++, +++) (Kruskal Wallis test: H (3, N=30) = 12.46 p<0.01). A moderately strong inverse relationship was established between level of expression of EGFR and expression of p53 among primary tumors (r_s= -0.62, p<0,001).

5. Higher expression of MMP-9 was directly linked to higher vascularization index (r_s= 0.43; p<0.05).

References

[1] Bikfalvi, A. (2012). *Angiogenesis and invasion in cancer. Handbook of Clinical Neurology Neuro-Oncology.* 104 HCN Series, 35-43. doi:10.1016/b978-0-444-52138-5.00003-7

[2] Bouvier-Labit, C., Chinot, O., Ochi, C, Gambarelli, D., Dufour, H., & Figarella-Branger, D. (1998). Prognostic significance of Ki67, p53 and epidermal growth factor receptor immunostaining in human glioblastomas. *Neuropathology and Applied Neurobiology,* 24(5), 381-388. doi:10.1046/j.1365-2990.1998.00137.x

[3] Brennan, C. W., Verhaak, R. G., McKenna, A., Campos, B., Noushmehr, H., Salama, … Chin, L., TCGA Research Network (2013). The somatic genomic landscape of glioblastoma. *Cell,* 155(2), 462-477. doi: 10.1016/j.cell.2013.09.034

[4] Dabbs, D. J. (2014). *Diagnostic immunohistochemistry theranostic and genomic applications.* Philadelphia, PA: Elsevier Saunders. eBook ISBN:9780323225090

[5] Ellis, L. M., & Hicklin, D. J. (2008). VEGF-targeted therapy: Mechanisms of anti-tumour activity. *Nature Reviews Cancer*, 8(8), 579-591. doi:10.1038/nrc2403

[6] Fletcher, C. D. (2013). *Diagnostic histopathology of tumors.* Philadelphia, PA: Elsevier Saunders. ISBN-13: 9781437715347

[7] Goldman, C. K., Kim, J., Wong, W. L., King, V., Brock, T., & Gillespie, G. Y. (1993). Epidermal growth factor stimulates vascular endothelial growth factor production by human malignant glioma cells: A model of glioblastoma multiforme pathophysiology. *Molecular Biology of the Cell,* 4(1), 121-133. doi:10.1091/mbc.4.1.121

[8] Hernández-Hernández, O. T., González-Garcia, T. K., & Camacho-Arroyo, I. (2012). Progesterone receptor and SRC-1 participate in the regulation of VEGF, EGFR and Cyclin D1 expression in human astrocytoma cell lines. *The Journal of Steroid Biochemistry and Molecular Biology,* 132(1-2), 127-134. doi:10.1016/j.jsbmb.2012.04.005

[9] Jain, R. K., Tomaso, E. D., Duda, D. G., Loeffler, J. S., Sorensen, A. G., & Batchelor, T. T. (2007). Angiogenesis in brain tumours. *Nature Reviews Neuroscience*, 8(8), 610-622. doi:10.1038/nrn2175

[10] Jain, R., Poisson, L. M., Gutman, D., Scarpace, L., Hwang, S. N., Holder, C. A., ... Flanders, A. (2014). Outcome Prediction in Patients with Glioblastoma by Using Imaging, Clinical, and Genomic Biomarkers: Focus on the Nonenhancing Component of the Tumor. *Radiology,* 272(2), 484-493. doi:10.1148/radiol.14131691

[11] Khalid, H., Shibata, S., Kishikawa, M., Yasunaga, A., Iseki, M., & Hiura, T. (1997). Immunohistochemical analysis of progesterone receptor and ki-67 labeling index in astrocytic tumors. *Cancer,* 80(11), 2133-2140. doi:10.1002/(sici)1097-0142(19971201)80:113.0.co;2-#

[12] Li, J., Liang, R., Song, C., Xiang, Y., & Liu, Y. (2018). Prognostic significance of epidermal growth factor receptor expression in glioma patients. *OncoTargets and Therapy*, Volume 11, 731-742. doi:10.2147/ott.s155160

[13] Louis, D. N. (2007). WHO classification of tumours of the central nervous system. Lyon: International Agency for Research on Cancer. ISBN: 9789283224302

[14] Louis, D. N., Ohgaki, H., Wiestler, O. D., & Cavenee, W. K. (2016). *WHO classification of tumours of the central nervous system.* Lyon: International Agency For Research On Cancer. ISBN-13:9789283244929

[15] Louis, D. N., Perry, A., Reifenberger, G., Deimling, A. V., Figarella-Branger, D., Cavenee, W. K., … Ellison, D. W. (2016). The 2016 World Health Organization Classification of Tumors of the Central Nervous System: A summary. *Acta Neuropathologica*, 131(6), 803-820. doi:10.1007/s00401-016-1545-1

[16] Malkoun, N., Chargari, C., Forest, F., Fotso, M., Cartier, L., Auberdiac, P., … Magne, N. (2011). Prolonged temozolomide for treatment of glioblastoma: Preliminary clinical results and prognostic value of p53 overexpression. *Journal of Neuro-Oncology,* 106(1), 127-133. doi:10.1007/s11060-011-0643-0

[17] Ostrom, Q., Gittleman, H., & Liao, P. (2017). CBTRUS statistical report: Primary brain and other central nervous system tumors diagnosed in the United States in 2010-2014. *Neuro-oncology,* 19, 1-88. doi:10.1093/neuonc/nox158
[18] Paul, I., Bhattacharya, S., Chatterjee, A., & Ghosh, M. K. (2013). Current Understanding on EGFR and Wnt/ -Catenin Signaling in Glioma and Their Possible Crosstalk. *Genes & Cancer,* 4(11-12), 427-446. doi:10.1177/1947601913503341
[19] Pearson, J. R., & Regad, T. (2017). Targeting cellular pathways in glioblastoma multiforme. *Signal Transduction and Targeted Therapy,* 2, 17040. doi:10.1038/sigtrans.2017.40
[20] Regad, T. (2015). Targeting RTK Signaling Pathways in Cancer. *Cancers*, 7(3), 1758-1784. doi:10.3390/cancers7030860
[21] Santosh, V., Shastry, A., Thota, B., & Arimappamagan, A. (2015). P53 stratification reveals the prognostic utility of matrix metalloproteinase-9 protein expression in glioblastoma. *Neurology India*, 63(3), 399. doi:10.4103/0028-3886.158227
[22] Shibuya, M. (2001). Structure and Function of VEGF/VEGF-receptor System Involved in Angiogenesis. *Cell Structure and Function*, 26(1), 25-35. doi:10.1247/csf.26.25
[23] Stoyanov, G. S., Dzhenkov, D. L., Kitanova, M., Donev, I. S., & Ghenev, P. (2017). Correlation Between Ki-67 Index, World Health Organization Grade and Patient survival in glial tumors with astrocytic differentiation. *Cureus*. doi:10.7759/cureus.1396
[24] Tamimi, A. F., & Juweid, M. (2017). Epidemiology and Outcome of Glioblastoma. In: De Vleeschouwer S, editor. Glioblastoma [Internet]. Brisbane (AU): Codon Publications; Chapter 8. doi: 10.15586/codon.glioblastoma.2017.ch8
[25] Tavares, C. B., Gomes-Braga, F. d., Costa-Silva, D. R., Escorcio-Dourado, C. S., Borges, U. S., Conde-Junior, A. M., … da-Silva, B. B. (2016). Expression of estrogen and progesterone receptors in astrocytomas: a literature review. *Clinics* (Sao Paulo, Brazil), 71(8), 481-486.
[26] Watanabe, K., Tachibana, O., Sato, K., Yonekawa, Y., Kleihues, P., & Ohgaki, H. (1996). Overexpression of the EGF Receptor and p53 Mutations are Mutually Exclusive in the Evolution of Primary and Secondary Glioblastomas. *Brain Pathology,* 6(3), 217-223. doi:10.1111/j.1750-3639.1996.tb00848.x
[27] Xue, Q., Cao, L., Chen, X., Zhao, J., Gao, L., Li, S., & Fei, Z. (2017). High expression of MMP9 in glioma affects cell proliferation and is associated with patient survival rates. *Oncology Letters*, 13(3), 1325-1330. doi:10.3892/ol.2017.5567
[28] Zhao, L., Xu, K., Wang, S., Hu, B., & Chen, L. (2012). Pathological significance of epidermal growth factor receptor expression and amplification in human gliomas. *Histopathology,* 61(4), 726-736. doi:10.1111/j.1365-2559.2012.04354.x

ПРОЛІФЕРАТИВНІ ОСОБЛИВОСТІ ДИФУЗНИХ АСТРОЦИТАРНИХ ПУХЛИН III-IV СТУПЕНЯ ЗЛОЯКІСНОСТІ ТА ЇХ ВПЛИВ НА ПРОГНОЗ

Яковцова І. І., Гаврилюк А. О., Чертенко Т. М.

Анапластичні астроцитоми та гліобластоми є високо злоякісними пухлинами з поганим прогнозом. Метою нашого дослідження було комплексне вивчення факторів, що сприяють формуванню агресивного потенціалу цих пухлин та впливають на їх проліферативну активність (Ki-67, EGFR, MMP-9, PR, p53, розвиненість судинного русла), а також визначення вірогідного прогностичного значення цих факторів та взаємозв'язків між ними, що в майбутньому могло б бути корисно для оптимізації таргетної терапії хворих на дифузні астроцитарні пухлини III-IV ступеня злоякісності. Для дослідження був відібраний післяопераційний матеріал від 30 вперше прооперованих з приводу пухлини пацієнтів, що були розподілені на 2 рівні групи: 15 пацієнтів, які мали рецидив протягом року після операції та 15 пацієнтів без рецидиву протягом року. Післяопераційний матеріал дифузних астроцитарних пухлин III-IV ступеня злоякісності був представлений парафіновими блоками, також додатково вивчалися історії хвороби досліджуваних пацієнтів. Методом імуногістохімії вивчалася експресія наступних маркерів: Ki-67, EGFR, MMP-9, PR, p53, VEGF та CD34. Для оцінки статистично значущих відмінностей між групами використовували наступні показники: χ^2 Пірсона, критерій Манна-Уїтні, критерій Краскера-Уоллиса. Кореляційний зв'язок між кількісними показниками оцінювали за допомогою коефіцієнта кореляції Спірмена. Визначена тенденція ($U_{емп}$=75,00; p>0,05) до більш високого індексу проліферації в групі пухлин, що дали рецидив протягом року після операції (18,29±3,44) порівняно з групою без рецидивів (16,57±3,09). Експресія EGFR була достовірно вищою у групі пухлин, що мали рецидив протягом року ($U_{емп}$=70,50; p<0,05). Більш висока експресія EGFR була пов'язана з більш високою експресією MMP-9 ($U_{емп}$=7,500; p<0,01) та більш низькою експресією p53 (r_s= -0,62, p<0,001). Більш висока експресія MMP-9 також була пов'язана з більш високими значеннями індексу васкуляризації (ЩМР(VEGF/ЩМР(CD34)) (r_s=0,43; p<0,05). Отримані дані свідчать про наявність тісного взаємозв'язку між різними факторами агресивного потенціалу пухлин, а також вказують на наявність молекулярно-біологічних відмінностей між однорідними за гістологією, але різними за прогнозом групами дифузних астроцитарних пухлин III-IV ступенів злоякісності, що в подальшому може бути використано для оптимізації стратегії лікування хворих на ці пухлини.

Ключові слова: *гліобластома, анапластична астроцитома, особливості проліферації, агресивний потенціал, прогноз, EGFR.*

ПРОЛИФЕРАТИВНЫЕ ОСОБЕННОСТИ ДИФФУЗНЫХ АСТРОЦИТАРНЫХ ОПУХОЛЕЙ III-IV СТЕПЕНИ ЗЛОКАЧЕСТВЕННОСТИ И ИХ ВЛИЯНИЕ НА ПРОГНОЗ

Яковцова И. И., Гаврилюк А. А., Чертенко Т. Н.

Анапластические астроцитомы и глиобластомы являются высоко злокачественными опухолями с плохим прогнозом. Целью нашей работы было комплексное изучение факторов, влияющих на их агрессивный потенциал и пролиферативную активность (Ki-67, EGFR, MMP-9, PR, p53, развитость сосудистого русла) для выявления вероятного прогностического значения этих факторов и взаимосвязей между ними, что в будущем помогло бы оптимизировать таргетную терапию для разных групп пациентов с диффузными астроцитарными опухолями Grade III-IV. Исследование включало 30 пациентов, прооперированных впервые по поводу диффузной астроцитарной опухоли III-IV степени злокачественности, которые были разделены на 2 равные группы: 15 пациентов с опухолями, которые дали рецидив в течение 1 года после операции и 15 пациентов без рецидива в течение года после операции. Изучили медицинские карты стационарных больных и послеоперационный материал, представленный в парафиновых блоках. Методом иммуногистохимии была изучена

экспрессия таких маркеров: Ki-67, EGFR, MMP-9, PR, p53, VEGF и CD34. Для оценки статистически значимых различий между группами использовали следующие критерии: χ² Пирсона, критерий Манна-Уитни, критерий Краскера-Уоллиса. Корреляционная связь между количественными показателями оценивали с помощью коэффициента корреляции Спирмена. Выявлена тенденция ($U_{эмп}$=75,00; p>0,05) к более высокому индексу пролиферации в группе опухолей, давших рецидив в течение года (18,29±3,44) по сравнению с группой без рецидивов (16,57±3,09). Экспрессия EGFR была достоверно выше в группе опухолей с рецидивами в течение года ($U_{эмп}$=70,50; p<0,05). Более высокая экспрессия EGFR была связана с более высокой экспрессией MMP-9 ($U_{эмп}$=7,500; p<0,01) и более низкой экспрессией p53 (r_s= -0,62, p<0,001). Более высокая экспрессия MMP-9 также была связана с более высоким индексом васкуляризации (ПМР(VEGF/ПМР(CD34)) (r_s=0,43; p<0,05). Полученные результаты свидетельствуют о тесной взаимосвязи различных проявлений агрессивного потенциала опухоли, а также наличии молекулярно-биологических различий между однородными по гистологии, но различными по прогнозу группами опухолей, что в дальнейшем может быть использовано для оптимизации стратегии лечения пациентов с диффузными астроцитарными опухолями III-IV степени злокачественности.

Ключевые слова: *глиобластома, анапластическая астроцитома, особенности пролиферации, агрессивный потенциал, прогноз, EGFR.*

REQUIREMENTS FOR ARTICLES

For publication, scientific articles are accepted only in English only with translation on Ukrainian or Russian, which contain the following necessary elements: UDC code; title of the article (in English, Ukrainian and Russian); surname, name and patronymic of the authors (in English, Ukrainian and Russian); the official name of the organization (institution) (in English, Ukrainian and Russian); city, country (in English, Ukrainian and Russian); structured annotations (in English, Ukrainian and Russian); keywords (in English, Ukrainian and Russian); introduction; purpose; materials and methods of research; research results; discussion; conclusions; bibliographic references.

The title of the article briefly reflects its contents and contains no more than 15 words.

Abstract. The volume of the annotation is 1800-2500 characters without spaces. The text of an annotation in one paragraph should not contain general phrases, display the main content of the article and be structured. The abstract should contain an introductory sentence reflecting the relevance of the study, the purpose of the study, a brief description of the methods of conducting research (2-3 sentences with the mandatory provision of the applied statistical methods), a description of the main results (50-70% of the volume of the abstract) and a concise conclusion (1 sentence). The abstract should be clear without familiarizing the main content of the article. Use the following expressions: "Detected ...", "Installed ...", "Fixed ...", "Impact assessed ...", "Characterized by regularities ...", etc. In an annotation, use an active rather than passive state.

Keywords: 4-6 words (or phrases).

"Introduction"

The introduction reflects the state of research and the relevance of the problem according to the world scientific literature (at least 15 references to English articles in international journals over the past 5 years). At the end of the entry, the purpose of the article is formulated (contains no more than 2-3 sentences, in which the problem or hypothesis is addressed, which is solved by the author).

"Materials and methods"

The section should allow other researchers to perform similar studies and check the results obtained by the author. If necessary, this section may be divided into subdivisions. Depending on the research objects, the ethical principles of the European Convention for the protection of vertebrate animals must be observed; Helsinki Declaration; informed consent of the surveyed, etc. (for more details, see "Public Ethics and its Conflict"). At the end of this section, a "statistical processing of results" section is required, which specifies the program and methods for processing the results obtained by the automobile.

"Results"

Requirements for writing this section are general, as well as for all international scientific publications. The data is presented clearly, in the form of short descriptions, and must be illustrated by color graphics (no more than 4) or drawings (no more than 8) and tables (no more than 4), the information is not duplicated.

"Discussion"

In the discussion, it is necessary to summarize and analyze the results, as possible, compare them with the data of other researchers. It is necessary to highlight the novelty and possible theoretical or practical significance of the results of the research. You should not repeat the information already listed in the "Introduction" section. At the end of the discussion, a separate paragraph should reflect the prospects for using the results obtained by the author.

"Conclusion"

5-10 sentences that summarize the work done (in the form of paragraphs or solid text).

"Acknowlegements"

Submitted after conclusion before bibliographic references.

"References"

References in the text are indicated by Arabic numerals in square brackets according to the numerology in the list of references. The list of references (made without abbreviations) sorted by alphabet, in accordance with the requirements of APA Style (American Psychological Association Style): with the obligatory referencing of all authors, work titles, journal names, or books (with obligatory publication by the publishing house, and editors when they are available), therefore, numbers or releases and pages. In the Cyrillic alphabets references, give the author's surnames and initials in English (Cyrillic alphabet in brackets), the title of the article or book, and the name of the magazine or the publisher first to be submitted in the original language of the article, and then in square brackets in English. If available, doi indexes must be provided on www.crossref.org (at least 80% of the bibliographic references must have their own doi indexes). Links to online publications, abstracts and dissertations are not welcome.

After the list of references, it is necessary to provide information about all authors (in English, Ukrainian and Russian): last name, first name and patronymic of the author, degree, place of work and position, **ORCID number** (each of the authors of the ORCID personal number if absence - free creation on the official website http://www.orcid.org) to facilitate the readers of this article to refer to your publications in other scientific publications.

The last page of the text should include the surname, name and patronymic of the author, degree, postal address, telephone number and e-mail of the author, with which the editors will maintain contact.

Concluding remarks

The manuscript should be executed in such a way that the number of refinements and revisions during the editorial of the article was minimal.

When submitting the article, please observe the following requirements. The volume of the article - not less than 15 and not more than 25 pages, Times New Roman, 14 pt, line spacing - one and a half, fields - 2 cm, sheet A4. Text materials should be prepared in the MS Word editor (* .docx), without indentations. Math formulas and equations to prepare in the embedded editor; graphics - in MS Excel. Use the units of the International Measurement System. Tables and drawings must contain the name, be numbered, and references to them in the text should be presented as follows: (fig. 1), or (table 1). The drawings should be in the format "jpg" or "tif"; when scanned, the resolution should be at least 800 dpi; when scanning half-tone and color images, the resolution should be at least 300 dpi. All figures must be represented in the CMYK palette. The statistical and other details are given below the table in the notes. Table materials and drawings place at the end of the text of the manuscript. All elements of the text in images (charts, diagrams, diagrams) must have the Times New Roman headset.

Articles are sent to the editorial board only in electronic form (one file) at the e-mail address nila@vnmu.edu.ua

Responsible editor - Gunas Igor Valeryovich (phone number: + 38-067-121-00-05; e-mail: gunas.red@gmail.com).

Signed for print 28.09.2018
Format 60x84/8. Printing offset. Order № 3113. Circulation 100.
Vinnytsya. Printing house “Tvory”, Keleckaya St., 51a
PO Box 8825, 600-Richchya Str., 21, Vinnytsya, 21007
Phone: +38 (0432) 603 000
+38 (096) 97-30-934, +38 (093) 89-13-852
e-mail: tvory2009@gmai.com
http://www.tvoru.com.ua